The University of Aston in Birmingham

Updating Finite Element Models using Measured Vibration Data

Michael Ian Friswell

Doctor of Philosophy August 1990

Summary

The modelling of mechanical structures using finite element analysis has become an indispensable stage in the design of new components and products. Once the theoretical design has been optimised a prototype may be constructed and tested. What can the engineer do if the measured and theoretically predicted vibration characteristics of the structure are significantly different? This thesis considers the problems of changing the parameters of the finite element model to improve the correlation between a physical structure and its mathematical model.

Two new methods are introduced to perform the systematic parameter updating. The first uses the measured modal model to derive the parameter values with the minimum variance. The user must provide estimates for the variance of the theoretical parameter values and the measured data. Previous authors using similar methods have assumed that the estimated parameters and measured modal properties are statistically independent. This will generally be the case during the first iteration but will not be the case subsequently.

The second method updates the parameters directly from the frequency response functions. The order of the finite element model of the structure is reduced as a function of the unknown parameters. A method related to a weighted equation error algorithm is used to update the parameters. After each iteration the weighting changes so that on convergence the output error is minimised.

The suggested methods are extensively tested using simulated data. An H frame is then used to demonstrate the algorithms on a physical structure.

Key Words: Vibration; Parameter Updating; Modal Testing; Finite Element;

Acknowledgements

This thesis was written while the author was employed as a Lecturer in the Department of Mechanical and Production Engineering at the University of Aston in Birmingham (1987-1990). The author would like to thank Dr J E T Penny, who was both project supervisor and Head of Department during this time.

Contents

List of Figures and Tables

Chapter 2

Chapter 4

Chapter 5

Chapter 6

Chapter 7

Chapter 8

Appendices

Chapter 1

Introduction

1.1 Problem Overview

Industry is investing increasing resources into Mechanical Computer Aided Engineering (MCAE). MCAE integrates computer based tools throughout the Engineering Department, allowing companies to develop mechanical products more cheaply and quicker than traditional methods. The aim is to use computer analysis to reduce the quantity of physical testing to an absolute minimum. This revolution has been aided by reducing hardware costs and the increasing availability of high quality software. Although MCAE covers a wide range of techniques, for example solid modelling, design visualisation, thermal analysis, drafting and manufacturing analysis, this thesis will concentrate on just two facets: Finite Element Analysis and Experimental Structural Testing as they relate to dynamic analysis.

Finite element analysis is commonly used to predict a structure's static strength and dynamic characteristics. These predicted characteristics are optimised during the theoretical design cycle to produce a satisfactory modelled structural response. A prototype is then produced. Experimental structural testing yields the dynamic response of the prototype which may then be compared to the predicted response. Should the responses agree then the modelling phase in general and the finite element model in particular are validated. What happens if the responses do not agree? Does it matter? Whether it matters will be answered in each individual case by consideration of the roles of the analytical and experimental phases. The finite element model of the structure allows a wide range of different configurations to be tried. These may be structural modifications. Or they may be complex loading patterns which are difficult to reproduce in a controlled experiment. The experimental model will be incomplete, for example no satisfactory transducer exists to measure the rotational degrees of freedom. Some structural modifications may be undertaken theoretically using the experimentally derived response although it is more difficult than using an analytical model. The experimental data does provide information on the idealisations made

during the finite element modelling (for example joints, bearings). Each case must be considered individually based on what information the engineer requires from the theoretical and experimental phases.

Suppose that the analytical and experimental responses do not agree. Often the structure has detail that cannot be accounted for within a finite element model without a vast increase in the number of degrees of freedom and therefore computational time. For example a particular finite element may have a small hole in it that is modelled by reducing the stiffness of the element. Equally the experimental responses will contain errors arising from the measurement process. The physical parameters of the modelled system could be adjusted to increase the correlation between the theoretical model and the actual structure. The result will be a more accurate simulation of the static and dynamic characteristics of the structure. But which parameters should be adjusted, how should they be adjusted and what criterion should be used to gauge the success of these changes? The majority of research in this area has used the correlation between the analytically derived and experimentally measured modal models (natural frequencies and mode shapes) as a measure of success. The natural frequencies are compared and the mode shapes are correlated, for example by using the Modal Assurance Criterion. The parameters of the analytical model are then updated often using the Taylor series expansion of the eigensystem in terms of the parameters. These methods assume that the natural frequencies and mode shapes of the prototype structure may be extracted. In many cases this is possible and given an accurate modal model these techniques can produce good results. Commercial software packages are available to perform the updating task systematically. In some instances the measured modal model is difficult to obtain accurately, especially where there are heavily damped or closely coupled modes present. Some algorithms have difficulty with data incorporating slight frequency shifts, for example due to the mass loading of a roving accelerometer. There are also problems with the interpretation of complex modes. In general, obtaining an accurate modal model requires a

great deal of care and engineering insight.

The main thrust of the research described in this thesis takes a different approach and attempts to update the unknown physical parameters directly from the frequency response function data. The problems associated with identifying an experimental modal model will not then arise. Some papers have appeared which update mass, damping and stiffness matrices from frequency response data directly. These algorithms generally update condensed theoretical models of the structure and require that the number of degrees of freedom and the number of measurement locations are equal. Most techniques cannot update the physical parameters of a finite element models with many degrees of freedom. Those algorithms that may be extended to a general finite element model would require an impractical amount of computation time.

1.2 Thesis Outline

There are many techniques used to update the parameters of finite element models. Theoretical finite element analysis and experimental structural testing have already been mentioned and are fundamental to any updating algorithm. The basic methods in theoretical and experimental vibration analysis are reviewed in Chapter 2. Also reviewed in this chapter are the methods to calculate eigensystem derivatives or sensitivities that are used in many updating algorithms. Chapter 2 can also be considered as an introduction to the notation used throughout the thesis. In particular damping matrices are included to provide the most general case and the equations of motion are written as a first order differential equation in terms of a state vector. Chapter 3 provides a summary of the methods used for parameter estimation or updating in structural dynamics.

The main thrust of this research is to investigate the possibility of updating

the model parameters directly from the frequency response data without computing the modal model. To produce a viable algorithm, the order of the finite element model must be considerably reduced while still maintaining the dependence of the modelled dynamic characteristics on the parameters of interest. The area of model order reduction has been considered in vibration analysis to enable modelled modal properties to be computed more quickly. Chapter 4 considers these reduction algorithms together with algorithms used in control engineering and assesses their applicability to the parameter updating problem.

Chapter 5 outlines a new method, based on a previously published minimum variance estimation algorithm, to update model parameters using the measured modal model. Previous authors using this method have assumed the estimated parameters and measured modal properties to be statistically independent. This will generally be the case during the first iteration of an updating scheme but will not be the case subsequently. The minimum variance algorithm uses the full finite element model.

Chapter 6 applies modal truncation, the chosen method to reduce the theoretical model order, to the general dynamic finite element model. An example is given to demonstrate the effect of reducing the model order on the frequency response functions.

Chapter 7 details the methods used to update the parameters of a structure using the reduced order model of Chapter 6. To highlight some of the problems and to introduce the updating algorithms, a simple one dof simulated example is demonstrated first. The updating algorithms are then outlined for the general multi dof system and evaluated using a simulated example.

Chapter 8 tries these new algorithms on an experimental structure, namely an H frame with bolted joints, and assesses the results.

Chapter 9 concludes the thesis by discussing the results in the context of possible practical application and considers the potential for further work in this area.

1.3 So What's New

The question which arises with any thesis is 'where is the original work?'. This section is designed to highlight those areas that are original. A number of journal and conference papers have been written on the work contained in this thesis and provides some justification of its originality.

Chapter 5 gives a corrected minimum variance estimator for updating procedures using the modal model. The correction is important because this technique, in its incorrect form neglecting the correlation between the estimated parameters and measured modal properties, is one of the most popular updating algorithms. Friswell (1989a) reports this work.

Previous methods for generating reduced order models of a finite element model have not explicitly retained the unknown parameters. Chapter 6 considers this problem in detail and forms the major part of the paper by Friswell (1990). The main thrust of the thesis is to couple the reduced order models to a suitable parameter estimation algorithm. Previous authors have updated condensed models of a structure. Chapter 7 considers this problem using simulated data and a paper on this research has been published (Friswell and Penny 1990c). Friswell (1989b) has also presented the state estimation and equation error algorithm results alone. The extension of Goyder's algorithm to a general multi degree of freedom method is also new. The author's experience of the methods on a simple experimental structure is outlined in Chapter 8 and was presented at IMAC 1990 (Friswell and Penny, 1990a).

Chapter 2

Review of Theoretical and Experimental Vibration Analysis

2.1 Chapter Summary

This chapter briefly reviews the dynamic modelling and analysis of structures. The treatment involves a rapid transit through some aspects of structural analysis and assumes the reader is already familiar with the techniques outlined. Since this chapter is not written for beginners in vibration analysis many textbooks are referenced which may be used to review the subject in more detail. The main purpose of this chapter is to introduce the notation used in the thesis, which is by no means standard throughout the literature.

2.2 Finite Element Modelling of Structures

The finite element method will now be considered briefly. Richards (1977), Irons and Shrive (1983), Meirovitch (1986), Przemieniecki (1968), Zienkiewicz (1977) and Zienkiewicz and Taylor (1989) review the subject in detail. A linear model is assumed throughout, that is the stress and strain in a system are linearly related. The purpose of a finite element model of a continuum is to replace the distributed or infinite dimensional system described by partial differential equations with a finite dimensional model described by ordinary differential equations. The modelling of a system using finite elements requires three stages which will now be outlined.

Finite Element Mesh Generation. The finite element method requires simple displacement models to be defined over a large number of small regions or elements. Thus the first task is to generate the element mesh, or equivalently to split the structure in regions of simple geometry. The form of the elements depends on whether the structure can be modelled as an assemblage of one dimensional or line elements, two dimensional elements (plane stress or strain) or general three dimensional elements. Bodies with axial symmetry can use ring type elements. Beam bending or beam extension may be approximated by using line elements and these elements are used for

the examples in this thesis. Thus beams are merely split into segments which need not be of constant length. The quality of the results from a finite element analysis is highly dependent on the form of the mesh that is used.

Displacement Model Selection. The unknown generalised coordinates for the system $q_1, q_2, \ldots, q_n$ usually correspond to the nodal displacements of the discretised system. The assumed displacement within each element must be written in terms of the generalised coordinates. Polynomial interpolating functions are particularly convenient for this purpose. Often the same form of the displacement model is used for all the elements in a model of a structure, although this is not necessary. In practice the choice of functions for the displacement model can be complex and sometimes requires the definition of additional nodes, either external nodes on boundaries between elements or internal nodes which are only associated with one element. The functions must be compatible between elements so the displacement and enough of its derivatives are continuous across element boundaries.

Equations of Motion Formulation. The formulation of the equations of motions reduces to computing the system mass matrix $\mathbf{M}_n$, stiffness matrix $\mathbf{K}_n$ and generalised force vector $\mathbf{Q}$. Note that n is the number of degrees of freedom of the modelled structure. The equations of motion are then

$$\mathbf{M}_n \ddot{\mathbf{q}} + \mathbf{K}_n \mathbf{q} = \mathbf{Q} \qquad (2.1)$$

where $\mathbf{q}$ is a vector of generalised coordinates. The required matrices and generalised force are usually derived by adding together the kinetic energy, the potential energy and the potential of the applied loads for all the individual elements.

In subsequent sections and chapters the basic equation 2.1 may be written in a slightly different form. The generalised co-ordinate vector $\mathbf{q}$ will often be written and called a state vector $\mathbf{x}$. The generalised force will usually consist

of a low number of point loads generated by shakers. In this case $\mathbf{Q}$ will be written as $\mathbf{B}_n \mathbf{u}$ where $\mathbf{B}_n$ is a matrix allocating the shaker input to the correct generalised co-ordinates (or states) and $\mathbf{u}$ is the input force excitation. This terminology is more in line with control engineering literature.

Damping has not been mentioned throughout this resumé of finite element analysis. In general damping is difficult to incorporate into a finite element analysis and is rarely undertaken in practice. Damping arises from two main sources. The material of which the structure is made may absorb energy and so give rise to damping that is distributed throughout the structure. This type of damping is sometimes modelled by adding a term $\mathbf{C}_n \dot{\mathbf{q}}$ into the equations of motion, equation 2.1, and is then called viscous damping. Experience with practical structures has shown that a more accurate model is given if the matrix $\mathbf{C}_n$ is frequency dependent. In the frequency domain the resulting model, called hysteretic damping, has a complex stiffness matrix. This model of the damping is really only valid for harmonic excitation. The alternative, and often the dominant, form of damping comes from joints in the structure. These are discrete energy absorbers but are usually highly nonlinear and are difficult to model accurately. If the damping is low then a very rough approximation, called proportional viscous damping, is that the damping is given by

$$\mathbf{C}_n = \alpha \mathbf{M}_n + \beta \mathbf{K}_n \qquad (2.2)$$

for some constants α and β . For proportional hysteretic damping the imaginary part of the stiffness matrix is assumed to be of the same form as equation 2.2 , where $\mathbf{K}_n$ is the real part of the stiffness matrix. Proportional damping is really only a convenient analytical fudge to include some damping into a model without a huge increase in computation, see section 2.4 .

2.3 The Nature of Unknown Parameters

It is very difficult to produce general guidelines on the choice of parameters to update. Suppose a structure has been manufactured from a homogeneous, isotropic material. Then the only possible unknown parameters are the material properties and the structure geometry. Because the finite element model cannot, in general, exactly reproduce the structure geometry there will be, for a particular form of finite element mesh, a set of dimensions that maximise the correlation of the model and structure characteristics. These dimensions may be difficult to estimate theoretically. It is unnecessary and unwise to try to identify the whole mass and stiffness matrices. Often it is impractical to include every detail of a structure's geometry. For example, a small hole may not be included. 'Average' values for the mass and stiffness coefficients are estimated for the element containing the hole.

A different form of the unknown parameters arises from applications involving fault detection. Assuming an adequate model exists for the perfect structure the task is to locate local faults, usually indicated by a local reduction in stiffness. All the parameters may be updated simultaneously and areas of large change highlighted. Alternatively sets of local parameters may be updated sequentially and the best agreement between model and measured characteristics chosen.

Finally proportional damping may be assumed with the constants of proportionality identified from the experimental data. Whatever parameters are chosen to be updated care must be taken that the parameter estimation problem does not become ill-conditioned. The probability of this happening increases as the number of unknown parameters increases. Physically problems will occur if two distinct sets of parameters give rise to the same change in measured characteristics. A simple method to overcome this problem, used later in the thesis, is to choose the set of parameters closest to the original estimates from the finite element analysis.

2.4 Structural Vibration Analysis

The general linear equations of motion for structure, obtained by extending equation 2.1 to include damping, are

$$\mathbf{M}_n \ddot{\mathbf{q}} + \mathbf{C}_n \dot{\mathbf{q}} + \mathbf{K}_n \mathbf{q} = \mathbf{Q} = \mathbf{B}_n \mathbf{u} \qquad (2.3)$$

where $\mathbf{M}_n$ is the mass matrix, $\mathbf{C}_n$ is the viscous damping matrix and $\mathbf{K}_n$ is the stiffness matrix, which is complex if hysteretic damping is included. These matrices are symmetric and positive semi-definite. $\mathbf{q}$ is the n dimensional vector of generalised displacements. $\mathbf{Q}$ is the vector of generalised forces which usually arises from predetermined shaker inputs or similar. Hence $\mathbf{Q}$ may be written as $\mathbf{B}_n \mathbf{u}$ where $\mathbf{B}_n$ is a matrix allocating the force input to the relevant degrees of freedom and $\mathbf{u}$ is the input force vector which has the same dimension as the number of force inputs. $\mathbf{M}_n$, $\mathbf{C}_n$ and $\mathbf{K}_n$ are usually symmetric matrices.

Suppose the structure is undamped. Then the ith eigenvalue μ_i (minus natural frequency squared) and the corresponding eigenvector ψ_i (mode shape) are the solution of

$$\left(\mathbf{M}_n \mu_i + \mathbf{K}_n \right) \psi_i = 0 \qquad (2.4)$$

where μ_i and ψ_i are both real (μ_i is also negative or zero). If μ_i and μ_k are distinct then it may be shown that

$$\psi_i^T \mathbf{M}_n \psi_k = 0 \qquad \psi_i^T \mathbf{K}_n \psi_k = 0 \qquad . \qquad (2.5)$$

A transformation matrix obtained by placing these eigenvectors into its columns will uncouple the equations of motion given by equation 2.3. If

proportional damping is assumed then this transformation matrix will also uncouple the resulting equations of motion. This method will not be expanded further as it is particular case of the general damping analysis which is used to generate the algorithms in this thesis. Meirovitch (1986) and Ewins(1984) give further details.

For general damping the analysis proceeds by changing the n second order equations given by equation 2.3 into the 2n first order equations

$$\mathbf{M}\,\dot{\mathbf{x}} + \mathbf{K}\,\mathbf{x} = \mathbf{B}\,\mathbf{u} \tag{2.6}$$

where $\mathbf{x} = \begin{Bmatrix} \mathbf{q} \\ \dot{\mathbf{q}} \end{Bmatrix}$

$$\mathbf{M} = \begin{bmatrix} \mathbf{C}_n & \mathbf{M}_n \\ \mathbf{M}_n & 0 \end{bmatrix} \qquad \mathbf{K} = \begin{bmatrix} \mathbf{K}_n & 0 \\ 0 & -\mathbf{M}_n \end{bmatrix}$$

$$\mathbf{B} = \begin{Bmatrix} \mathbf{B}_n \\ 0 \end{Bmatrix}$$

Usually not all the generalised displacements will be measured. Thus the measured output vector $\mathbf{y}$ has dimension m and is given by

$$\mathbf{y} = \mathbf{C}\,\mathbf{x} \tag{2.7}$$

for some matrix $\mathbf{C}$. Note that the matrix $\mathbf{C}$ is NOT damping. The 2n eigenvalues λ_i and right hand eigenvectors ϕ_i of equation 2.6 are the solutions of

$$\left(\mathbf{M}\,\lambda_i + \mathbf{K} \right) \phi_i = 0 \quad . \tag{2.8}$$

Without hysteretic damping λ_i and ϕ_i occur in complex conjugate pairs. In

any event the left and right hand eigenvectors are equal. If λ_i and λ_k are distinct then it may be shown that

$$\phi_i^T \mathbf{M} \phi_k = 0 \qquad \phi_i^T \mathbf{K} \phi_k = 0 \quad . \tag{2.9}$$

Since any multiple of the eigenvectors given by equation 2.8 is also an eigenvector, the eigenvectors may be chosen so that

$$\phi_i^T \mathbf{M} \phi_i = 1 \quad . \tag{2.10}$$

Then

$$\phi_i^T \mathbf{K} \phi_i = -\lambda_i \quad . \tag{2.11}$$

The equations of motion equation 2.6 can now be transformed using the transformation

$$\mathbf{x} = \Phi \mathbf{z} \tag{2.12}$$

where $\Phi = [\, \phi_1 , \phi_2 , \ldots , \phi_{2n} \,]$.

Premultiplying the transformed equation by the transpose of Φ gives the uncoupled equations of motion

$$\left.\begin{aligned} \dot{\mathbf{z}} + \Lambda \mathbf{z} &= \Phi^T \mathbf{B} \mathbf{u} \\ \mathbf{y} &= \mathbf{C} \Phi \mathbf{z} \end{aligned}\right\} \tag{2.13}$$

where $\Lambda = -\mathrm{diag}(\lambda_1 , \lambda_2 , \ldots , \lambda_{2n})$.

On taking the Fourier Transform of equation 2.13 and after some rearrangement the frequency response function (or receptance) defining the input to output characteristics of the system may be obtained as

$$F(\omega) = \left[\frac{X}{U}\right](\omega) = \sum_{i=1}^{2n} \frac{C\,\phi_i\,\phi_i^T\,B}{(j\omega - \lambda_i)} \quad . \qquad (2.14)$$

The expression $\left[\frac{X}{U}\right]$ is defined by $\left[\frac{X}{U}\right]_{ik} = \frac{\{X\}_i}{\{U\}_k}$.

Each receptance, linking a single input to a single output, is a complex function of the frequency ω. Two methods of presentation are generally used to plot graphs of the frequency response functions. The most popular, called the Bode plot, requires two graphs: the modulus of the FRF vs frequency and the phase of the FRF vs frequency. The modulus and/or frequency axes are often logarithmic to allow for the wide range of values encountered in practice. The second, called the Nyquist plot, shows the FRF on an Argand plane. The frequency information, if required, must be marked on the plot at individual points.

2.5 Computational Aspects of Structural Vibration

Some computational aspects of structural vibration will now be described. Generally a finite element model is used to compute estimates of the eigenvalues and eigenvectors of a structure. If required, these may then be used to calculate the frequency response functions given by equation 2.14. For the sensitivity analysis used by many model updating algorithms the derivatives of the eigenvalues and eigenvectors with respect to physical parameters are also required.

2.5.1 Computing Eigenvalues and Eigenvectors

The system eigenvalues and eigenvectors are given by equation 2.8 with the eigenvector normalisation given by equation 2.10. Essentially computing the eigensystem is a numerical analysis problem that has received much attention over many years. For a model with a large number of degrees of freedom not all the eigenvalues will be computed. In any case only the lower eigenvalues are likely to be close to those of the actual system. Wilkinson (1965), Jennings (1981) and Gourlay and Watson (1973) give more detail.

Transformation methods such as Givens, Householder, LR and QR methods (Wilkinson, 1965) work well for most systems. All the eigenvalues and eigenvectors are computed and so the amount of computation required for these methods is proportional to n^3, where n is the dimension of the matrices. The other major problem with these methods is that they do not preserve the sparseness that is inevitably present in the mass and stiffness matrices (Jennings, 1981). Jacobi's method for real symmetric matrices (Wilkinson, 1965) is an older method that uses plane rotations to reduce the matrix to diagonal form.

The alternative methods are based on iteration. Initial estimates for some of the system eigenvalues and eigenvectors are updated using only multiplication by the sparse matrices. Such methods include the power method, simultaneous iteration and the Lanczos' method. Eigenvalues may also be estimated using Sturm sequences with a bisection process (Jennings, 1981).

2.5.2 Computing Eigensystem Derivatives

The computation of eigensystem derivatives has not received as much prominence as eigensystem calculations and so will be summarised in more

detail here. Probably the most straightforward method to calculate the derivatives of the system eigenvalues and eigenvectors with respect to parameters of the system model matrices is by perturbing the parameters one at a time. The resulting perturbations of the eigensystem are then used to numerically calculate the derivative. Of course a new eigensystem has to be calculated for each parameter.

Fox and Kapoor [1968] outlined a method to compute the eigensystem derivatives analytically. Consider the eigenproblem given by equation 2.8 and assume that the eigenvalues and eigenvectors have been computed. Differentiating equation 2.8 with respect to unknown parameter $\{\theta\}_k$ gives

$$\left(\frac{\partial \mathbf{M}}{\partial \{\theta\}_k} \lambda_i + \frac{\partial \mathbf{K}}{\partial \{\theta\}_k} + \mathbf{M} \frac{\partial \lambda_i}{\partial \{\theta\}_k} \right) \phi_i +$$

$$\left(\mathbf{M} \lambda_i + \mathbf{K} \right) \frac{\partial \phi_i}{\partial \{\theta\}_k} = 0 \qquad (2.15)$$

Premultiplying equation 2.15 by ϕ_i^T gives, assuming the eigenvectors are normalised as in equation 2.10,

$$\frac{\partial \lambda_i}{\partial \{\theta\}_k} \phi_i^T \mathbf{M} \phi_i = \frac{\partial \lambda_i}{\partial \{\theta\}_k} =$$

$$- \phi_i^T \left(\frac{\partial \mathbf{M}}{\partial \{\theta\}_k} \lambda_i + \frac{\partial \mathbf{K}}{\partial \{\theta\}_k} \right) \phi_i \ . \qquad (2.16)$$

Equation 2.16 provides a very simple and convenient way of computing eigenvalue derivatives. The derivatives of the eigenvectors are obtained by realising that the eigenvectors form a basis for 2n dimensional Euclidian

space. Thus any vector, including the eigenvector derivatives, may be written as a linear combination of all the eigenvectors. Hence

$$\frac{\partial \phi_i}{\partial \{\theta\}_k} = \sum_{h=1}^{2n} {}_k a_{ih}\, \phi_h \qquad (2.17)$$

where the constants ${}_k a_{ih}$ are to be determined. If one or more eigenvalue is repeated then a linearly independent set of eigenvectors may still be generated. But the method is not able to calculate the derivatives of eigenvectors associated with such eigenvalues. Premultiplying equation 2.15 by ϕ_h^T , substituting the expression given in equation 2.17 gives, using equations 2.9 , 2.10 and 2.11,

$${}_k a_{ih} = \frac{1}{\lambda_h - \lambda_i}\, \phi_h^T \left(\frac{\partial \mathbf{M}}{\partial \{\theta\}_k} \lambda_i + \frac{\partial \mathbf{K}}{\partial \{\theta\}_k} \right) \phi_i \qquad i \neq h \ . \qquad (2.18)$$

The term ${}_k a_{ii}$ is found in a similar manner by differentiating equation 2.10 instead of equation 2.8 to give

$$2\, \phi_i^T\, \mathbf{M}\, \frac{\partial \phi_i}{\partial \{\theta\}_k} + \phi_i^T\, \frac{\partial \mathbf{M}}{\partial \{\theta\}_k}\, \phi_i = 0 \qquad (2.19)$$

Substituting the expression given by equation 2.17 into equation 2.19 yields, on application of equations 2.9 and 2.10,

$${}_k a_{ii} = -\frac{1}{2}\, \phi_i^T\, \frac{\partial \mathbf{M}}{\partial \{\theta\}_k}\, \phi_i \ . \qquad (2.20)$$

These expressions for the eigensystem derivatives are used in chapter 6 to gain some insight into the quality of the proposed reduced order models.

Another algebraic method for calculating the eigenvector derivatives is also contained in the paper by Fox and Kapoor (1968). Assuming that the derivative of the eigenvalue has been calculated from equation 2.16 then equations 2.15 and 2.19 represent 2n+1 equations in the 2n unknown elements of the eigenvectors derivative. These equations may be assembled into matrix form and solved using a pseudo inverse technique. Note that equation 2.15 cannot be used alone to compute the eigenvector derivative since $\mathbf{M}\lambda_i + \mathbf{K}$ is singular. For systems with many degrees of freedom computing the pseudo inverse is a lengthy computation. The resulting 2n dimensional matrix to be inverted will also be fully populated even though the original eigensystem matrices are sparse and the inversion may be poorly conditioned. Nelson (1976) produced an algorithm which solved the equations more efficiently. The derivative of the i th eigenvector is written as

$$\frac{\partial \phi_i}{\partial \{\theta\}_k} = \mathbf{V}_{ik} + c_{ik}\,\phi_i \qquad (2.21)$$

for some vector $\mathbf{V}_{ik}$ and constant c_{ik}. By fixing one element of the vector $\mathbf{V}_{ik}$ the other elements may be found from equation 2.15, whilst maintaining any sparseness that is present. The element chosen must be such that the corresponding element in ϕ_i is relatively large. The constant c_{ik} is then computed using equation 2.19.

The alternative method is based on an iterative method, originally proposed by Rudisill and Chu (1975). The original paper and others extending the method considered the standard eigenproblem, that is, $\mathbf{M}$ is the identity matrix and $\mathbf{K}$ is an arbitrary matrix. Applied to the vibration problem gives the following iteration scheme, derived from equation 2.15,

$$\left(\frac{\partial \phi_i}{\partial \{\theta\}_k}\right)^{h+1} = \mathbf{M}^{-1}\left(\left(\frac{\partial \mathbf{M}}{\partial \{\theta\}_k}\lambda_i + \frac{\partial \mathbf{K}}{\partial \{\theta\}_k} + \mathbf{M}\frac{\partial \lambda_i}{\partial \{\theta\}_k}\right)\phi_i + \mathbf{K}\left(\frac{\partial \phi_i}{\partial \{\theta\}_k}\right)^{h}\right) / \lambda_i \qquad (2.22)$$

where the superscript h denotes the h th iterate, and the eigenvalue derivative is given by equation 2.16. If the eigenvalues are arranged in descending absolute value then this scheme only converges for i = 1, the dominate eigenvalue (Andrew, 1978). For subdominant eigenvalues a modification analogous to the standard deflation process for the classical eigenproblem was suggested by Rudisill and Chu (1975) and Andrew (1978). Tan (1987) and Tan and Andrew (1989) have produced algorithms that are similar but have increased computational efficiency.

2.6 Experimental Vibration Analysis Theory

Experimental Vibration Analysis can cover a vast range of techniques, for example identifying nonlinearities or the investigation of the dynamics of rotating machines. In the context of this thesis the aim of any experiment is to obtain a frequency response function (FRF) between predetermined force input positions and response locations for a given structure. The modal parameters, natural frequencies, damping coefficients and mode shapes, are then computed from these FRFs, although some algorithms use the time series data directly. Snoeys *et al.* (1987) review most techniques in Experimental Modal Analysis and also give a detailed evaluation of the methods against numerous cost and quality criteria. Ewins (1984) and Allemang *et al.* (1987) give more comprehensive details.

2.6.1 Excitation Methods

In order to obtain a system response the structure must be excited in some way. Excitation methods may be broadly split into three types: harmonic, random and transient. One of the oldest and certainly the most simple method is stepped sine testing. Here the structure is excited with a sinusiodally varying force. Assuming the structure is linear the response will be sinusoidal at the excitation frequency. This method is extended by using a sinusoid whose frequency varies slowly, or swept sine excitation. Friswell and Penny (1990b) consider the possibility of using more than one sinusoid at a time.

The other available techniques tend to use broadband excitation and Fourier Transforms, implemented as the FFT, to obtain the FRFs. Either pseudo random or random vibration can be applied to the structure. Since the measurement time is finite the calculation of the Fourier Transforms have problems with leakage (see section 2.6.2). Recently new broadband signals have been successfully used that have reduced leakage properties and improved signal to noise ratios, for example burst random (Olsen, 1983) obtained by combining random and transient signals.

Transient excitation is easily implemented using a force impact or a step relaxation, for example a large weight may be released from a concrete bridge. The Fourier Transform of an impulse applied to a structure generally shows a fairly constant power level for all frequencies up to a cut off frequency which is dependent on the physical parameters of the excitation hardware.

Recently multipoint excitation methods have been developed (Allemang *et al.*, 1983, and Zaveri, 1984). With these methods the FRFs are calculated for multiple, simultaneous force inputs. The result should be more consistent data sets and a more uniform distribution of energy throughout the structure.

2.6.2 Digital Signal Processing

Generally the time signals generated by the force and response transducers are sampled by an analogue to digital converter (ADC) and then processed digitally either by a computer or microprocessor system. To prevent aliasing, before the signal is sampled it must be filtered to remove frequencies above half the sampling frequency. The effect of aliasing is to make high frequencies in the signal appear as a contribution to a lower frequency component in the sampled signal (Ewins, 1984).

The problems in signal processing occur with the broadband signals that require processing using a Fourier Transform (strictly speaking a Discrete Fourier Transform or DFT). The major source of error is called leakage. Leakage arises because the signals are only sampled for a finite period of time. The DFT algorithms then assume, in effect, that the signal is periodic for times outside the time interval sampled. The solution is to make the signal periodic in the sampling window, for example by using burst random excitation. If this is not possible then the partial solution is to apply a window to the time series data before the DFT is computed. Windows are functions that are zero where the signal is non-zero at the ends of the sampling interval. The time signal is weighted by the window and the window is designed to influence the resulting DFT as little as possible. Leakage usually causes the damping in a structure to be overestimated.

What processing is required to calculated the FRFs of a structure from the time series data? The easiest method would be to take the DFT of both force input and response and then their ratio, in the case of only one input, will be the required FRF. Formally the FRFs may be computed using Auto and Cross Spectral Densities. The Cross Spectral Density between time series u(t) and y(t), $S_{yu}(\omega)$, is defined as the Fourier Transform of the Cross Correlation Function $R_{yu}(\tau)$ given by

$$R_{yu}(\tau) = E[\, y(t)\, u(t+\tau)\,] \qquad (2.23)$$

where $E[\ ]$ denotes expected value. The Auto Spectral Densities, $S_{uu}(\omega)$ and $S_{yy}(\omega)$, are defined as the Fourier Transforms of the corresponding Autocorrelation Functions. It may be shown that the FRF between input u and output y may be written in two ways, designated H1 and H2 as follows

$$\left.\begin{aligned} H_1(\omega) &= \frac{S_{yu}(\omega)}{S_{uu}(\omega)} \\ H_2(\omega) &= \frac{S_{yy}(\omega)}{S_{yu}(\omega)} \end{aligned}\right\} . \qquad (2.24)$$

These derivations of the FRF estimates are formally correct although more efficient algorithms exist for their computation. The H1 estimate minimises the effect of noise that occurs on the system output whereas the H2 estimate minimises the effect of noise that occurs on the system input. Recently methods that take into account errors on both the system input and output and minimise them in a total least squares sense, called the Hv estimate, have been proposed (Vold *et al.*, 1985).

2.6.3 Modal Model Extraction

In experimental vibration analysis the most important information is the modal model, that is the natural frequencies, damping coefficients and mode shapes. This information provides insight into the critical excitation frequencies and usually the mechanisms that give rise to a particular mode of vibration. Often the solution to rectify any inadequacies in the dynamic response of a structure may be derived directly. For example an extra stiffening bar may be used to increase a natural frequency out of a problem

range. The experimental modal model has been used extensively to update theoretical structural models, see Chapter 3.

Leuridan *et al.* (1988), Snoeys *et al.* (1987), Brown *et al.* (1979) and Allemang *et al.* (1987) review parameter estimation methods in the context of identifying a modal model. This section will only give a brief introduction to the commonly used algorithms. Simple, single degree of freedom (SDOF) methods, where each mode is assumed to be distinctly separated from the others, sometimes provides meaningful results in elementary cases. Almost all modern algorithms are multiple degree of freedom (MDOF) methods which are well suited to closely spaced modes (Brown *et al.*, 1979). There are two other classification criteria concerned with these estimation methods. First the algorithm may be implemented using data in either the frequency or time domain and this determines the type of model derived. Time domain algorithms requiring impulse response functions have become more popular since efficient and fast DFT algorithms have allowed the impulse response to be calculated from the frequency response function. Second the algorithm may or may not identify a single 'optimal' set of global parameters, which are the parameters that do not vary with forcing or response location, for example natural frequency and damping.

The simplest SDOF method is the **Peak and Mode Picking Method** and is mainly used for lightly damped systems. The natural frequency is estimated by the frequency at which the amplitude of the FRF is maximum. The damping is estimated using the frequencies at which the ratio of the amplitude of the FRF relative to the peak amplitude is $1 / \sqrt{2}$ (the half power points). The mode shape is estimated using the relative magnitude and phase of the FRFs at resonance. If the damping is negligible then the value of the maximum amplitude of the FRFs is very difficult to estimate.

The **Circle Fit Method** is another SDOF method that gives more accurate estimates of the modal parameters. The method is based on the fact that

for a simple one DOF system Nyquist plots of particular frequency response functions (the receptance for hysteretic damping) are circles. The natural frequency is estimated from the point of maximum sweep rate around the circle. Damping is estimated using points on the circle at frequencies above and below resonance. The modal constant is obtained from the diameter of the circle. The effect of other modes may be evaluated from the position offset of the circle. The modal properties may also be computed by fitting straight lines to the inverse of the receptance (Dobson, 1987).

For lightly damped systems Ewins and Gleeson (1982) proposed a MDOF **Least Squares Frequency Domain Method** that uses natural frequencies obtained by peak picking. Assuming negligible damping the FRF is a linear function of the modal constants. These constants may be found using sufficient points from the full FRF, by including mass and stiffness residuals to allow for modes outside of the measurement range. If required damping can be estimated from the peak value of the FRF modulus and the relevant modal constant.

The **Least Squares Complex Exponential Method** is a MDOF time domain technique which produces global estimates of the natural frequencies and damping coefficients. The method works by curve fitting to the experimental impulse response. Because sampled data is used, the exponentials in the theoretical impulse response function are replaced by a power series. The end result is that an autoregressive (AR) model must be fitted to the experimental data. Statistical analysis of the input data can provide an insight into the order of the AR model, and hence the number of modes, required. The poles, or natural frequency and damping coefficients, are then computed from this autoregressive model. The extension of this method to allow for multiple force inputs is relatively straightforward but important enough to be given a separate name, the **Polyreference Method.**

The **Ibrahim Time Domain Technique** is similar to the Least Squares Complex

Exponential Method but uses sampled data from free decay responses. The method constructs a matrix whose eigenvalues and eigenvectors are related to the measured system's natural frequencies, damping coefficients and mode shapes.

The **Orthogonal Polynomial Method** is a global, frequency domain method which can account for modes outside the measurement range explicitly by including mass and stiffness residuals. The method assumes that the system's frequency response function may be written as a ratio of two polynomials in $(j\omega)$. Orthogonal polynomials are usually used to produce a well conditioned problem. After rearranging the equations the coefficients of these polynomials may be found by a linear least squares algorithm. The method may be extended to data from multiple input experiments.

The **Time Domain Direct Parameter Identification Method** is similar to the Least Squares Complex Exponential Method but estimates the parameters of an autoregressive moving average model (ARMA) rather than an autoregressive model. If fact both the Least Squares Complex Exponential Method and the Ibrahim Time Domain Technique are special cases of these direct parameter identification techniques. The method is described, along with the corresponding Z-Transform, by Mickleborough and Pi (1989).

More recently the **Eigensystem Realisation Algorithm** has been suggested. The method uses sampled time domain data to produce a representative state space model of the measured system. The algorithm originated in Control Theory and constructs the model via a block Hankel Matrix and singular value decomposition. The method gives insight into to the model order required from the singular values and the system's modal characteristics are found from the state space model's eigensystem.

2.7 Experimental Vibration Analysis in Practice

Section 2.6 outlined the theory of experimental vibration analysis. What guidelines determine which method and equipment should be used for a given experiment? In particular what method and equipment will be used for the experimental work documented later in the thesis? This section tries to address some general considerations. The description of the experimental procedure adopted by the author is given in chapter 8. Ewins (1984) gives more detail.

2.7.1 Choice of Method

The choice of method used to measure the frequency response functions of a system is closely linked to the equipment available and the ultimate use of the data. In principle any modal extraction routine may then be used, although many of the global algorithms may have difficulties with inconsistent measured data. These inconsistencies mainly occur when the response of the system is measured using only one accelerometer that is repeatedly moved. This causes slight changes in the mass and stiffness distribution of the structure that produces changes in its natural frequencies. The solution is to use many accelerometers and measure the response at all the required points simultaneously.

The first decision to be taken is the choice of excitation type. Suppose that only the natural frequencies of a structure were required. The impact excitation using an instrumented hammer or similar would be ideal. The method is quick to set up and can provide good estimates of natural frequencies. Problems occur in ensuring that each impact is essentially the same as previous ones, in avoiding multiple impacts or 'hammer bounce' and in not entering nonlinear regimes by overloading the structure. If spatial information, such as mode shapes, is required then the decision is not so

clear. Generally the processing involved in stepped sine testing is negligible and so the length of a vibration test is independent of the number of accelerometers. Broadband excitation signals require far more processing to obtain the FRFs of a structure. With many accelerometer signals the processing time may negate the speed advantage inherent in exciting the structure at many frequencies simultaneously.

2.7.2 Equipment Used

The equipment used in a vibration test will ultimately depend on the excitation signal type chosen. Also there is a trend towards measuring the response at all locations required simultaneously. Thus computer workstations with associated ADCs and DACs have become more popular. All the excitation signal generation and signal processing functions, such as correlations and FFTs, may be performed in software albeit at the expense of longer computational times. The alternative is to have a dedicated analyser that performs the signal generating and processing functions which is usually interfaced to a controlling computer for further data analysis.

Transducers for measuring force and acceleration based on piezoelectric material are readily available, are reliable and have good dynamic characteristics. Transducers exist that measure displacement or velocity but they tend to be more expensive and more difficult to operate. Electrodynamic exciters that can convert excitation signals generated as voltages into a force input to the structure are also readily available. Impact excitation may be applied using a hammer that contains a force transducer just behind the impact tip.

Before measurements are taken the transducers used should be calibrated. Both force and acceleration transducers may be calibrated absolutely, usually using an expensive and highly accurate standard transducer. If only the frequency response function of a structure is required then the force

transducer and accelerometer may be calibrated together very simply. A 'rigid' mass is suspended and then excited horizontally. The system is forced, for example using an exciter, and the force input to the mass and its resulting acceleration are measured using the transducers requiring calibration, see figure 2.1. Any of the force excitation signals may be used. Assuming the mass is rigid then the mass will satisfy Newton's second law of motion and the frequency response function will be constant and equal to the inverse of the mass of the moving part of the system. This mass can be measured accurately and compared to the value obtained from the FRF to calibrate the transducer pair.

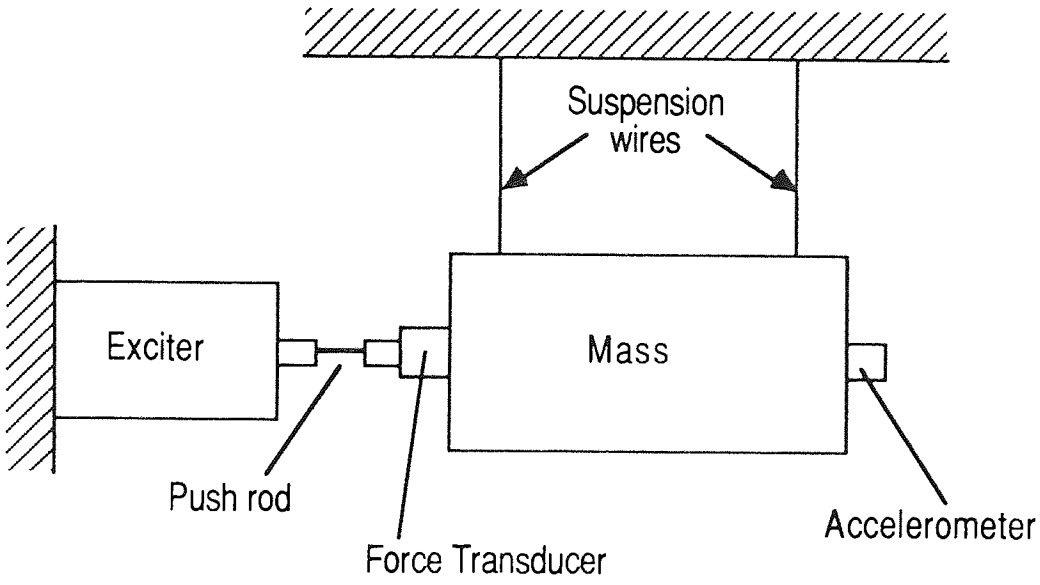

Figure 2.1 Calibration of Force / Acceleration Transducer Combination

Chapter 3

Review of Structural Parameter Estimation

3.1 Chapter Summary

This chapter reviews existing methods used to estimate or update the parameters of a finite element model. Methods to assess the agreement between the experimental and theoretical model are outlined first. The algorithms are then grouped and reviewed according to the type of experimental data they use, for example time, frequency or modal domain data. The methods using modal data, that is natural frequencies and mode shapes, are further grouped into direct (or non iterative) and iterative methods.

Although the application of system identification and parameter estimation to structural dynamics problems is relatively new there is a huge number of papers on the subject. With at least one major conference a year and three or four journals mainly devoted to modal analysis the problem is becoming even worse. Natke (1988) mentions this problem in his paper. Although the number of papers is large most of the algorithms are based on a small number of basic ideas. These ideas will be reviewed thoroughly in this chapter but it is almost impossible and also undesirable to consider every paper written on structural parameter estimation.

3.2 Correlation Between the Theoretical and Experimental Models

Model updating attempts to improve a finite element model by adjusting parameters of the model. Thus a method is required to assess how good the correlation is between the original model and the experimental results, and to measure the subsequent improvement (hopefully!) in this correlation. Also in methods using the experimental modal model the modes in the theoretical model and experimental data must correspond. Thus, for example, the first torsion mode in the theoretical model must correspond to the first torsion mode in the experimental data.

The simplest check is to compare the resonant frequencies predicted from theory and experiment, provided the modes correspond. Two main methods exist to check the consistency of the mode shape vectors: the Orthogonality Check and the Modal Assurance Criterion (MAC).

The **Orthogonality Check** uses the fact that the eigenvectors of an undamped, or proportionally damped, system are orthogonal when weighted by either the mass or stiffness matrices. The condition that the system be undamped or proportionally damped is not strictly necessary but implies that the eigenvectors are real. The interpretation of complex mode shapes is not straightforward and the visualisation of the motion of the system difficult. The orthogonality checks may be extended to the general damping case although they become more involved (see for example Heylen, 1987). The basis of the Mass Orthogonality Check is to compute the matrix

$$\Phi_m^T \, \mathbf{M}_a \, \Phi_m \tag{3.1}$$

where Φ_m is a matrix containing the measured mode shapes and $\mathbf{M}_a$ is the theoretical mass matrix for the system. The corresponding Stiffness Orthogonality Check uses the matrix

$$\Phi_m^T \, \mathbf{K}_a \, \Phi_m \tag{3.2}$$

where $\mathbf{K}_a$ is the theoretical stiffness matrix for the system. The measured modes shapes may be scaled so that the diagonal terms in matrix 3.1 are unity. If the measured mode shapes correspond exactly to the theoretical mode shapes then the off diagonal terms in this matrix are zero. Values above 0.1 for these terms are generally regarded as showing an inadequate correlation between theory and experiment. Similarly for the Stiffness Orthogonality Check.

The basis of the Modal Assurance Criterion is that if two vectors are describing the same mode shape then they should be proportional. A

constant of proportionality, the Modal Scale Factor (MSF) may be calculated together with a correlation coefficient, the Modal Assurance Criterion, (Allemang and Brown, 1982). If a measured mode shape ϕ_m and an analytical mode shape ϕ_a are given then the Modal Scale Factor and the Modal Assurance Criterion are

$$MSF = \frac{\phi_a^T W \phi_m}{\phi_m^T W \phi_m} \tag{3.3}$$

$$MAC = \frac{\left| \phi_a^T W \phi_m \right|^2}{\phi_a^T W \phi_a \quad \phi_m^T W \phi_m} \tag{3.4}$$

where W is a positive semi-definite weighting matrix. This weighting matrix could be, for example, the analytical mass or stiffness matrix but for simplicity is often chosen to be the identity matrix. Remember that the eigenvectors of any model are only orthogonal when weighted by the corresponding mass or stiffness matrices. Therefore even if the analytical and experimental mode shapes were identical the off diagonal terms in the MAC matrix would not necessarily be zero. The MAC values range from zero indicating no correlation between the vectors, to unity which indicates that the vectors are proportional.

In the preceding discussion two problems have been ignored. The major problem is that the number of degrees of freedom in the theoretical and experimental models are different. That is, the number of nodes in the finite element model will in general be far greater than the number of measurement locations. In any case no satisfactory transducer exists to measure the rotational degrees of freedom. This problem is overcome by either the extension of the measured mode shape vectors or the reduction of the finite

element model to correspond with the measurement locations. Several methods exist to extend the mode shape vector including geometric interpolation, the modal scale factor principle, the modal co-ordinate method and the static and dynamic equilibrium methods (Heylen, 1987). Model reduction will be reviewed more fully in the Chapter 4. The most popular methods in this particular application are static condensation techniques, for example Guyan reduction. Since these reductions are usually only approximate care must be exercised in the interpretation of the orthogonality matrices (Chu *et al.*, 1989). Of course the only reason that the difference in the number of degrees of freedom is a problem is the use of analytical mass and stiffness matrices in the orthogonality checks. Hence the popularity of the unweighted Modal Assurance Criterion. A subsidiary problem is that the finite element model may not contain nodes at the measurement locations. The second problem is that the number of modes in the experimental and analytical models may differ. This is not too great a problem since once the modes are paired any modes left over are ignored.

To demonstrate the idea of Orthogonality Checks and the Modal Assurance Criterion consider a theoretical system whose reduced mass and stiffness matrices are

$$\mathbf{M}_a = \begin{bmatrix} 2 & 0 & 0 & 0 & 0 \\ 0 & 1 & 0 & 0 & 0 \\ 0 & 0 & 1 & 0 & 0 \\ 0 & 0 & 0 & 2 & 0 \\ 0 & 0 & 0 & 0 & 3 \end{bmatrix}$$

$$\mathbf{K}_a = \begin{bmatrix} 20 & -5 & -1 & 0 & 0 \\ -5 & 15 & -3 & -4 & 0 \\ -1 & -3 & 5 & -3 & -1 \\ 0 & -4 & -3 & 40 & -5 \\ 0 & 0 & -1 & -5 & 25 \end{bmatrix} \qquad (3.5)$$

All mass terms are in kilograms and all stiffness terms are in Newtons/metre. Suppose that the 'measured' mode shapes are in fact from a simulated system with the same mass matrix but with the stiffness matrix

$$\mathbf{K} = \begin{bmatrix} 16 & -5 & -1 & 0 & 0 \\ -5 & 15 & -3 & -4 & 0 \\ -1 & -3 & 5 & -3 & -1 \\ 0 & -4 & -3 & 40 & -5 \\ 0 & 0 & -1 & -5 & 29 \end{bmatrix} \tag{3.6}$$

(Notice that only the first and fifth diagonal terms have changed). The analytical natural frequencies are 1.75, 2.85, 3.01, 4.04 and 4.66 rad/s. The 'measured' natural frequencies are 1.70, 2.73, 3.08, 4.01 and 4.66 rad/s, which are close in magnitude to the analytical frequencies. Since the mass matrix in the analytical and simulated systems are identical, the mass orthogonality matrix 3.1 is the identity matrix. The stiffness orthogonality matrix is

$$\begin{bmatrix} 1.000 & 0.123 & -0.020 & -0.031 & 0.013 \\ 0.123 & 1.000 & 0.039 & -0.049 & 0.011 \\ -0.020 & 0.039 & 1.000 & 0.007 & 0.016 \\ -0.031 & -0.049 & 0.007 & 1.000 & -0.005 \\ 0.013 & 0.011 & 0.016 & -0.005 & 1.000 \end{bmatrix}$$

Although the (1,2) term is a little high overall the check is reasonably satisfactory. Now consider the MAC matrix which is

$$\mathrm{MAC} = \begin{bmatrix} 0.993 & 0.071 & 0.032 & 0.001 & 0.013 \\ 0.036 & 0.107 & 0.769 & 0.005 & 0.010 \\ 0.011 & 0.905 & 0.170 & 0.089 & 0.009 \\ 0.001 & 0.018 & 0.007 & 0.995 & 0.045 \\ 0.013 & 0.003 & 0.005 & 0.062 & 0.999 \end{bmatrix}$$

The first, fourth and fifth modes correlate well with MAC values above 0.99 . The second and third mode have interchanged between the analytical and experimental models. Also, because of their close natural frequencies, there is some correlation between the second and third modes. This example shows the danger of only using Orthogonality Checks which cannot highlight any difference in the ordering of the modes between the analytical and experimental data. The MAC will therefore be used when necessary in this thesis.

3.3 Direct Model Updating using Modal Information

The methods that will be reviewed in this section update parameters using non-iterative algorithms. The methods generally minimise parameter deviations from analytical estimates under certain constraints. These constraints may be the modal form of the equations of motion (equations 2.4 or 2.8), the orthogonality conditions (equations 2.9 to 2.11) or other equations linear in the parameters, for example the total mass may be given. The mass and stiffness matrices must be linear functions of the unknown parameters. Then the constraint equations are also linear functions of the unknown parameters. The main methods will be considered in 3 groups; pseudo inverse, inverse orthogonality and Lagrange multiplier methods.

A number of authors have used various implementations of the **pseudo inverse method**. The constraint equations are assembled into a set of linear simultaneous equations. Thus

$$\mathbf{A}\,\theta = \mathbf{b} \,. \qquad (3.7)$$

where $\mathbf{A}$ contains the coefficients of the unknown masses and stiffnesses. For example, if the orthogonality conditions are used then $\mathbf{A}$ will have elements incorporating products of the elements of the mode shape vectors. $\mathbf{b}$ contains terms in the known masses and stiffnesses and the right hand

sides of the orthogonality conditions. Different authors use different sets of equations to generate equation 3.7. Berman and Flannelly (1971) used the mass orthogonality and total mass only. Tlusty (1976) and Tlusty and Ismail (1980) used all the equations available.

The method of solution of equation 3.7 depends on whether it is under or over determined. Thus if there are too many equations there is no solution to the problem. A pseudo inverse solution will produce a set of parameters that satisfy the equations as close as possible in a least squares sense. If there are too few equations there are an infinite number of sets of parameters would reproduce the measured data. The parameter values closest to the theoretical ones should be chosen by changing equation 3.7 to

$$\mathbf{A} (\theta - \theta_a) = \mathbf{b} - \mathbf{A} \theta_a \qquad (3.8)$$

where θ_a is the theoretical parameter estimates. The pseudo inverse solution of equation 3.8 then gives the solution required. The parameters may also be weighted to reflect confidence in the theoretical parameter values (see for example Berman and Flannelly, 1971). Nalitolela *et al.* (1990) considers adding mass or stiffness to a system to increase the number of equations available.

The second group are **inverse orthogonality methods**, where only the orthogonality conditions, equations 2.9 to 2.11, are used. Assuming that all the modes are measured then Φ, the matrix containing the eigenvectors, is square and

$$\mathbf{M} = \Phi^{-T} \Phi^{-1} \qquad \mathbf{K} = \Phi^{-T} \Lambda \Phi^{-1} \qquad (3.9)$$

where Λ is the diagonal matrix of eigenvalues. In general not all the

eigenvectors are measured and so Φ cannot be inverted. This difficulty is overcome in one of three ways: reduce the mass and stiffness matrices to the number of measured modes, use the flexibility matrix rather than the stiffness matrix or increase the number of eigenvectors. The number of elements in the mode shape vectors may be reduced to obtain a square matrix Φ that may be inverted although interpreting the resulting mass and stiffness matrices would be very difficult. The flexibility matrix is given by the inverse of the stiffness matrix, that is

$$K^{-1} = \Phi \Lambda^{-1} \Phi^{T} \tag{3.10}$$

The flexibility matrix may be constructed when with a low number of measured modes but is singular and cannot be inverted to produce the stiffness matrix. Gravitz (1958) and Ross (1971) considered this approach in more detail. The final option is to define additional vectors to make the eigenvector matrix square. These may be the high frequency eigenvectors from the analytic model (Heylen, 1982) or they may be obtained from energy considerations (Ross, 1971).

The final group of techniques are the **Lagrange multiplier methods**. These techniques minimise the difference between the updated and analytical parameter estimates with constraints based on equation 3.7. The constraints are incorporated into the problem using the Lagrange multiplier technique. For example, to obtain an updated stiffness matrix the following matrix norm is minimised

$$\left| M_a^{-1/2} \left(K - K_a \right) M_a^{-1/2} \right| \tag{3.11}$$

where M_a and K_a are the analytical mass and stiffness matrices (Baruch and Bar Itzhack, 1978, Baruch, 1978 and 1979, Berman and Nagy, 1983).

The constraints used by Berman and Nagy (1983) were the stiffness orthogonality condition, the equations of motion and the symmetry of the stiffness matrix. The mass orthogonality condition was used to optimise the mass matrix prior to the optimisation of the stiffness matrix producing an updated matrix $\mathbf{M}_u$. The updated stiffness matrix is

$$\mathbf{K}_u = \mathbf{K}_a + \left(\Delta + \Delta^T \right) \tag{3.12}$$

where $\Delta = \frac{1}{2} \mathbf{M}_u \Phi \left(\Phi^T \mathbf{K}_a \Phi + \Lambda \right) \Phi^T \mathbf{M}_u - \mathbf{K}_a \Phi \Phi^T \mathbf{M}_u$

Equation 3.12 is a sum of simple matrix products and the square root of the mass matrix that appears in the function to be minimised, equation 3.11, does not have to be computed. Caesar (1986) considers a range of objective functions and constraints and compares them using a simulated example. Brown (1988) uses these techniques to locate regions of modelling error.

The direct methods of parameter identification suffer from a number of disadvantages. Apart from the pseudo inverse method, these techniques derive condensed models which consist of full mass and stiffness matrices whose elements have little physical significance. All the techniques produce a model which exactly reproduces the mode shapes although in practice they cannot be measured accurately. The advantage of these methods is their relatively low computational requirement.

3.4 Iterative Model Updating using Modal Information

The iterative methods are, in some ways, similar to the direct methods but generate the equations in the parameters using a Taylor series expansion for the eigenvalues and eigenvectors. For example, the first order Taylor series expansion of the i th eigenvalue λ_i in the parameters is

$$\lambda_i(\theta) = \lambda_i(\theta_e) + \sum_{k=1}^{p} \left(\{\theta\}_k - \{\theta_e\}_k \right) \frac{\partial \lambda_i}{\partial \{\theta\}_k}(\theta_e) + o(\delta\theta^2) \quad (3.13)$$

where θ_e is the current estimate of the unknown parameters θ, $\{\theta\}_k$ is the k th element of θ and $\delta\theta = \theta - \theta_e$. Thus the first order Taylor series produces equation that are linear in the unknown parameters. The methods are iterative because the Taylor series expansion is only a linear approximation because the terms of order $\delta\theta^2$ are ignored. Linear approximations to the eigenvectors may be produced in a similar way. The eigenvalue and eigenvector derivatives are calculated using the methods of section 2.5.2.

The parameters to be updated can now be chosen arbitrarily, for example submatrices of the mass and stiffness matrices, element mass and stiffness matrices or even geometric parameters such as element dimensions. Convergence of the iterative techniques depends on a large number of factors but some general observations can be made. Convergence may be difficult if the theoretical and experimental results differ widely, if the measurements are inaccurate or if the selected parameters do not allow adequate representation of modelling error. The convergence properties of the methods may be improved by giving some weight to the original theoretical parameter estimates.

The **pseudo inverse technique** may be applied to solve the equations produced by the Taylor series expansion. The principles, including the treatment of analytically derived parameter estimates, are much the same as for the direct updating methods. The differences are the source of the equations and the necessity to iterate. Chen and Garba (1980) consider this technique in more detail.

One of the most popular techniques is the **statistical or minimum variance method** initially proposed by Collins *et al.* (1974). Essentially the method is very similar to a weighted pseudo inverse technique where the weights are related to the parameter and measurement noise variances and change at each iteration. The derivation by Collins *et al.* (1974) that has been used by many authors since (for example Robinson, 1982) overlooks the correlation between the current parameter estimates and the measured quantities. Chapter 5 gives the correct equations and considers the minimum variance updating procedure in more detail.

Heylen (1987) introduced a **combined method** which used the equations derived from mass and stiffness orthogonality and also equations from the Taylor series. These equations are combined into one set and solved using a pseudo inverse technique.

Recently Janter *et al.* (1988) developed the **QA model updating** approach. The QA stands for quality (Q) and acceptance (A). The method attempts to make the analytical frequencies converge to the experimental frequencies, to have the experimental mode shapes satisfy the mass and stiffness orthogonality checks (say the off diagonal terms less than 10% of the diagonal terms) and to have the parameters remain inside a user defined range. The solution strategies include linear, quadratic and nonlinear programming approaches. Liefooghe *et al.* (1988) give case studies using this method.

The iterative methods suffer from one major disadvantage. Each iteration of these schemes requires the solution of at least one eigenvalue problem. This difficulty is eased because a reasonable estimate for the new eigendata is available from the previous iteration. The main advantage of the methods is the ability to choose physically meaningful parameters to update thereby helping the engineering design process (Wei *et al.*, 1988).

3.5 Frequency Domain Estimation Methods

This section reviews the techniques available to update the physical parameters of a finite element model using frequency response function data. Most of the methods optimise the equation error or the output error of the structure and these will now be defined using the notation of Chapter 2. The equation error is given by

$$\sum_{k=1}^{N} \left| \left(\mathbf{M}(\theta)\, j\omega_k + \mathbf{K}(\theta) \right) \mathbf{F}_m(\omega_k) - \mathbf{B} \right|^2 \qquad (3.14)$$

where $\mathbf{F}_m$ is the measured frequency response function and ω_k are the measurement frequencies. Equation 3.14 requires that the response is measured at every degree of freedom of the theoretical model. Essentially the equation error is a measure of the difference between the predicted and actual force input into the structure. The output error is given by

$$\sum_{k=1}^{N} \left| \mathbf{F}(\omega_k) - \mathbf{F}_m(\omega_k) \right|^2 . \qquad (3.15)$$

Thus the output error is a measure of the difference between the predicted and actual frequency response functions of the structure. The main disadvantage of the output error approach is that the objective function is always a nonlinear function in the parameters, thus significantly increasing the computational burden and risking divergence of the parameter estimates. Both the equation and output error formulations may also be arranged to use acceleration and force data directly instead of the frequency response functions. Weighting matrices may be included to reflect the relative uncertainty of the forces or FRFs. A number of methods will now be outlined which use a range of error criterion and optimisation techniques.

Mottershead *et al.* (1987 and 1988) minimise the equation error using a filter based on the recursive algorithm of Detchmendy and Sridhar (1966). The

method, which is very similar to a recursive least squares algorithm, was demonstrated using a portal frame rig and seemed to work reasonably well. Mottershead *et al.* (1988) uses increased a priori information about the structure and assumes that the mass matrix is positive definite.

Fritzen (1986) minimises the equation error using least squares and instrumental variable algorithms. Fritzen considers the inaccuracy of the parameters derived from a least squares solution of the equation error is due to bias on the parameters due noise on the observations. The instrumental variable method premultiplies the difference in the predicted and actual force levels by a matrix that is uncorrelated with the measurement noise. This matrix is generated from an additional auxiliary model of the structure which produces an undisturbed output of the system. The resulting parameter estimates are then unbiased and the method seems to work very well. The computational load is certainly higher than the equation error method. Mottershead (1988) applies an instrumental variable method using the filter suggested by Detchmendy and Sridhar (1966).

The simplest method to optimise the output error is to use a nonlinear optimisation algorithm such as Gauss-Newton or quasilinearization (Kalaba and Spingarn, 1982 or Cottin *et al.*, 1984). These methods give good results in the presence of noise but have the disadvantages of the computational burden and convergence problems. Mottershead and Stanway (1986) performed the nonlinear optimisation using a variant of the filter suggested by Detchmendy and Sridhar (1966). The example given in the paper certainly required lengthy computations but no convergence problems seem to have arisen.

Natke (1988) and Santos and Arruda (1990) use a Bayesian or statistical approach applied to the system output error to update the parameters. This method requires the calculation of the sensitivity of the FRFs to the unknown parameters. Hart and Martinez (1982) updated the unknown parameters

using an extended Kalman Filter. To obtain the parameters of a system with a moderate number of DOF this method is likely to require a large amount of computation.

3.6 Time Domain Estimation Methods

Although time domain methods have been used in structural testing to obtain modal models, for example the Ibrahim Time Domain Technique, they have not been used extensively for updating physical structural parameters. The major reason is undoubtedly the extensive computational burden required to update models with many DOF. Time domain methods are used, and preferred to frequency domain methods, in control engineering where the model orders are relatively small. It is unlikely that any of the techniques will be used to update the parameters of a full order finite element models. Reducing the model order by the techniques outlined in Chapter 6 may produce workable algorithms. Roemer and Mook (1990) used a method based on the Eigensystem Realisation Algorithm to obtain condensed mass, stiffness and damping matrices.

Chapter 4

Review and Analysis of Reduced Order Models

4.1 Chapter Summary

This chapter reviews the techniques available to reduce the order of the model of a structure and assesses their suitability to form part of an updating algorithm.

4.2 Philosophy of Order Reduction

Finite element models of realistic structures are generally high order and produce a correspondingly high number of natural frequencies, damping coefficients and mode shapes. The natural frequency of most of these modes will be outside of the frequency range of interest in practical applications. For example, when measurements of the structure are taken using a computerised data acquisition system the resulting frequency response functions (inertance, mobility or receptance) have an upper limit on the usable frequency range determined by the sampling rate through the Nyquist Frequency. Thus it should be possible to reduce the number of degrees of freedom in the theoretical model for little loss of accuracy over the measured frequency range. This assumes sufficient degrees of freedom are included to provide at least the same number of modes, within the frequency range, in the reduced model as were in the original model. The accuracy of the response function of the reduced order model within the frequency range of interest will be improved by including a reasonable number of modes outside the measured frequency range. In many practical applications this would produce enormous savings.

Methods of order reduction have been used extensively in control and filter applications to reduce the cost of designing or implementing a high order controller or filter. The application to structural dynamics is slightly different for two reasons: generally control engineers deal with transfer functions, that is input/output relations, and the models used in control engineering are of

lower order. One requirement for reduced order models for structural dynamics is that the natural frequencies should be invariant. When the full model is predicting the system natural frequencies adequately, the reduced order model should also predict the lower natural frequencies adequately.

4.3 Padé Approximation and Continued Fractions

The oldest and least computationally demanding algorithms are based on Padé approximations or continued fractions, for example Shamash (1975). In the continued fraction method the transfer function is written as a sum and product of continued fractions. This sum is then truncated to produce the reduced order model. From the Routh stability criterion, if the high order system is stable then so is the low order system. The Padé approximation basically truncates the power series expansion of the transfer function in terms of the Laplace variable s. Shamash (1975) combined the continued fraction and Padé approximation methods to guarantee the stability of the reduced order model. These methods are not suitable to reduce the order of structural models for two reasons: they use the input/output transfer functions not the model matrices and they alter the eigenvalues, or natural frequencies, of the system. The eigenvalues can usually be measured quite accurately and the continued fraction method will change the lower eigenvalues by a small but significant amount. For example, consider a system with the following transfer function

$$G(s) = \frac{1}{s^4 + 0.1\,s^3 + 10\,s^2 + s + 9}$$

where s is the Laplace variable. The eigenvalues of this system are -0.0562 $\pm$ 0.998 j and 0.0062 $\pm$ 3.000 j. Applying the reduction technique outlined by Shamash (1975) gives the reduced transfer function

$$R(s) = \frac{1}{9.1\,s^2 + s + 9} \quad .$$

The eigenvalues of the reduced system are -0.0549 ± 0.993, which are quite close but not equal to the lower eigenvalues of the full order system.

4.4 Static and Dynamic Condensation

Static condensation, for example Guyan (1965) and Irons (1965), has been used to reduce the order of static structural problems. Equations that do not include an external force term are used to eliminate spatial variables. Generally these methods must be handled with extreme care as important natural frequencies may be changed considerably, or omitted altogether (Thomas 1982). Static condensation is most effective when the coordinates that are eliminated are associated with low mass or high stiffness (Urgueira *et al.*, 1990). Consider, for example, Guyan reduction. The state or co-ordinate vector $\mathbf{x}$ is split into two parts: the master co-ordinates $\mathbf{x}_1$ to be retained and the slave co-ordinates $\mathbf{x}_2$ to be eliminated. To use the Guyan reduction method there must not be any force applied to the slave co-ordinates. The undamped equations of motion are then

$$\begin{bmatrix} \mathbf{M}_{11} & \mathbf{M}_{12} \\ \mathbf{M}_{21} & \mathbf{M}_{22} \end{bmatrix} \begin{Bmatrix} \ddot{\mathbf{x}}_1 \\ \ddot{\mathbf{x}}_2 \end{Bmatrix} + \begin{bmatrix} \mathbf{K}_{11} & \mathbf{K}_{12} \\ \mathbf{K}_{21} & \mathbf{K}_{22} \end{bmatrix} \begin{Bmatrix} \mathbf{x}_1 \\ \mathbf{x}_2 \end{Bmatrix} = \begin{Bmatrix} \mathbf{F}_1 \\ 0 \end{Bmatrix} \qquad (4.1)$$

where the $\mathbf{M}_{ij}$ and $\mathbf{K}_{ij}$ are submatrices of the full order mass and stiffness matrices and $\mathbf{F}_1$ is the force applied to the master co-ordinates. The slave co-ordinates are eliminated using the transformation $\mathbf{T}$ derived from the static equations which is given by

$$\begin{Bmatrix} x_1 \\ x_2 \end{Bmatrix} = \begin{bmatrix} I \\ -K_{22}^{-1} K_{21} \end{bmatrix} x_1 = T x_1 \quad . \qquad (4.2)$$

Using this transformation the reduced mass and stiffness matrices M_R and K_R are given, with reference to the master co-ordinates, by

$$M_R = T^T \begin{bmatrix} M_{11} & M_{12} \\ M_{21} & M_{22} \end{bmatrix} T \qquad K_R = T^T \begin{bmatrix} K_{11} & K_{12} \\ K_{21} & K_{22} \end{bmatrix} T \qquad (4.3)$$

Consider the simple mass spring system shown in figure 4.1. The first three eigenvalues, or natural frequencies squared, for this system are 58.1, 503.0 and 1290.8 $(rad/s)^2$. Suppose we eliminate the displacement of the sixth mass by Guyan reduction. The first three eigenvalues of the reduced model are 59.1, 559.3 and 1535.8 $(rad/s)^2$. Alternatively eliminating the displacement of the fifth mass gives eigenvalues of 58.6, 510.0 and 1299.2 $(rad/s)^2$. The result for the first eigenvalue is quite good but even so, because natural frequencies can be measured very accurately, Guyan reduction is not suitable as a method of order reduction. Also notice that the choice of master and slave co-ordinates makes a considerable difference to the quality of the eigenvalues of the reduced model.

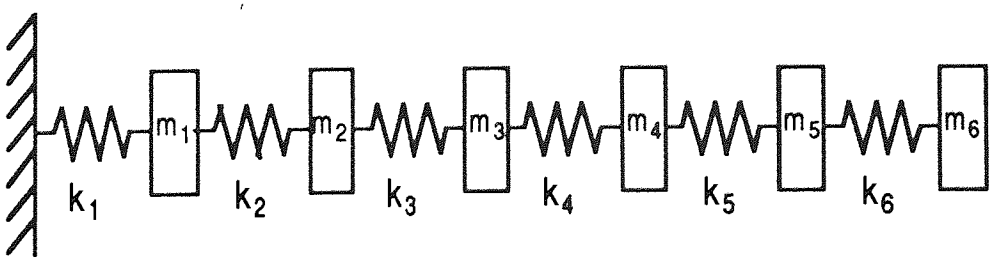

$m_i = 1$ kg $\qquad k_i = 1000$ N/m $\qquad i = 1, . . , 6$

Figure 4.1 Simple Discrete Mass and Spring System

Paz (1984) suggested a method of dynamic condensation that is really limited to solving the theoretical eigenproblem. The technique is iterative and reduces the full order mass and stiffness matrices to reduced matrices using a transformation based on the latest frequency estimate.

4.5 Modal Truncation

Modal truncation, or reducing the model order by retaining only the modes with the lowest natural frequencies, is slightly more complex and computationally more demanding. The state vector is transformed using the matrix consisting of an incomplete set of eigenvectors. The transformation and resulting equations are very similar to equations 2.12 and 2.13 which used the complete set of eigenvectors. Modal truncation has the advantage that the lower natural frequencies remain unchanged and providing that enough modes are included the reduced model can approximate the full model sufficiently accurately. This method shows the most promise and is developed further in Chapter 6.

Modal truncation has been refined to allow a choice of master and slave co-ordinates and is called the System Equivalent Reduction Expansion Process (SEREP) (O'Callahan *et al.*, 1989). The method has been used for a wide variety of tasks including forced response calculations, estimation of rotational dofs (O'Callahan *et al.*, 1986) and orthogonality checks between theoretical and experimental models.

4.6 Balanced Realisations and Hankel Norms

There has been considerable interest recently on methods based on balanced realisations and the Hankel singular values of a system. Moore (1981) proposed the balanced realisation approach based on the transformation

given by Laub (1980). Glover (1984) develops optimal Hankel-norm approximations for multivariable systems. These methods of reduction are inappropriate for the identification of structural parameters for three reasons. First, the large dimension of a finite element model makes the computation times involved prohibitive. Second, the methods do not allow for unknown parameters. The linearisation of the equations and the solution of a series of balanced realisations or Hankel-norm approximations could extend the methods at the expense of additional computation. Finally the lower eigenvalues of the system are not guaranteed to remain unchanged although for structural models with light damping the lower eigenvalues effectively remain unchanged. Thus for practical structural systems, providing there are more degrees of freedom than identifiable modes, the reduced order model would accurately reproduce the full model in the frequency range of interest. As an example consider the application of Moore's algorithm (Moore, 1981) to the six DOF mass and spring system of figure 4.1. Reducing the number of DOF in the system to five gives values for the first three eigenvalues of 58.1, 503.0 and 1292.2 $(rad/s)^2$. These values closely reproduce those from the full order model, which are 58.1, 503.0 and 1290.8 $(rad/s)^2$. Notice that the lower eigenvalues are most accurate.

Chapter 5

A New Minimum Variance Estimation Algorithm

5.1 Chapter Summary

This chapter outlines a corrected statistical updating method. Currently one of the most popular updating methods uses a minimum variance updating algorithm. Unfortunately these algorithms assume that the experimental data and the current parameter estimates are statistically independent. This will be the case for the first updating iteration but not subsequently. The method given in this Chapter converges faster and to more correct results than the incorrect minimum variance algorithm. Natural frequencies are always measured more accurately than mode shape data, and they are also more sensitive to parameter changes. Thus natural frequencies are more useful inputs to parameter updating algorithms.

5.2 Updating Procedure

The method for updating an analytical or prior model of a structure using the minimum variance unbiased estimator based on the incomplete measurement of the modal model is now described. Much of the detailed derivation of the expressions given in this section is outlined in Appendix E. The notation is summarised in Appendix A and Chapter 2. Damping is assumed to be negligible although the method is easily extended to the general or proportional damping cases.

The real, symmetric mass and stiffness matrices $\mathbf{M}_n$ and $\mathbf{K}_n$ depend in a predetermined way on the vector of the p parameters to be updated θ. Thus

$$\mathbf{K}_n = \mathbf{K}_n(\theta) \qquad \mathbf{M}_n = \mathbf{M}_n(\theta) \quad . \tag{5.1}$$

$\mathbf{K}_n$ and $\mathbf{M}_n$ are the analytical matrices which define the assumed dependence of the mass and stiffness matrices on the chosen unknown parameters θ. If $\mathbf{x}$ is the displacement of the structure at the n

co-ordinates defined by the analytical model then the equation for free vibration is

$$\mathbf{M}_n(\theta)\,\ddot{\mathbf{x}} + \mathbf{K}_n(\theta)\,\mathbf{x} = 0 \tag{5.2}$$

In general a model of the structure contains many more degrees of freedom than measured points. If $\mathbf{y}$ is the vector of the m (< n) measurements predicted by the theoretical model then

$$\mathbf{y} = \mathbf{C}\,\mathbf{x} \tag{5.3}$$

for some (m,n) matrix $\mathbf{C}$. Note that the matrix $\mathbf{C}$ is NOT damping. Usually the measurements will be taken at selected points of the structure relating to nodes of the model. Then $\mathbf{C}$ will mainly consist of zeros with 1s where necessary to pick out the required position.

Suppose that the first r natural frequencies and/or modes are measured. Let μ_{mi} and $\mathbf{v}_{mi}$ for $i = 1, \ldots, r$ denote these measurements where μ_{mi} denotes minus natural frequency squared. These will correspond to the analytically derived frequencies and modes which are given by

$$\left(\mathbf{M}_n(\theta)\,\mu_i + \mathbf{K}_n(\theta)\right)\,\psi_i = 0 \tag{5.4}$$

$$\mathbf{v}_i = \mathbf{C}\,\psi_i \tag{5.5}$$

The natural frequencies and modes can be assembled into a measurement vector $\mathbf{z}$ where

$$\mathbf{z}^T = \left(\mu_1, \mathbf{v}_1^T, \mu_2, \ldots, \mu_r, \mathbf{v}_r^T\right)^T \tag{5.6}$$

and similarly for the measured quantities

$$\mathbf{z}_m^T = \left(\mu_{m1}, \mathbf{v}_{m1}^T, \mu_{m2}, \ldots, \mu_{mr}, \mathbf{v}_{mr}^T\right)^T \tag{5.7}$$

Although this suggests that the number of eigenvalues and mode shapes must be equal this is not necessary and $\mathbf{z}$ may contain any information available. Usually mode shape data is used only to relate theoretical modes to the experimental modes using, for example, the Modal Assurance Criterion (Section 3.1). Mode shape data may be included in statistical updating algorithms although their influence will be small because of the high variances assigned to them. If more than one experiment were undertaken two or more measurements of the same quantity could be included. Whatever data is contained in the vector $\mathbf{z}_m$ the information in $\mathbf{z}$ must correspond with it. $\mathbf{z}$ and $\mathbf{z}_m$ will not be equal due to measurement noise, which in this case includes errors which cannot be accounted for within the analytical model given by equations (5.1), (5.2) and (5.3). Thus

$$\mathbf{z}_m^T = \mathbf{z}^T + \varepsilon \tag{5.8}$$

where ε is the measurement noise with

$$E[\varepsilon] = 0 \qquad Var(\varepsilon) = E[\varepsilon^T \varepsilon] = V_\varepsilon \tag{5.9}$$

where $E[\ ]$ denotes the expected value. Let θ_0 be the original estimate of the unknown mass and stiffness parameters, for example from a finite element analysis. Assume that the mean and covariance of θ_0 are

$$E[\theta_0] = \theta \qquad Var(\theta_0) = V_0 \tag{5.10}$$

The object is to produce an iterative method to provide successive, improved estimates θ_j of the parameters θ. The method proposed linearises the system about the current parameter estimate and updates the parameter estimate using this approximation.

Let the current estimate be θ_j with corresponding modal properties at the measurement locations $\mathbf{z}_j$ and variance $\mathbf{V}_j$. If the difference between the current estimate and the actual parameters is small then truncating the Taylor expansion for $\mathbf{z}$ after the first order term gives

$$\mathbf{z} = \mathbf{z}_j + \mathbf{H}_j (\theta - \theta_j) \tag{5.11}$$

$$\text{where} \quad [\mathbf{H}_j]_{ks} = \frac{\partial \{\mathbf{z}\}_k}{\partial \{\theta\}_s} \quad \text{evaluated at } \theta = \theta_j \tag{5.12}$$

and $\mathbf{z}(\theta)$ is given by equations (5.4) - (5.6).

The form of $\mathbf{H}_j$ will be discussed later.

Although the initial parameter estimate and the measurement error are independent, subsequent parameter estimates are not since the measurements would have been used in the updating process. This has been overlooked in previous papers (for example Collins *et al.*, 1974) resulting in an unbiased but not minimum variance estimator.

$$\text{Let} \quad E[\, \theta_j \, \varepsilon \,] = \mathbf{D}_j \quad \text{and assume} \quad \mathbf{D}_0 = \mathbf{0} \tag{5.13}$$

Thus $\mathbf{D}_j$ is the correlation matrix between the j th parameter estimate and the measurement noise. Suppose that the updated parameter estimate θ_{j+1} using the prior estimate θ_j is

$$\theta_{j+1} = \theta_j + \mathbf{T} (\mathbf{z}_m - \mathbf{z}_j) \tag{5.14}$$

where $\mathbf{T}$ is a matrix to be determined. Then (see Appendix E for details)

$$E[\theta_{j+1}] = E[\theta_j] = \theta \qquad (5.15)$$

And the covariance of the new parameter estimate is (Appendix E), using equation 5.14,

$$\mathbf{V}_{j+1} = \mathbf{V}_j + \left(\mathbf{D}_j - \mathbf{V}_j\mathbf{H}_j^T\right)\mathbf{T}^T + \mathbf{T}\left(\mathbf{D}_j^T - \mathbf{H}_j\mathbf{V}_j\right) + \mathbf{T}\,\mathbf{V}_{zj}\mathbf{T}^T \qquad (5.16)$$

where

$$\mathbf{V}_{zj} = \mathbf{H}_j\,\mathbf{V}_j\,\mathbf{H}_j^T - \mathbf{H}_j\,\mathbf{D}_j - \mathbf{D}_j^T\,\mathbf{H}_j^T + \mathbf{V}_\varepsilon \quad . \qquad (5.17)$$

Minimising the covariance of the new parameter estimate $\mathbf{V}_{j+1}$ with respect to $\mathbf{T}$ gives

$$\mathbf{T} = \left(\mathbf{V}_j\mathbf{H}_j^T - \mathbf{D}_j\right)\mathbf{V}_{zj}^{-1}$$

and thus the minimum variance unbiased estimator θ_{j+1} is

$$\theta_{j+1} = \theta_j + \left(\mathbf{V}_j\mathbf{H}_j^T - \mathbf{D}_j\right)\mathbf{V}_{zj}^{-1}\left(\mathbf{z}_m - \mathbf{z}_j\right) \quad . \qquad (5.18)$$

The parameter estimate/measurement noise correlation matrix, $\mathbf{D}_j$, and the covariance of the parameter estimate, $\mathbf{V}_j$, may be updated by (Appendix E)

$$\mathbf{D}_{j+1} = \mathbf{D}_j - \left(\mathbf{V}_j\mathbf{H}_j^T - \mathbf{D}_j\right)\mathbf{V}_{zj}^{-1}\left(\mathbf{H}_j\mathbf{D}_j - \mathbf{V}_\varepsilon\right) \qquad (5.19)$$

$$\mathbf{V}_{j+1} = \mathbf{V}_j - \left(\mathbf{V}_j\mathbf{H}_j^T - \mathbf{D}_j\right)\mathbf{V}_{zj}^{-1}\left(\mathbf{V}_j\mathbf{H}_j^T - \mathbf{D}_j\right)^T \qquad (5.20)$$

The iterations defined by equations (5.19) and (5.20) are initiated using the estimated analytical parameter variance $\mathbf{V}_0$ and the definition in equation (5.13), $\mathbf{D}_0 = \mathbf{0}$. Due to the large number of equations required to derive the estimation procedure the actual algorithm is somewhat obscured. Figure 5.1 shows a flow chart of the steps defined by the above equations and forms the basis of the algorithm used in the examples which follow. Note that if the

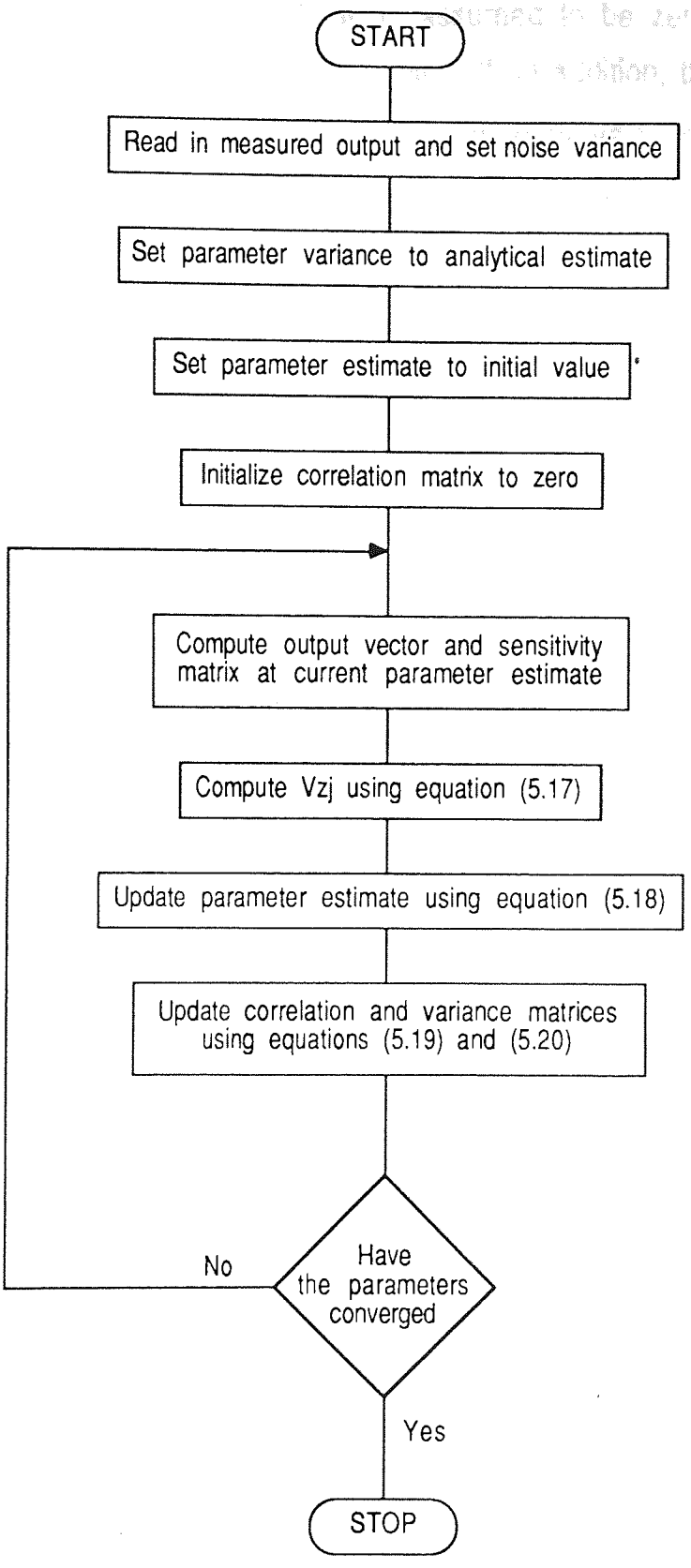

Figure 5.1 Flow Chart Showing the Parameter Updating Procedure

variance of the measurement noise is assumed to be zero (that is no measurement noise) then $\mathbf{D}_j = \mathbf{0}$ for all j. If, in addition, the number of parameters is less than the number of measurements then $\mathbf{V}_{zj}$ will be singular. Thus the algorithm breaks down and the parameters are likely to diverge. In this case a pseudo inverse solution based on the sensitivity equation 5.11 could be used.

Before discussing practical aspects of the method the relationship between the minimum variance estimator and the least squares estimator will be explored. Least squares estimators are derived by minimising a cost function which is a weighted sum of square terms. Let the cost function to be minimised be

$$J(\theta) = \varepsilon \mathbf{W}_\varepsilon \varepsilon^T + \left(\theta - \theta_j\right)^T \mathbf{W}_\theta \left(\theta - \theta_j\right) \tag{5.21}$$

where $\mathbf{W}_\varepsilon$ and $\mathbf{W}_\theta$ are weighting matrices. Then using equations (5.8) and (5.11) to express the measurement noise in terms of the parameters to be estimated and minimising $J(\theta)$ produces (see Appendix E) the least squares estimate θ_{j+1} as

$$\theta_{j+1} = \theta_j + \left[\mathbf{H}_j^T \mathbf{W}_\varepsilon \mathbf{H}_j + \mathbf{W}_\theta\right]^{-1} \mathbf{H}_j^T \mathbf{W}_\varepsilon \left(\mathbf{z}_m - \mathbf{z}_j\right) \tag{5.22}$$

which is the minimum variance unbiased estimator providing the weighting matrices vary with each iteration and are given by (see Appendix E)

$$\mathbf{W}_\varepsilon = \mathbf{V}_{zj}^{-1} \tag{5.23}$$

$$\mathbf{W}_\theta \left(\mathbf{V}_j \mathbf{H}_j^T - \mathbf{D}_j\right) = - \mathbf{H}_j^T \mathbf{V}_{zj}^{-1} \left(\mathbf{H}_j \mathbf{D}_j - \mathbf{V}_\varepsilon\right)^T \tag{5.24}$$

Notice that $\mathbf{W}_\theta$ requires the calculation of a psuedo inverse, the form of

which will depend on the number of parameters to be updated compared to the number of measurements.

5.3 Practical Considerations

One of the major steps in the algorithm is the calculation of the sensitivity matrices $\mathbf{H}_j$ which are defined by equation (5.12). This computation involves the evaluation of the derivative of the system eigenvalues and mode shapes given by equations (5.4) and (5.5) with respect to the individual parameters evaluated at the current parameter estimates. Many algorithms to calculate these derivatives have been given in the literature and are reviewed in Section 2.5.2. The derivative of the mode shape is related to the derivative of the eigenvector by

$$\frac{\partial \mathbf{v}_i}{\partial \{\theta\}_s} = \mathbf{C} \frac{\partial \psi_i}{\partial \{\theta\}_s} \quad . \tag{5.25}$$

If the measurement vector can be partitioned into independent sub vectors then the proposed method may be applied successively to each sub vector starting with the latest parameter estimate and parameter variance. Thus the order of the matrix inversion in equations (5.18) - (5.20) can be reduced. Any potential savings in computer time will depend on the eigensystem extraction algorithm used. For example, suppose three natural frequencies of a system are measured. The unknown parameters are updated using the first natural frequency alone. On convergence the second natural frequency is used to update the parameters, and so on. Thus the eigensystem extraction algorithm must compute a single eigenvalue / eigenvector pair efficiently. If eigenvalues and mode shapes are measured repeatedly, it will always be quicker to average the measured data prior to input into the updating algorithm.

5.4 A Simple Numerical Example

A two degree of freedom example will be used to demonstrate the proposed method. Although very simple, this example highlights the problems in neglecting the correlation between the estimated parameters and the measurement noise.

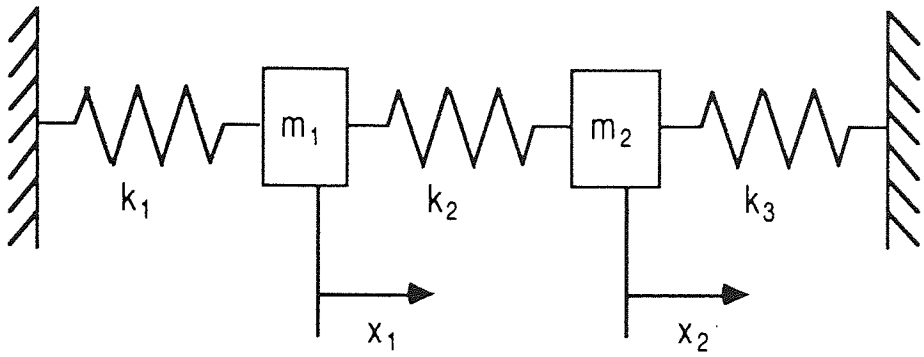

$$\mathbf{M}_n = \begin{bmatrix} m_1 & 0 \\ 0 & m_2 \end{bmatrix} \qquad \mathbf{K}_n = \begin{bmatrix} k_1 + k_2 & -k_2 \\ -k_2 & k_2 + k_3 \end{bmatrix}$$

Figure 5.2 Example Two dof System

Figure 5.2 shows the system and the form of the mass and stiffness matrices. Assume that the values of the masses m_1 and m_2 are known accurately and are 4 kg and 9 kg respectively. The prior estimates of k_1, k_2 and k_3 are

$$k_1 = 130 \text{ N/m} \quad k_2 = 50 \text{ N/m} \quad k_3 = 220 \text{ N/m}$$

giving eigenvalues of 26.3 s^{-2} and 48.7 s^{-2}. Assume these estimates are independent with variances of 10 $(N/m)^2$. Hence

$$\mathbf{V}_0 = \begin{bmatrix} 10 & 0 & 0 \\ 0 & 10 & 0 \\ 0 & 0 & 10 \end{bmatrix}$$

Only the eigenvalues of the system are measured. The assumed eigenvalue measurements are independent with values of 25 s^{-2} and 50 s^{-2}. The measurement noise variances for the two eigenvalues are assumed to be equal but will be changed to demonstrate different features. The eigenvalues are derived from a system with spring constant values of

$$k_1 = 120 \text{ N/m} \quad k_2 = 60 \text{ N/m} \quad k_3 = 210 \text{ N/m}$$

The estimated parameters are unlikely to converge to these parameters even with no measurement noise because the measured eigenvalues can be produced by an infinite number of alternative spring constant values.

The convergence criterion is taken to be the maximum absolute percentage change in the individual parameters from one iteration to the next. The initial value of the parameter estimate/measurement noise correlation $\mathbf{D}_0$ is zero as the analytical parameter estimate and the measurement noise are assumed to be independent.

If the measurement noise variance is taken to be 0.1 s^{-4} then on convergence (using a convergence criterion of 10^{-3} %) the parameter vector and parameter covariance matrix (after 5 iterations) are

$$\theta_5 = \begin{bmatrix} 129.8 \\ 53.8 \\ 213.6 \end{bmatrix} \qquad \mathbf{V}_5 = \begin{bmatrix} 7.2 & -3.9 & -1.4 \\ -3.9 & 2.9 & 0.46 \\ -1.4 & 0.46 & 5.7 \end{bmatrix}$$

with an output of

$$z_5 = \begin{bmatrix} 25.7 \\ 49.9 \end{bmatrix}$$

The correlation matrix between the new parameter estimate and the measurement vector is

$$D_5 = \begin{bmatrix} 0.109 & 0.128 \\ 0.205 & -0.089 \\ -0.027 & 0.473 \end{bmatrix} .$$

The parameter variances have been reduced as would be expected with more information available. The measured eigenvalues yield most information about k_2 and least about k_1. This may be seen from the relative reductions in the parameter variances and the relative magnitudes of the parameter changes. The off diagonal terms in the covariance matrix have become quite large and show that the parameter estimates are no longer independent of each other. This is expected as the individual parameter updates have used the same measured information. The updated parameters have also become correlated with the measurements. Figure 5.3 shows the values of the parameters after each of the 5 iterations and indicates that almost all of the change in the parameters occurs during the first iteration. Similar plots for the elements of the parameter variance, parameter/measurement correlation and the estimated output vector would indicate that all the visible change occurs in the first iteration.

If the correlation between the parameter estimates and the measurement noise is set to zero at each iteration to simulate previous author's methods, for example Collins *et al.* (1972 and 1974) and Thomas *et al.* (1986), then the results are very different. With the same noise variance and convergence criterion as the previous example the estimated parameter vector and parameter covariance matrix (after 85 iterations) are

$$\theta_{85} = \begin{bmatrix} 128.1 \\ 55.5 \\ 206.5 \end{bmatrix} \qquad V_{85} = \begin{bmatrix} 6.8 & -3.9 & -2.5 \\ -3.9 & 2.3 & 1.4 \\ -2.5 & 1.4 & 1.1 \end{bmatrix}$$

with an output of

$$z_{85} = \begin{bmatrix} 25.0 \\ 50.0 \end{bmatrix} .$$

The most important feature shown in this example is that the output vector computed from the estimated parameters, or eigenvalues in this case, converges to the measured output vector even in the presence of measurement noise. This phenomenon also occurred in the papers by Collins *et al.* (1972) and Thomas *et al.* (1986) and effectively the method is assuming a zero measurement noise variance. The estimation algorithm should weight the prior model and the measurement to obtain a compromise model which will not reproduce the measured output unless there is no measurement noise. Thus methods neglecting the correlation between the parameters and the measurements ultimately converge to an incorrect solution. Using these methods the first iteration gives the same result as the method described in this chapter and produces a reasonable parameter estimate in this example.

The large difference in the number of iterations required show that the rate of convergence is very much slower when the correlation between the parameter estimates and measurement noise is neglected. This is highlighted in figure 5.4 by plotting the changes in the values of the parameters as the iteration progresses. The rate of convergence is extremely slow compared to that plotted in figure 5.3 derived by the algorithm described in this chapter. Figure 5.5 shows the convergence of elements of the parameter variance.

Returning to the algorithm proposed in this chapter, the effect on the output produced by the estimated model, due to the relative magnitudes of the prior

parameter estimate variance and the measurement noise variance can easily be demonstrated. Figure 5.6 shows the effect of measurement noise variance on the two eigenvalues produced by the updated model after the algorithm has converged. As may be expected as the noise variance reduces the model output becomes closer to the measured output. Figure 5.7 shows the effect of measurement noise on the updated parameter values after the algorithm has converged as a percentage of the assumed analytically derived values. As expected if the measurement noise variance is large then the parameters do not change significantly from their initial values. Figure 5.8 shows the effect of measurement noise variance on the variance of the parameters updated by the algorithm. Although the variance of the updated parameters broadly reduces as the measurements become more accurate some discontinuities are obvious in the plots. These discontinuities, also visible in figures 5.6 and 5.7, show that the estimation process is non-linear. This may be compared with the Newton-Raphson method for minimising a non-linear function. For different initial values of the independent variables the Newton-Raphson algorithm may converge to different local minima. Since the decision to converge to one local minima or another occurs at a saddle point a discontinuity will appear in a graph of initial value of the independent variable against the minimum value of the function. The algorithm in this chapter is slightly different because the initial parameter value is constant. Changing the assumed measurement noise variance effectively alters the function to be minimised. Although the updated parameter values and variances are most sensitive to the non-linear nature of the algorithm, discontinuities can just be seen in the plots of the output vector and the parameter/measurement noise correlation, figures 5.6 and 5.9 respectively.

5.5 Pin Jointed Frame Example

The method will now be used to update the stiffness parameters of a pin jointed frame. The ten degree of freedom frame arrangement is shown in

figure 5.10 and consists of ten beams. Each beam has a mass of 1 kg per metre length and the horizontal and vertical beams are 1 m long. The stiffness of the equivalent unit length beams, or equivalently the product of the Young's Modulus and cross-sectional area of the beam EA_i, will be updated. The effective stiffness of an actual beam is found by dividing this parameter by the beam's length. Initially all these parameters are equal and have a value of 3×10^7 N with a standard deviation of 1×10^6 N. Only the first two natural frequencies and mode shapes are measured. The output vector consists of the vertical displacements and so the measurement vector has twelve elements. Numerically the output vector based on the initial parameters and the assumed measurement vector are

$$\mathbf{z}_0 = (580.8, 0.179, 0.381, 0.151, 0.367, 0.539, 1931.3, 0.447, 0.004, 0.396, 0.066, -0.578)^T$$

$$\mathbf{z}_m = (576.0, 0.186, 0.388, 0.172, 0.377, 0.506, 1931.9, 0.420, -0.006, 0.387, 0.072, -0.580)^T$$

Thus the measured natural frequencies are 576.0 and 1931.9 rad/s. These correspond to computed natural frequencies based on the initial parameters of 580.8 and 1931.3 rad/s.

Suppose that the natural frequency and mode shape co-ordinate measurements are independent with standard deviations of 2 and 0.02 rad/s respectively. The measured output vector was obtained by adding noise with the above standard deviations to the output of a simulated system using the following parameter values

$EA_1 = 3.04 \times 10^7$ N $\quad EA_2 = 2.98 \times 10^7$ N $\quad EA_3 = 2.96 \times 10^7$ N

$EA_4 = 2.96 \times 10^7$ N $\quad EA_5 = 3.22 \times 10^7$ N $\quad EA_6 = 2.95 \times 10^7$ N

$EA_7 = 2.88 \times 10^7$ N $\quad EA_8 = 2.91 \times 10^7$ N $\quad EA_9 = 3.07 \times 10^7$ N

$EA_{10} = 3.00 \times 10^7$ N

After the algorithm has converged the updated parameters are

$EA_1 = 3.168 \times 10^7$ N $\quad EA_2 = 3.250 \times 10^7$ N $\quad EA_3 = 3.180 \times 10^7$ N

$EA_4 = 3.142 \times 10^7$ N $\quad EA_5 = 3.249 \times 10^7$ N $\quad EA_6 = 3.157 \times 10^7$ N

$EA_7 = 3.119 \times 10^7$ N $\quad EA_8 = 3.135 \times 10^7$ N $\quad EA_9 = 3.194 \times 10^7$ N

$EA_{10} = 3.108 \times 10^7$ N

which produces an output of

$$\mathbf{z} = (576.8, 0.179, 0.381, 0.152, 0.367, 0.538, 1931.7, 0.447, 0.003, 0.396, 0.065, -0.578)^T$$

The natural frequencies of the system with the updated parameters are close to measured values but the mode shape elements are very close to the values obtained using the original analytical parameters. This is because the frequencies are measured far more accurately than the mode shape elements. This is reflected in the frequency and mode shape variances. Also the natural frequencies are more sensitive than mode shapes to parameter changes. Thus natural frequencies are always more useful in updating algorithms than mode shapes. The measured mode shapes are in fact compatible to the analytical modes based on the initial parameter values. The Modal Assurance Criterion Matrix between the measured and analytical mode shapes is

$$MAC = \begin{bmatrix} 0.997 & 0.057 \\ 0.031 & 0.999 \end{bmatrix}$$

The Modal Assurance Criterion Matrix between the measured and updated analytical mode shapes is also equal to this matrix to 3 decimal places. The

increase in quality of the updated parameters may be seen from their standard deviations which in this case are

$$10^{6} \times (0.883, 0.533, 0.561, 0.987, 0.984, 0.952, 0.949, 0.994, 0.971, 0.992)\ N$$

EA_2 and EA_3 have been obtained most accurately but the quality of the other estimates has hardly improved. Physically EA_2 and EA_3 strongly influence the first two modes which are shown in figure 5.11.

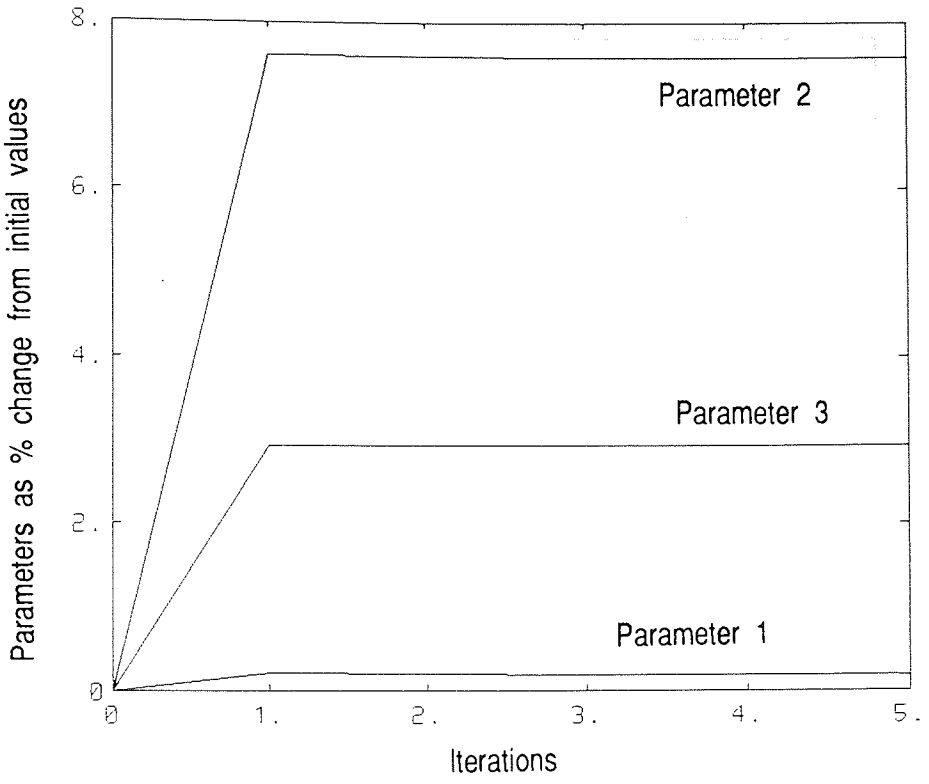

Figure 5.3 Convergence of Parameter Estimates

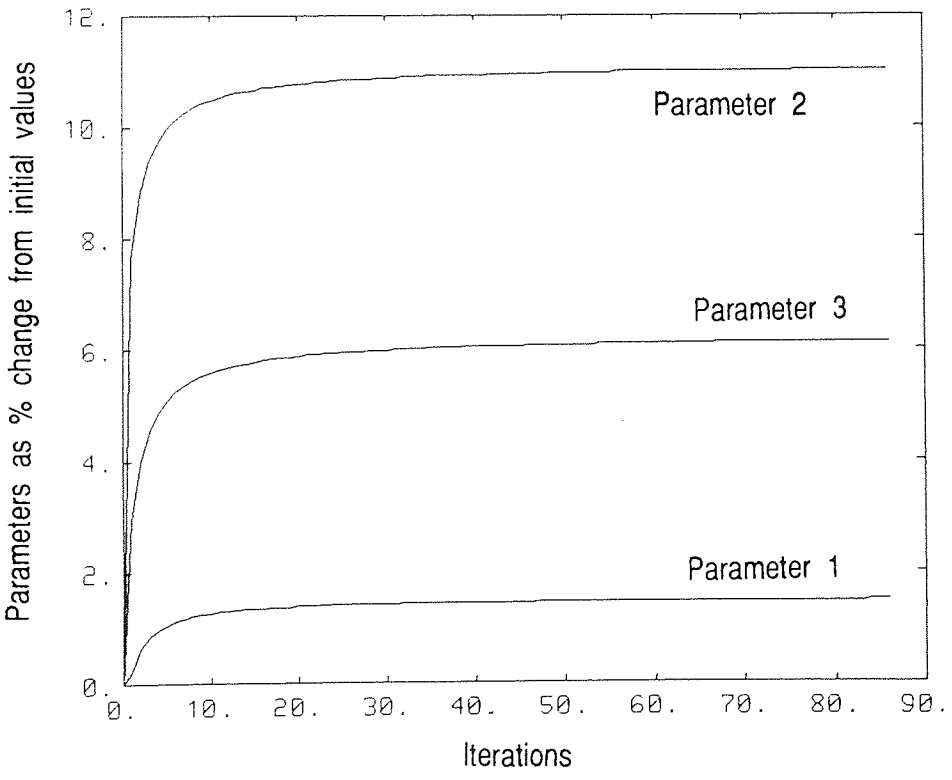

Figure 5.4 Convergence of Parameter Estimates (Parameter to Noise Correlation Ignored)

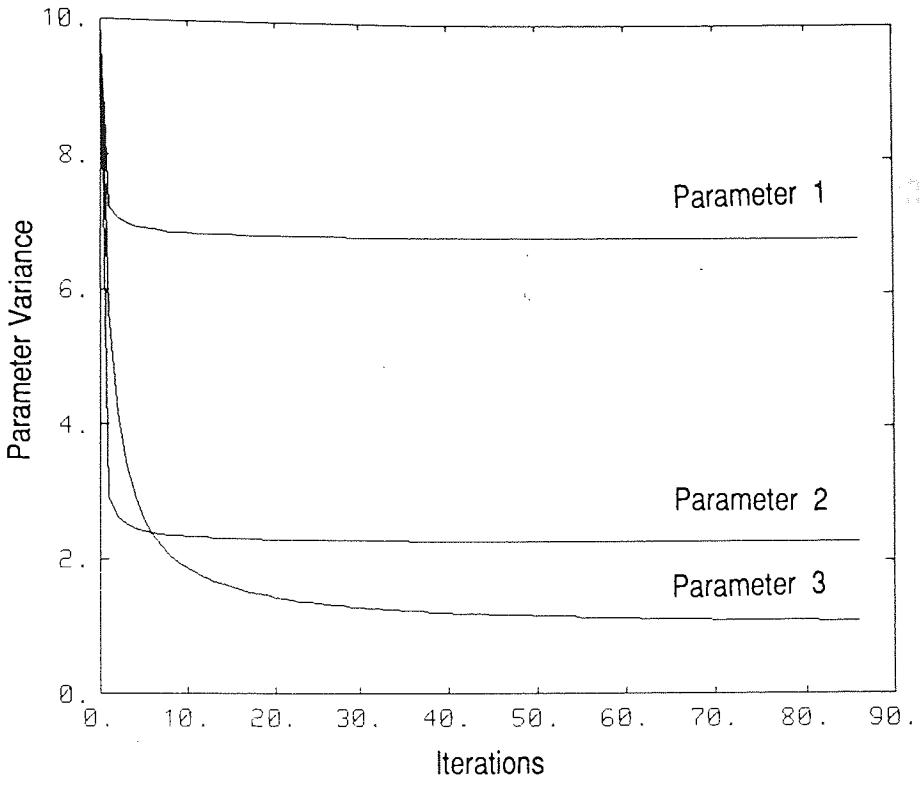

Figure 5.5 Convergence of Parameter Variances (Parameter to Noise Correlation Ignored)

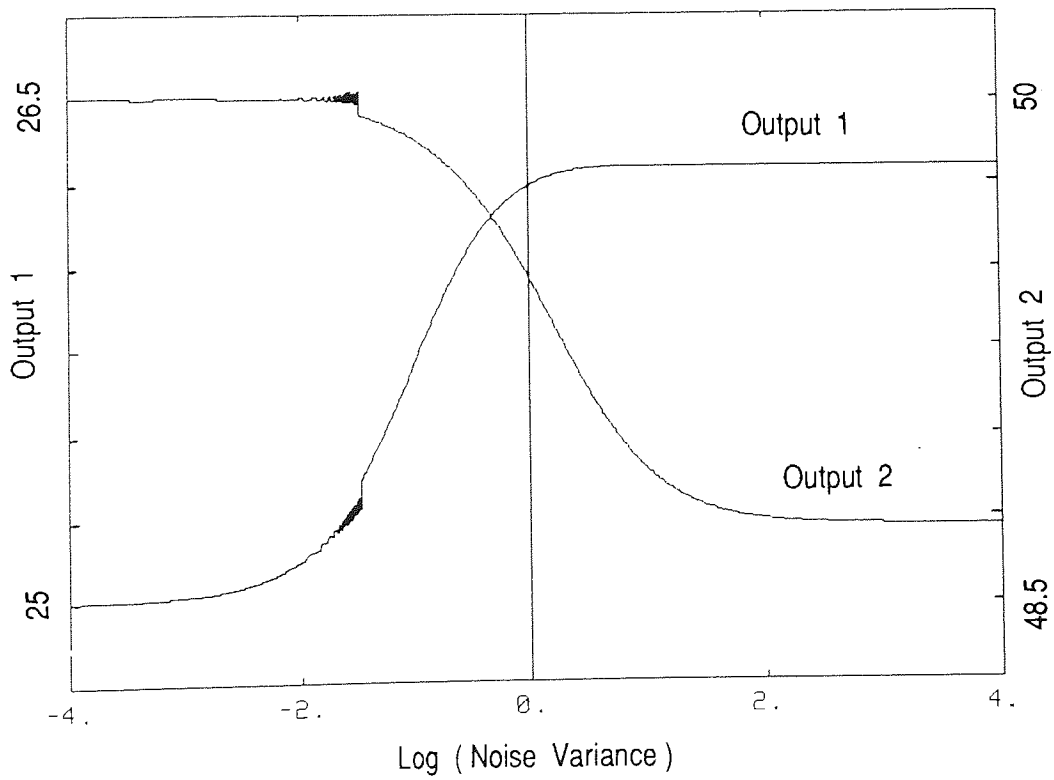

Figure 5.6 The Effect of Measurement Variance on the Estimated System Output

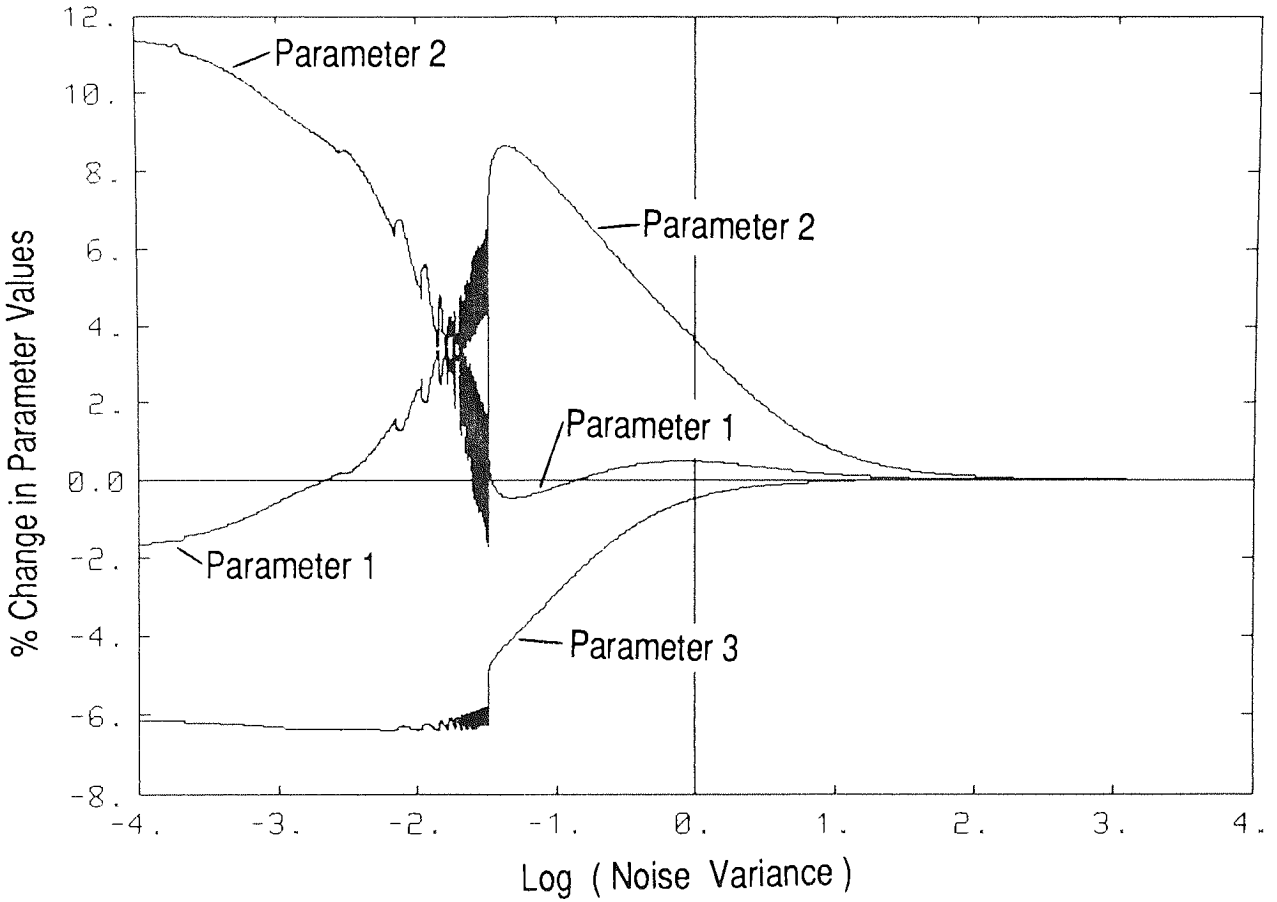

Figure 5.7 The Effect of Measurement Variance on the Updated Parameter Values

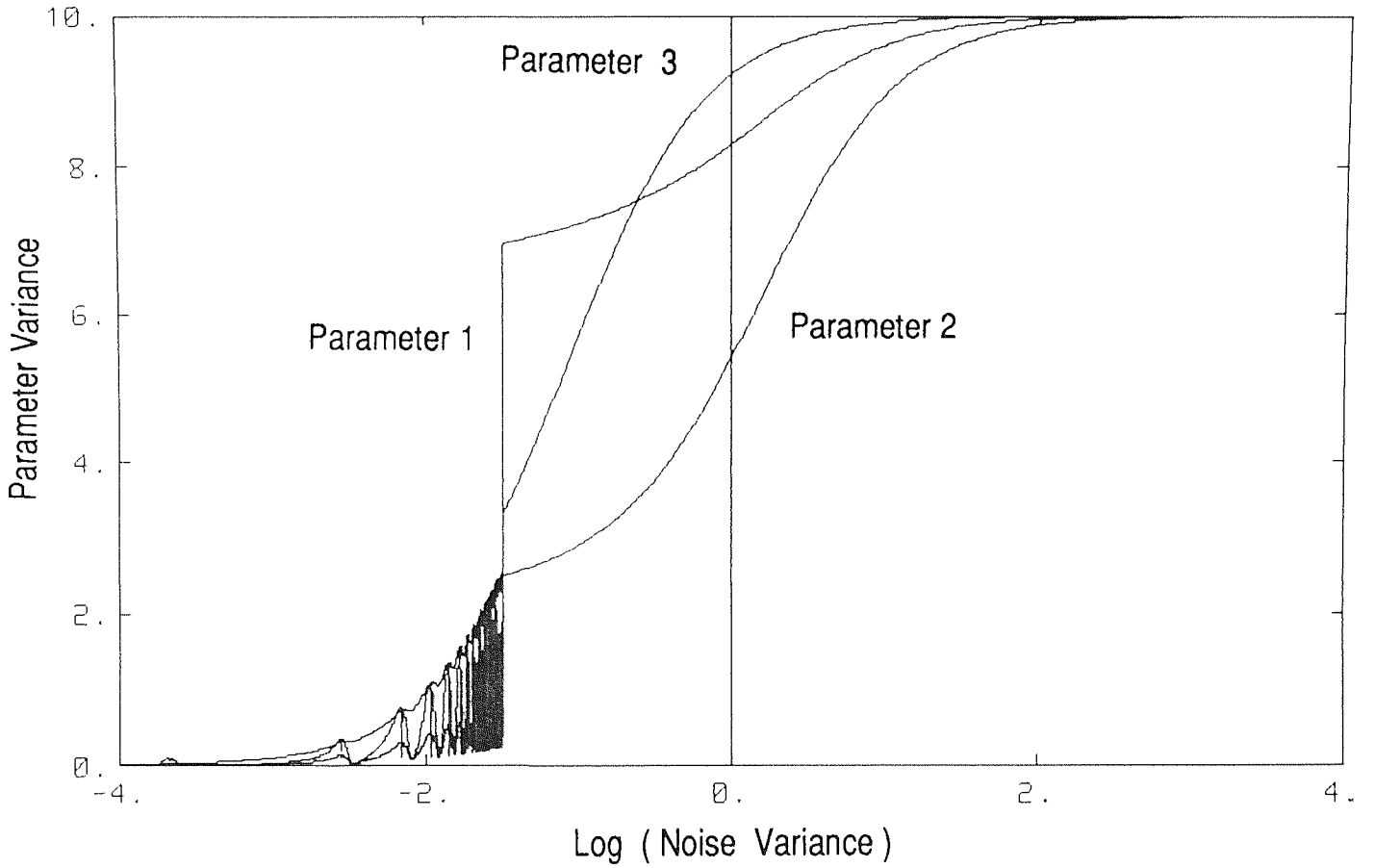

Figure 5.8 The Effect of Measured Noise Variance on the Parameter Variance after Convergence

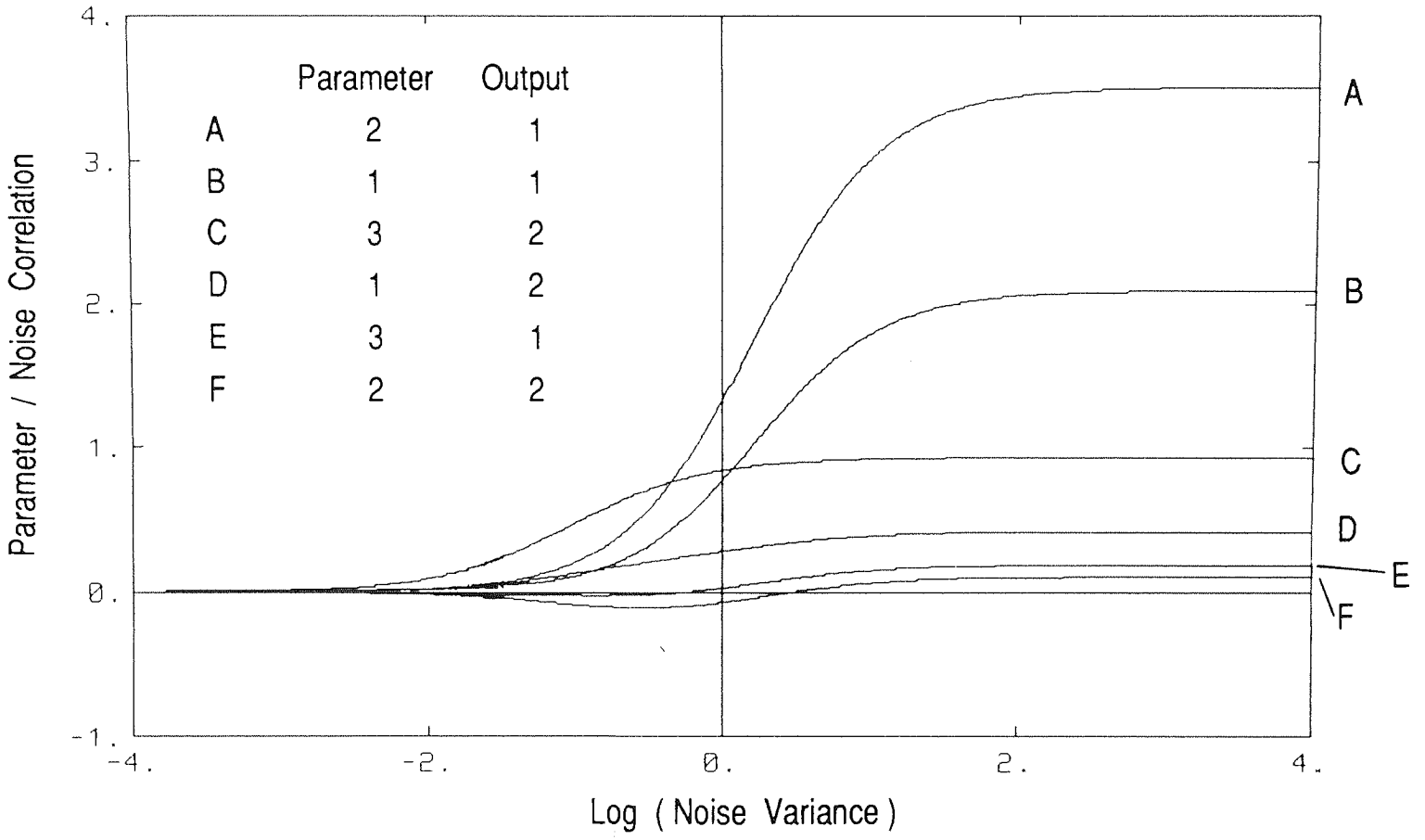

Figure 5.9 The Effect of Measurement Noise Variance on the Parameter / Noise Correlation after Convergence

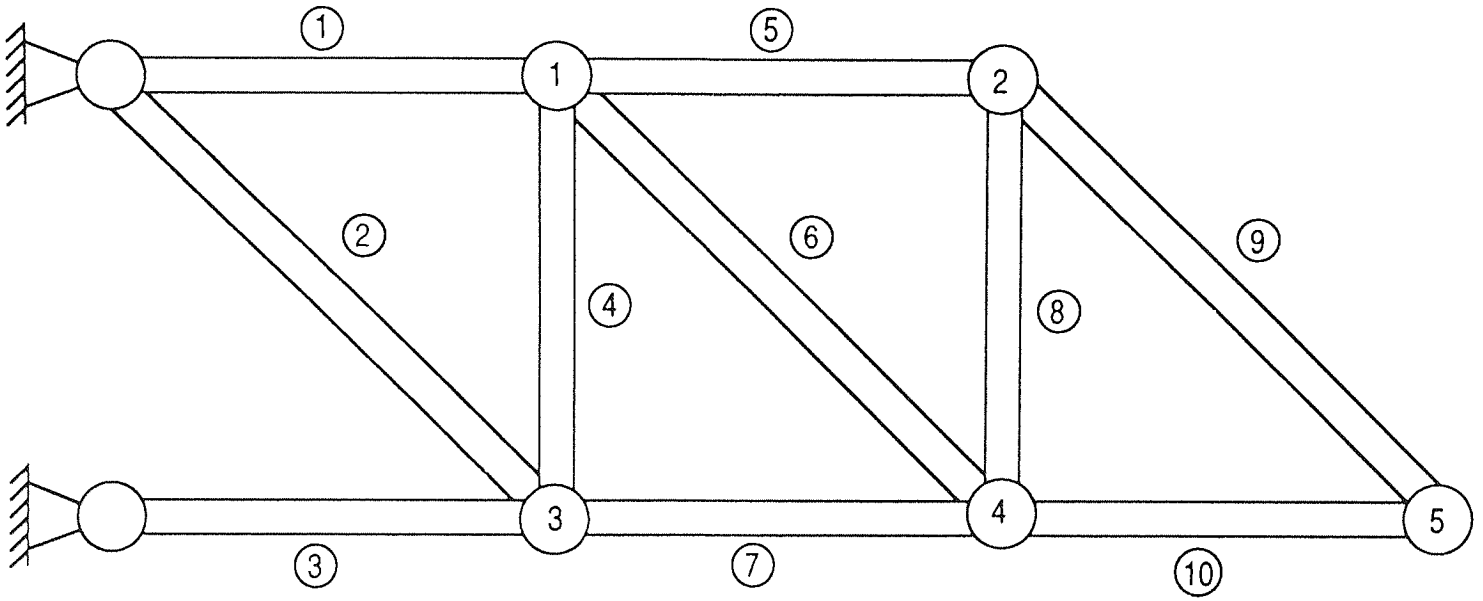

Numbers at joints are node numbers

Numbers near beams are element numbers

Figure 5.10 Example Pin Jointed Frame Arrangement

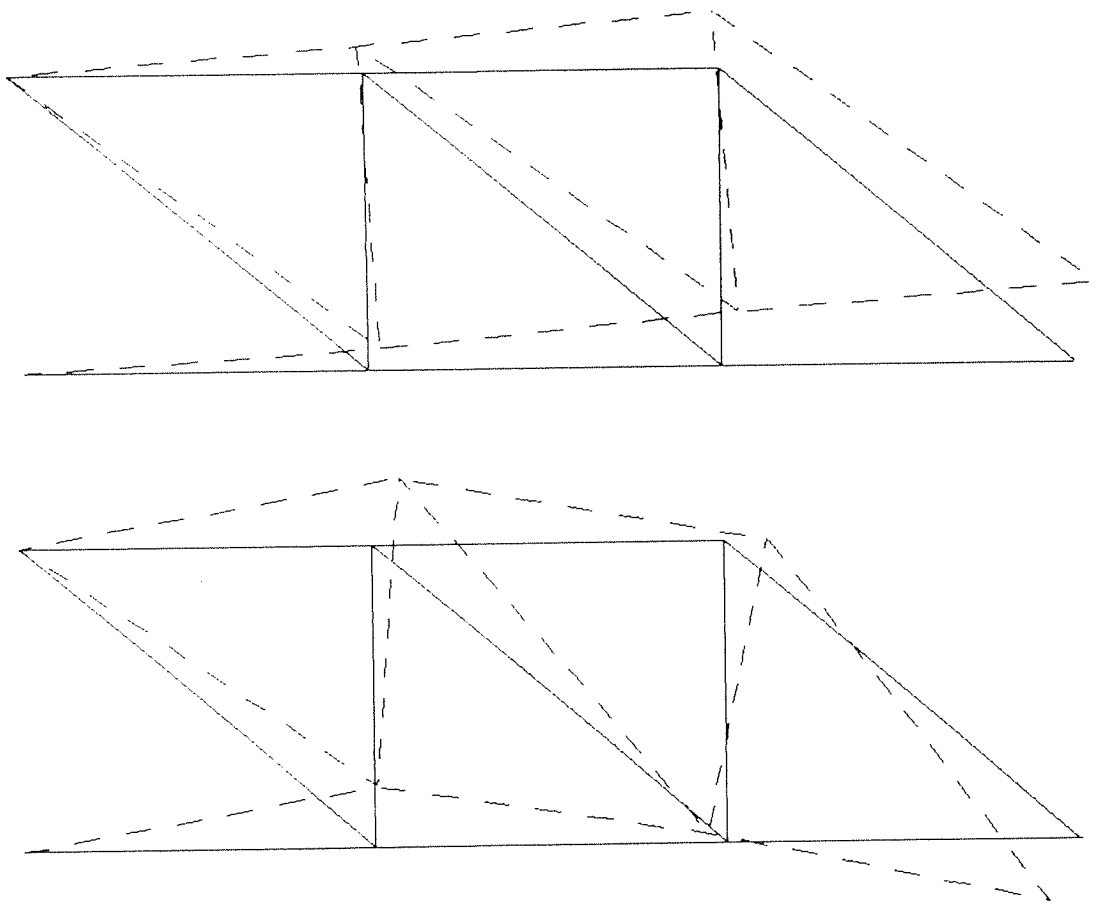

Figure 5.11 The First Two Mode Shapes of the Pin Jointed Frame

Chapter 6

Application of Modal Truncation to Structural Models

6.1 Chapter Summary

This chapter outlines the theory behind modal truncation and its application to structural models. This reduction technique will be required in Chapter 7 to update parameters using FRF data. It is of little use in updating algorithms which use modal data, that is natural frequencies and mode shapes (for example Chapter 5). Modal truncation is a standard technique for systems with known coefficients. This chapter extends the theory to allow for unknown parameters so that the reduced order model may be used in the parameter estimation routines in the following chapters. In principle the approach is simple. The eigenvectors are expressed as a linear functions of the parameters about a given initial parameter estimate by computing the eigenvector derivatives. These functions may then be used in the same way as eigenvectors in standard modal truncation to produce a model that is correct to first order in the parameter variations. The main difficulty in this approach is the calculation of the eigenvector derivatives. Much of this chapter considers a transformation using just the values of the eigenvectors at the initial parameter estimate, or zeroth order transformation. This transformation can give very good results and is shown to be equivalent to a first order transformation where the eigenvector derivatives have been approximated, as would occur in practical situations. A section on proportional viscous damping is included to highlight the computational advantages for systems with this damping model.

6.2 Modal Truncation Applied to Structural Models

From Chapter 2 the linear model of a structure with n degrees of freedom exhibiting viscous or hysteretic damping may be written as the following first order differential equation in the unknown parameter vector θ,

$$\left.\begin{aligned} \mathbf{M}(\theta)\,\ddot{\mathbf{x}} + \mathbf{K}(\theta)\,\mathbf{x} &= \mathbf{B}\,\mathbf{u} \\ \mathbf{y} &= \mathbf{C}\,\mathbf{x} \end{aligned}\right\} \quad . \tag{6.1}$$

The notation is described fully in Chapter 2 and is also given in Appendix A.

Assume that a current estimate of the unknown parameters θ_e is available from a theoretical analysis or previous iterations of the estimation scheme. Then equation 6.1 may be rewritten using a Taylor series expansion for the 'mass' and 'stiffness' matrices. In some instances the model may be formulated so that this expansion is exact, for example if the unknown parameters were the material damping and stiffness properties. Thus the first equation of 6.1 becomes,

$$\left[\mathbf{M}_0 + \delta\theta_1\mathbf{M}_1 + \ldots + \delta\theta_p\mathbf{M}_p\right]\ddot{\mathbf{x}} + \left[\mathbf{K}_0 + \delta\theta_1\mathbf{K}_1 + \ldots + \delta\theta_p\mathbf{K}_p\right]\mathbf{x} = \mathbf{B}\,\mathbf{u} + o\left(\delta\theta^2\right) \tag{6.2}$$

where $\delta\theta = \theta - \theta_e = (\delta\theta_1, \delta\theta_2, \ldots, \delta\theta_p)$

$$\mathbf{M}_0 = \mathbf{M}(\theta_e)$$

$$\mathbf{K}_0 = \mathbf{K}(\theta_e)$$

$$\mathbf{M}_i = \frac{\partial \mathbf{M}}{\partial \{\theta\}_i}(\theta_e) \qquad \text{for } i = 1, 2, \ldots, p$$

$$\mathbf{K}_i = \frac{\partial \mathbf{K}}{\partial \{\theta\}_i}(\theta_e) \qquad \text{for } i = 1, 2, \ldots, p$$

The eigenvalues and mass normalised eigenvectors at the current parameter

estimate, ${}_0\lambda_i$ and ${}_0\phi_i$, are

$$\left[\mathbf{M}_0\ {}_0\lambda_i + \mathbf{K}_0\right]\ {}_0\phi_i = 0 \qquad \text{for } i = 1, \ldots, 2n \ . \tag{6.3}$$

The eigenvalues are arranged in ascending order of natural frequency and since the 'mass' and 'stiffness' matrices are symmetrical the left and right eigenvectors are equal. The normalisation of the eigenvectors implies that

$${}_0\phi_i^T\ \mathbf{M}_0\ {}_0\phi_k = \delta_{ik} \qquad \text{the Kronecker delta} \ .$$

Let the reduced order model have r degrees of freedom. Generally the number of degrees of freedom in the reduced model is much lower than that in the full model, that is $r \ll n$ in general. Usually in modal truncation the full order state is transformed to a reduced order state using a matrix consisting of the first 2r eigenvectors. The situation is more complex because the eigenvectors depend on the unknown parameters. One solution is to write the eigenvectors as a Taylor series in $\delta\theta$ which is then truncated to produce the required transformation matrix. This approach will be adopted here with truncation after the constant, or zeroth order term, and after the first order terms, thus producing a zeroth and first order transformation. If $\Phi(\theta)$ is the transformation matrix which has dimension (2n,2r) then it may be written as

$$\Phi(\theta) = \Phi_0 + \delta\theta_1\Phi_1 + \delta\theta_2\Phi_2 + \ldots + \delta\theta_p\Phi_p + o\left(\delta\theta^2\right) \tag{6.4}$$

where $\Phi_0 = \left[\ {}_0\phi_1,\ {}_0\phi_2, \cdots,\ {}_0\phi_{2r}\right]$

$$\Phi_i = \frac{\partial\Phi}{\partial\{\theta\}_i}\left(\theta_e\right) \qquad \text{for } i = 1, 2, \ldots, p \ .$$

Similarly the eigenvalues may be considered as a Taylor series in $\delta\theta$. Writing

the negated eigenvalues on the diagonal of a matrix of dimension (2r,2r) gives

$$\Lambda(\theta) = \Lambda_0 + \delta\theta_1\Lambda_1 + \delta\theta_2\Lambda_2 + .. + \delta\theta_p\Lambda_p + o(\delta\theta^2) \qquad (6.5)$$

where $\Lambda_0 = -\,\mathrm{diag}\left({}_0\lambda_1, {}_0\lambda_2, \ldots, {}_0\lambda_{2r} \right)$

$$\Lambda_i = \frac{\partial \Lambda}{\partial \{\theta\}_i}\left(\theta_e\right) \qquad \text{for } i = 1, 2, \ldots, p \ .$$

The matrices Λ_i and Φ_i may be determined in a number of ways although evaluating the eigenvector sensitivity matrices is the most time consuming. Section 6.3 addresses this problem in providing some understanding of the nature of the approximation and Section 6.4 discusses the problems in computing these matrices.

Having defined the transformation matrices the reduced order models may now be determined. The zeroth order transformation is

$$\mathbf{x} = \Phi_0 \mathbf{w} \qquad (6.6)$$

where $\mathbf{w}$ is the reduced order state vector which has dimension 2r. Applying this transformation to equation 6.2 and premultiplying by $\Phi_0{}^T$ produces the reduced order equation

$$\left.\begin{aligned} \left[I_{2r} + \delta\theta_1 M_{z1} + .. + \delta\theta_p M_{zp}\right]\dot{\mathbf{w}} + \\ \left[\Lambda_0 + \delta\theta_1 K_{z1} + .. + \delta\theta_p K_{zp}\right]\mathbf{w} = B_z\mathbf{u} + o(\delta\theta^2) \\ y_z = C_z\mathbf{w} \end{aligned}\right\} \qquad (6.7)$$

where

$$\mathbf{M}_{zi} = \Phi_0^T \mathbf{M}_i \Phi_0$$

$$\mathbf{K}_{zi} = \Phi_0^T \mathbf{K}_i \Phi_0$$

$$\mathbf{B}_z = \Phi_0^T \mathbf{B}$$

$$\mathbf{C}_z = \mathbf{C} \Phi_0$$

$\mathbf{I}_{2r}$ = the (2r , 2r) identity matrix

$\mathbf{y}_z$ = the output from the reduced model .

The reduced model based on the first order transformation may be defined in a similar way. If $\mathbf{v}$ is the reduced order state vector, which has dimension 2r, then the transformation is

$$\mathbf{x} = \left[\Phi_0 + \delta\theta_1\Phi_1 + \delta\theta_2\Phi_2 + .. + \delta\theta_p\Phi_p\right] \mathbf{v} \; . \qquad (6.8)$$

Applying this transformation to equation 6.2 and premultiplying by the matrix inside the square brackets in equation 6.8 gives the reduced model equation based on the first order transformation as

$$\left.\begin{aligned} \dot{\mathbf{v}} + \left[\Lambda_0 + \delta\theta_1\Lambda_1 + \delta\theta_2\Lambda_2 + .. + \delta\theta_p\Lambda_p\right] \mathbf{v} = \\ \left[\mathbf{B}_{F0} + \delta\theta_1\mathbf{B}_{F1} + \delta\theta_2\mathbf{B}_{F2} + .. + \delta\theta_p\mathbf{B}_{Fp}\right]\mathbf{u} + o\left(\delta\theta^2\right) \\ \mathbf{y}_F = \left[\mathbf{C}_{F0} + \delta\theta_1\mathbf{C}_{F1} + \delta\theta_2\mathbf{C}_{F2} + .. + \delta\theta_p\mathbf{C}_{Fp}\right] \mathbf{v} \end{aligned}\right\} \qquad (6.9)$$

where $B_{Fi} = \Phi_i^T B$

$C_{Fi} = C \Phi_i$

y_F = the output from the reduced model.

This first order transformation has the advantage that it diagonalises the system equations providing an easy inversion when the frequency response function is required. The computational implications of both schemes are discussed in section 6.4. In principle, though, we have two methods to considerably reduce the order of the full model. The accuracy of these schemes will now be discussed.

6.3 The Nature of the Approximation

Now that the transformations have been defined the nature of the approximations of the reduced models to the full model may be investigated. Of course the full model is still an approximation to the real structure due to the inherent deficiencies in modelling a continuum with a discrete finite element mesh. A further approximation may be caused by the mass, damping and stiffness matrices not being linear functions of the parameters.

To see the specific effect of the unknown parameters the frequency response function will be written as the sum of contributions from individual modes. Standard modal truncation then truncates this series after the required number of modes as shown in Chapter 4. Writing the eigenvector transformation matrix as a function of the unknown parameters produces the transformation

$$x = \Phi(\theta)\, z \qquad (6.10)$$

where $\Phi(\theta) = \left[\phi_1(\theta) , \phi_2(\theta) , \ldots , \phi_{2r}(\theta) \right]$

z = the reduced order state vector.

Applying this to equation 6.1 produces the frequency response function for the reduced system as

$$F(\omega) = C\, \Phi(\theta) \left[j\omega I_{2r} + \Lambda(\theta) \right]^{-1} \Phi(\theta)^T B \qquad (6.11)$$

where $\Lambda(\theta) = \text{diag}\left(\lambda_1(\theta) , \lambda_2(\theta) , \ldots , \lambda_{2r}(\theta) \right)$

and $\lambda_i(\theta)$ is the i th eigenvalue of the system. j is, of course, $\sqrt{-1}$.

The frequency response function may be written as the following series,

$$F(\omega) = \sum_{i=1}^{2r} \frac{C\, \phi_i(\theta)\, \phi_i(\theta)^T B}{j\omega - \lambda_i(\theta)} \qquad (6.12)$$

which is the truncation of the full dimensional series. In this form the approximations due to writing the transformation matrix as a zeroth or first order series in the parameters may be related to the frequency response function. For the first order approximation, defined by equations 6.8 and 6.9, both the eigenvalues and eigenvectors in equation 6.12 are, as defined, correct to first order in $\delta\theta$.

The situation for the zeroth order approximation is better than might be expected. The eigenvalues are actually correct to first order in $\delta\theta$. At the current estimated parameter values the zeroth and first order transformations are equal. Hence the eigenvalues of the corresponding reduced models given by Λ_0 will be equal. From Chapter 2 the eigenvalue

sensitivity matrices Λ_i are

$$\left.\begin{aligned} \Lambda_i &= -\,\mathrm{diag}\left(\frac{\partial \lambda_1}{\partial \{\theta\}_i}(\theta_e) \,,\, \frac{\partial \lambda_2}{\partial \{\theta\}_i}(\theta_e) \,,\, \ldots \,,\, \frac{\partial \lambda_{2r}}{\partial \{\theta\}_i}(\theta_e) \right) \\ \\ \frac{\partial \lambda_k}{\partial \{\theta\}_i}(\theta_e) &= -\; {}_0\phi_k^T \left[{}_0\lambda_k \mathbf{M}_i + \mathbf{K}_i \right] {}_0\phi_k \quad . \end{aligned}\right\} \qquad (6.13)$$

The eigenvector of the zeroth order model at the current parameter estimate corresponding to the eigenvalue ${}_0\lambda_k$ is a unit vector in the k th coordinate direction. Call this vector $\mathbf{u}_k$. Then the eigenvalue derivatives for the zeroth order model are

$$\left.\begin{aligned} \frac{\partial \lambda_k}{\partial \{\theta\}_i}(\theta_e) &= -\,\mathbf{u}_k^T \left[{}_0\lambda_k \mathbf{M}_{zi} + \mathbf{K}_{zi} \right] \mathbf{u}_k \\ &= -\,\mathbf{u}_k^T \Phi_0^T \left[{}_0\lambda_k \mathbf{M}_i + \mathbf{K}_i \right] \Phi_0 \mathbf{u}_k \end{aligned}\right\} \qquad (6.14)$$

Since $\Phi_0 \mathbf{u}_k = {}_0\phi_k$ equation 6.14 is equivalent to the expression for the eigenvalue derivative given in equation 6.13. Thus the eigenvalues of the reduced order model based on the zeroth order transformation are correct to first order in the parameter variations.

The nature of the approximation to the eigenvector sensitivity matrices Φ_i is

slightly more complex. From Chapter 2 these matrices may be written as

$$\left.\begin{aligned} \Phi_i &= \left[\frac{\partial \phi_1}{\partial \{\theta\}_i}(\theta_e) , \frac{\partial \phi_2}{\partial \{\theta\}_i}(\theta_e) , \ldots , \frac{\partial \phi_{2r}}{\partial \{\theta\}_i}(\theta_e) \right] \\ \frac{\partial \phi_h}{\partial \{\theta\}_i}(\theta_e) &= \sum_{k=1}^{2n} {}_i a_{hk}\, {}_0\phi_k \end{aligned}\right\} \qquad (6.15)$$

where $${}_i a_{hk} = \frac{1}{{}_0\lambda_k - {}_0\lambda_h} {}_0\phi_k^T \left[{}_0\lambda_h \mathbf{M}_i + \mathbf{K}_i \right] {}_0\phi_h \qquad \text{if } k \neq h$$

$${}_i a_{hh} = \frac{1}{2} \left[{}_0\phi_h^T \mathbf{M}_i \, {}_0\phi_h \right] .$$

Equations 6.15 define the sensitivities used for the first order approximation to the eigenvector given in equation 6.4. Note that the eigenvector derivatives are a linear combination of all of the eigenvectors. The zeroth order approximation actually truncates the series in equation 6.15 after 2r terms. It has already been established that the eigenvalues resulting from the zeroth and first order transformations are equal to first order in $\delta\theta$. By analogy to equation 6.15 the eigenvector derivative obtained from the reduced model based on the zeroth order transformation are

$$\frac{\partial u_h}{\partial \{\theta\}_i}(\theta_e) = \sum_{k=1}^{2r} {}_i b_{hk}\, u_k \qquad (6.16)$$

where $${}_i b_{hk} = \frac{1}{{}_0\lambda_k - {}_0\lambda_h} u_k^T \Phi_0^T \left[{}_0\lambda_h M_i + K_i \right] \Phi_0 u_h = {}_i a_{hk} \qquad \text{if } k \neq h$$

$${}_i b_{hh} = \frac{1}{2} \left[u_h^T \Phi_0^T M_i \Phi_0 u_h \right] = {}_i a_{hh} \quad .$$

Applying the transformation given in equation 6.6 gives, for the zeroth order transformation

$$\frac{\partial \phi_h}{\partial \theta_i}\left(\theta_e\right) = \sum_{k=1}^{2r} {}_i a_{hk}\, \phi_k \quad . \qquad (6.17)$$

What effect does this truncation have on the frequency response function defined in equation 6.12? If h « k then $|\lambda_h| \ll |\lambda_k|$ and so, from the definition of the series coefficient in equation 6.15, ${}_i a_{hk}$ is small. Thus in general the derivatives of the eigenvectors with low natural frequency are more accurate than those with higher natural frequency when the model based on the zeroth order transformation is used. From the definition of the frequency response function given by equation 6.12 the value of the eigenvector derivative has most influence close to its corresponding natural frequency. Thus the reduced order model based on the zeroth order transformation is most accurate at low frequencies and least accurate at high frequencies. Usually enough modes may be included to make this reduced order model sufficiently accurate within the frequency range of interest.

6.4 Computational Aspects

Suppose a reduced order model were required for a given system and current parameter estimate. To compute the first order transformation directly

requires the calculation of the derivatives of the first 2r eigenvectors, or equivalently the sensitivity matrices Φ_i. Methods to calculate these matrices have been fully described in Chapter 2 but will be considered briefly here.

The sensitivity matrices may be evaluated from the series given in equation 6.15 although in theory all the eigenvectors of the system must first be computed. In practice the series may be truncated so that all the eigenvectors need not be computed. If 2r eigenvectors are used, Section 6.3 has shown that the zeroth and first order transformations will give the same model. An alternative, given by Nelson (1976), involves computing the inverse of a matrix of dimension 2n, clearly a time consuming task.

Iterative schemes, for example the algorithm described by Rudisill and Chu (1975), may be used. The vector ε - algorithm described by Tan (1987) is a more advanced iterative method which, with exact computation, gives the exact solution in 4n-2 iterations, where n is the number of degrees of freedom in the original model. It may be possible to calculate the eigenvector derivatives numerically by changing the parameter value slightly and computing the change in the eigenvectors. This requires computing a new set of eigenvectors for every parameter. Both the iterative and the numerical methods are best suited to small numbers of unknown parameters and to low dimensional reduced order models.

Because of the high computational burden necessary to accurately compute the eigenvector derivatives, the zeroth order transformation should be used where possible. Should the estimation algorithm be more efficiently executed with a diagonal mass and stiffness matrices then there are two choices. Either the model resulting from the zeroth order transformation may be diagonalised or the eigenvector derivatives may be formed using the first 2r terms in the series defined by equation 6.15 .

6.5 Numerical Example Assuming Proportional Viscous Damping

So far no assumptions have been made about the nature of the damping. Proportional viscous damping assumes that the viscous damping matrix is

$$\mathbf{C}_n(\theta) = \alpha\, \mathbf{M}_n(\theta) + \beta\, \mathbf{K}_n(\theta) \qquad (6.18)$$

for some constants α and β. It has been shown in Chapter 2 that with this form of damping the eigenvectors of the undamped model are real and are also the eigenvectors of the damped model. Thus all of the computation can be conducted using real vectors and matrices. This, combined with the matrices having dimension n rather than 2n, produces enormous savings in computational time.

Consider a ten degree of freedom system whose damping matrix is proportional to its mass matrix although the numerical value of the constant has only been estimated. The mass matrix is assumed fixed and the stiffness matrix is dependent on a second parameter. Force is applied at one position and only one response is measured. The numerical values of the relevant matrices are given in Appendix C. The reduced models are obtained based on the parameter estimate θ_e = (0.01,3.0). Figure 6.1 shows the receptance of the system over a frequency range that includes three modes. Also shown is the receptance of the system reduced to four degrees of freedom with the same parameter values. The major discrepancies occur where the magnitude of the response is small and where an experimental receptance would be susceptible to noise. Although the approximation is very accurate at the current estimated parameter values the reduced model must retain adequate accuracy over a range of parameter values. Figure 6.2 shows the receptance of the full model for parameter values, θ, of (0.01,3.0)

(0.02,4.0) and also the zeroth and first order reduced models evaluated at the same parameter values. Even though the parameter change is large, and could not be described as first order, the first mode is still modelled accurately. The second and third modes are more inaccurate because of the magnitude of their natural frequencies relative to those of the unmodelled modes. The coefficients in the expansion for the FRF given by equation 6.12 depend on the reciprocal of the difference between the frequency of interest and the eigenvalues. Since the reduced model consists of four modes the difference between the fifth natural frequency and the frequency range of interest is relatively small. This problem also causes large discrepancies in the anti-resonance regions. For the zeroth order model the eigenvector derivatives are obtained using only the first four modes of the system. This causes the small difference between the zeroth and first order models in figure 6.3.

Modal truncation seems an effective method to reduce the order of a model. To reduce errors the natural frequency of the lowest neglected mode should be considerably higher than the frequency range of interest. In this case the extra complexity in calculating the eigenvector sensitivities to the parameter variations does not yield a significantly better approximation.

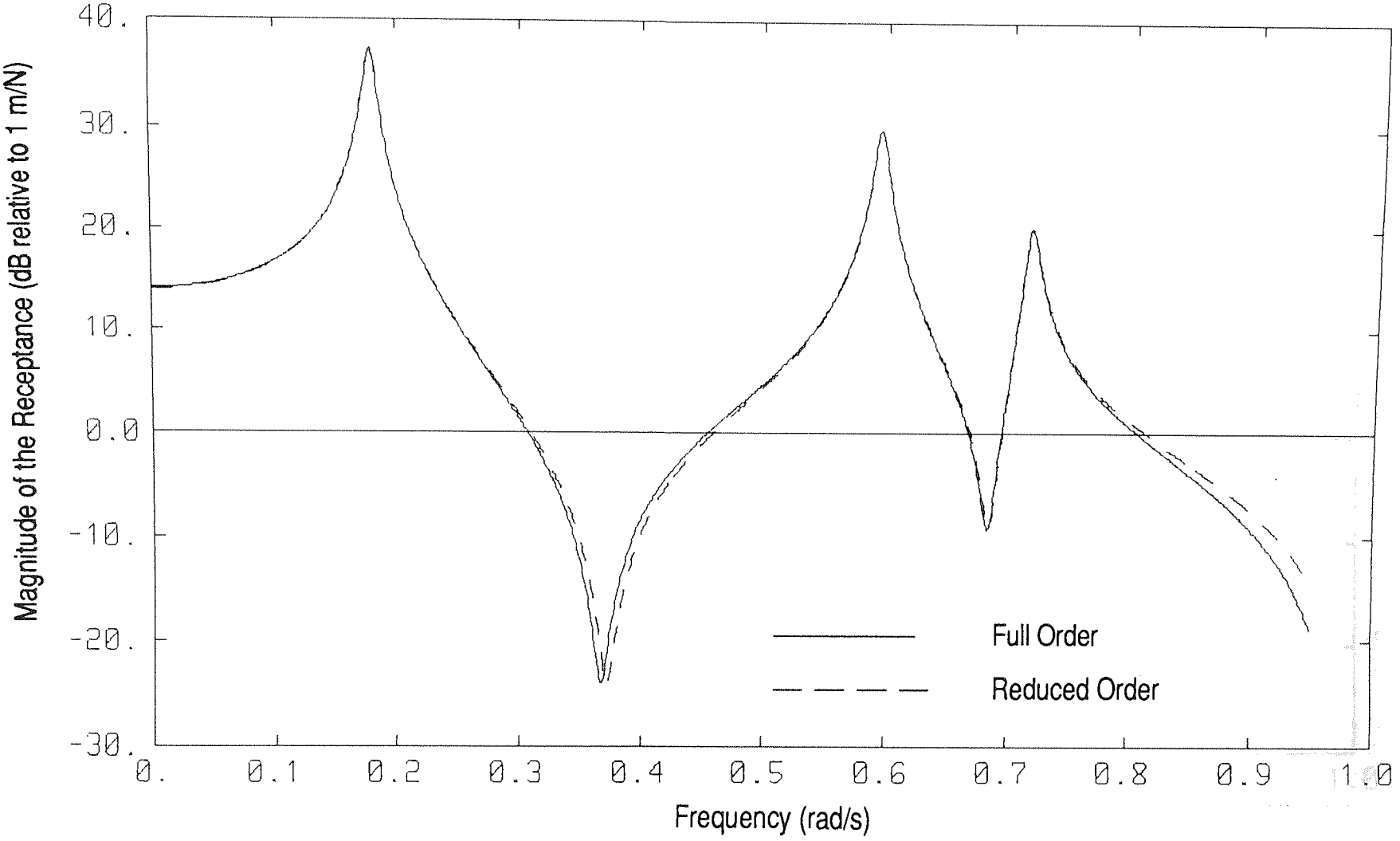

Figure 6.1 The Effect of Modal Trucation

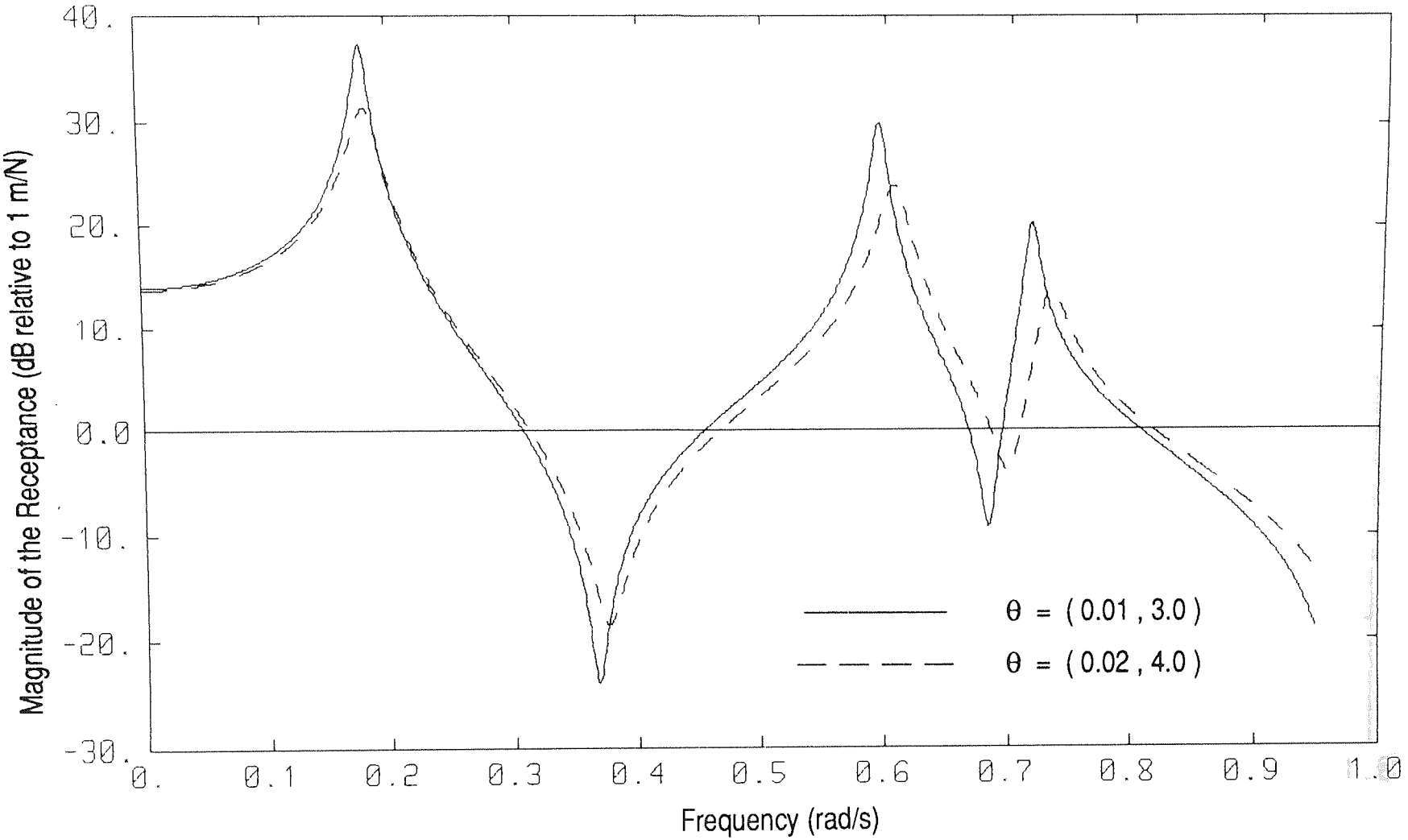

Figure 6.2 The Receptance at Different Parameter Values

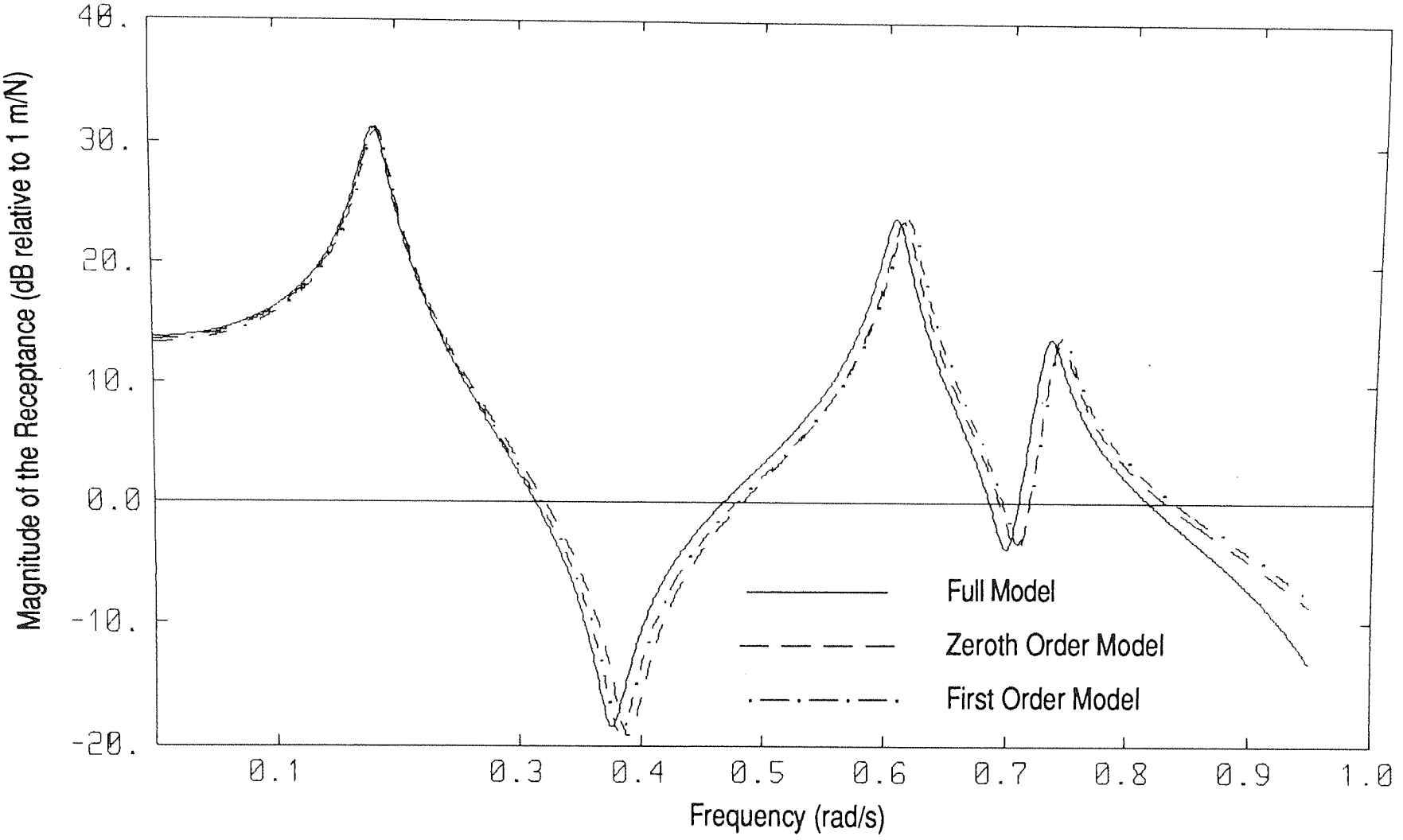

Figure 6.3 The Effect of Parameter Variations on Modal Truncation

Chapter 7

Structural Parameter Estimation in the Frequency Domain

7.1 Chapter Summary

This chapter outlines some of the algorithms that can be used to update the parameters of structural models directly from frequency data. The algorithms are first demonstrated on a one degree of freedom system to introduce the methods and highlight their advantages and shortcomings. After outlining some of the problems associated with estimating parameters in real systems the first of the practical algorithms are introduced. The main thrust of this thesis is the use of reduced order models to help the parameter estimation process. In section 7.4 the number of reduced degrees of freedom is chosen so that the frequency response functions based on the state of the modelled system may be estimated. Algorithms are then introduced which use this frequency data to update the system parameters. A simulated example is used to assess the quality of the proposed methods.

7.2 The One Degree of Freedom System

Although applications using one degree of freedom models are limited this section serves two purposes. First, many of the features of the estimation schemes and the difficulties they encounter may be understood more easily in a simple system. Second, the modal properties of a multi degree of freedom system may be identified using an iterative scheme where only one degree of freedom is identified at a time (Goyder 1980). In a one degree of freedom system the identification of modal properties is equivalent to the identification of structural properties (mass, damping and stiffness). Only estimation schemes which directly identify, or may be reformulated to identify, structural parameters are considered.

Let f(ω,a,b,c) be the computed frequency response function for the system, which depends on the unknown constants a, b and c, given by

$$f(\omega, a, b, c) = \frac{c}{a - \omega^2 + bj\omega} \quad . \tag{7.1}$$

Obviously a, b and c can readily be associated with either the natural frequency, damping ratio and modal participation factor or the mass, damping coefficient and stiffness of a one degree of freedom system. The value of the measured frequency response function, denoted $f_m(\omega)$ will only be available at a finite number N of frequencies ω_k. The conventional least squares, or output error, problem is to find the values of a, b and c that minimise

$$J(a, b, c) = \sum_{k=1}^{N} \left| f_m(\omega_k) - f(\omega_k, a, b, c) \right|^2 \quad . \tag{7.2}$$

From the definition of the computed frequency response function, equation 7.1, J(a,b,c) is a highly nonlinear function of the constants a and b and thus requires some form of iterative method for its minimisation.

The first method to be tried was the Newton-Raphson algorithm which effectively approximates equation 7.2 by a three term Taylor series. Gaukroger *et al.* (1973) used such an algorithm to obtain the properties of up to five modes simultaneously. This method will work well providing the initial parameter estimates are sufficiently accurate. Suppose the measured frequency response function is taken from a system with (a,b,c) = (1.0,0.02,1.0) and no measurement noise. The frequency response function is measured at 1024 equally spaced points between 0.75 rad/s and

1.25 rad/s. Assume the values of b and c are available and so the parameter a is the only unknown parameter. This situation is not particularly realistic but will serve as an illustration of the problems with this algorithm. Figure 7.1 shows the cost function J for parameter values between 0.85 and 1.1. For much of the parameter range this graph is convex and will produce a divergent estimation algorithm. For example, if the initial estimate of a is 0.97, that is the natural frequency is estimated with a 1.5% error, then the next estimate for a is 0.913. Figure 7.1 also shows the three term Taylor series expansion about this point which graphically illustrates the problem. In fact the algorithm tries to estimate the maximum of the cost function J, as it will for any convex function.

Mottershead and Stanway (1986) outline an algorithm which overcomes these problems using a recursive filter. Consider the measured frequency response function given above and assume a, b and c are to be updated. One sweep through the frequency range with an initial parameter estimate of (a,b,c) = (0.9,0.0,1.1) gives an updated parameter estimate correct to three significant figures. This filter is highly nonlinear and uses large amounts of computer time. One way of reducing the computational burden is to minimise the equation error instead of the output error considered so far. Mottershead *et al.* (1987) have implemented the recursive filter to minimise, in the one dimensional case,

$$J(a,b,c) = \sum_{k=1}^{N} \left| \left(a - \omega_k^2 + b j \omega_k \right) f_m(\omega_k) - c \right|^2 . \qquad (7.3)$$

This has transformed the nonlinear problem into a linear least squares problem.The algorithm described by Mottershead *et al.* (1987) is very similar to a recursive linear least squares algorithm and minimising equation 7.3 presents no problem. The minimisation of J given by equation 7.3 for the current example gives a parameter estimate correct to the accuracy of the

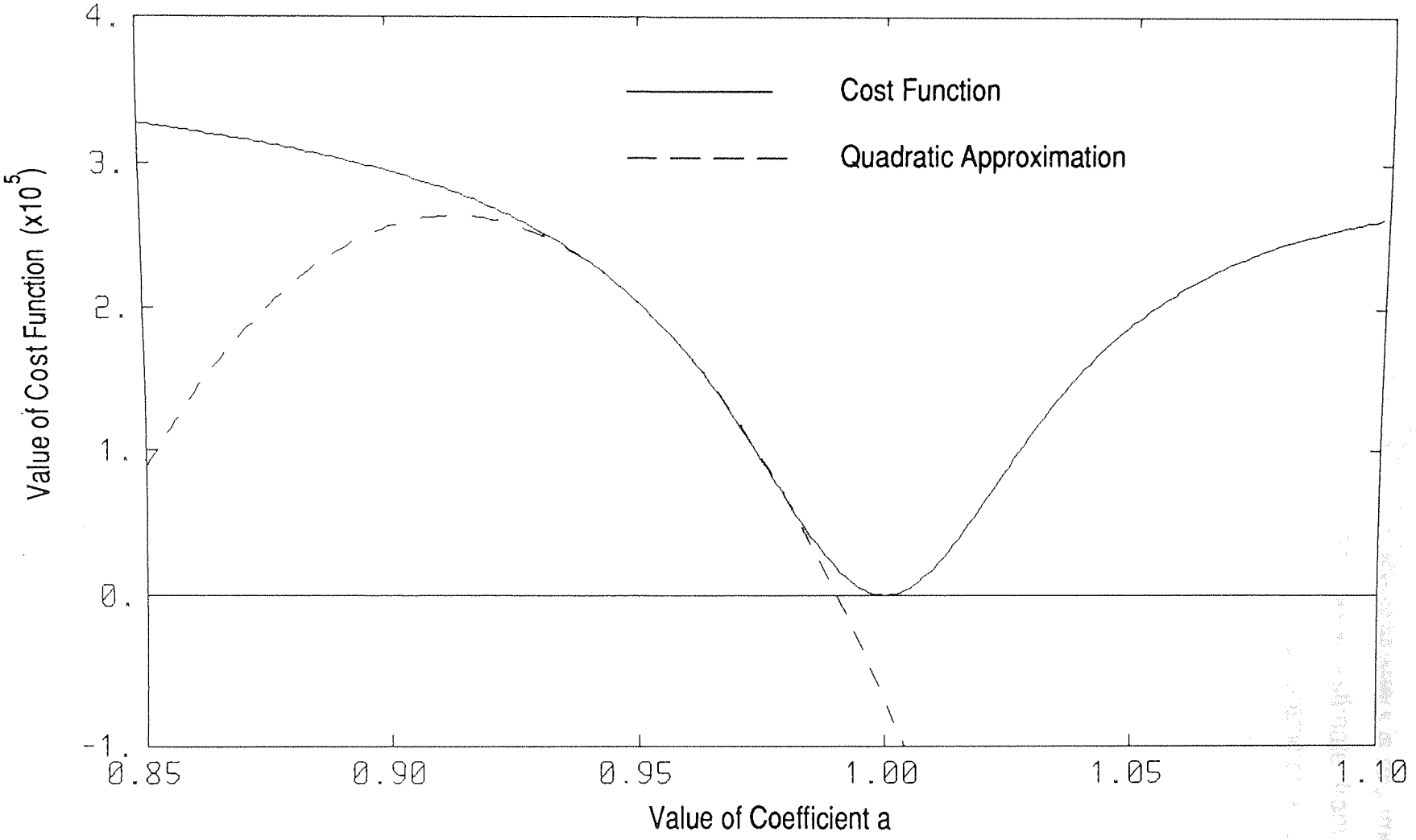

Figure 7.1 Cost Function and Quadratic Approximation - No Noise

computer used. Note that no initial estimate of the parameters is required. In the presence of measurement noise the parameter estimate from this equation error method is biased, that is the mean of the parameter estimate is not equal to the actual unknown parameter value (Fritzen 1986). A method called the Instrumental Variable Method has been proposed to produce an unbiased parameter estimate. The problem may be formulated in a number of ways (for example see Fritzen, 1986 or Mottershead, 1988). The most common way is to rewrite equation 7.1 as

$$\left(a - \omega^2 + bj\omega\right) f_m(\omega) - c = \text{Noise} \qquad (7.4)$$

and then assemble the equations at all the measured frequencies as the matrix equation

$$\begin{bmatrix} f_m(\omega_1) & j\omega_1 f_m(\omega_1) & -1 \\ f_m(\omega_2) & j\omega_2 f_m(\omega_2) & -1 \\ . & . & . \\ . & . & . \end{bmatrix} \begin{Bmatrix} a \\ b \\ c \end{Bmatrix} = \begin{Bmatrix} \omega_1^2 f_m(\omega_1) \\ \omega_2^2 f_m(\omega_2) \\ . \\ . \end{Bmatrix} + \text{Noise} \qquad (7.5)$$

or equivalently $\mathbf{A}_c \begin{Bmatrix} a \\ b \\ c \end{Bmatrix} = \mathbf{b}_c$.

Because the matrix $\mathbf{A}_c$ and the vector $\mathbf{b}_c$ are complex and the parameters are real, the real and imaginary parts of the equations should be separated to obtain

$$\begin{bmatrix} \text{Re}(\mathbf{A}_c) \\ \text{Im}(\mathbf{A}_c) \end{bmatrix} \begin{Bmatrix} a \\ b \\ c \end{Bmatrix} = \mathbf{A}_r \begin{Bmatrix} a \\ b \\ c \end{Bmatrix} = \mathbf{b}_r = \begin{Bmatrix} \text{Re}(\mathbf{b}_c) \\ \text{Im}(\mathbf{b}_c) \end{Bmatrix} . \qquad (7.6)$$

The equation error, or least squares error, is obtained from equation 7.6 using

the pseudo inverse of $\mathbf{A}_r$ formally giving

$$\begin{Bmatrix} a \\ b \\ c \end{Bmatrix} = \left[\mathbf{A}_r^T \mathbf{A}_r \right]^{-1} \mathbf{A}_r^T \mathbf{b}_r \quad . \tag{7.7}$$

To obtain the instrumental variable solution equation 7.6 is premultiplied by the transpose of a matrix $\mathbf{W}_r$ instead of $\mathbf{A}_r$. This matrix $\mathbf{W}_r$ is chosen to be statistically independent of the measurement noise. Usually $\mathbf{W}_r$ is obtained by replacing the measured FRF, f_m, in the derivation of $\mathbf{A}_r$, equations 7.5 and 7.6, by the FRF calculated at the current parameter estimate. Then the updated parameter estimate is given by

$$\begin{Bmatrix} a \\ b \\ c \end{Bmatrix} = \left[\mathbf{W}_r^T \mathbf{A}_r \right]^{-1} \mathbf{W}_r^T \mathbf{b}_r \quad . \tag{7.8}$$

Since the current parameter estimates are used to estimate the new parameter values the procedure is iterative. Using the example frequency response function with no measurement noise the correct parameters are obtained, to three significant figures after one iteration.

A method which tries to retain the computational advantages of the equation error approach whilst minimising the output error has been described by Goyder (1980). The latest estimate of the transfer function is used as a weighting function and the object is to minimise

$$J(a,b,c) = \sum_{k=1}^{N} |W_k|^2 \left| \left(a - \omega_k^2 + b j \omega_k \right) f_m(\omega_k) - c \right|^2 \tag{7.9}$$

where $W_k = \dfrac{1}{\hat{a} - \omega_k^2 + \hat{b} j \omega_k}$ and $\hat{a}$ and $\hat{b}$ are the current estimates of a and b.

On convergence the values of the parameters also minimise the output error given by equation 7.2. Using the example frequency response function after one iteration the parameter estimate to three significant figures is given by (1.00,0.0201,1.00), again very close to the actual parameters.

So far the methods have only been demonstrated on measurements taken from a linear one degree of freedom system with no measurement noise. This is unrealistic for three reasons: there will be other modes with low amplitudes present, the system may be slightly nonlinear and the measurement noise is not negligible. Secondary modes are a very real problem in the identification of the modal properties of a system taken one mode at a time (Goyder 1980). The main thrust of this chapter is the identification of parameters using the whole frequency response function available. Even so the model mismatch created because the theoretical model order and the actual model order are different produces convergence problems for many algorithms. This problem is considered in more detail later in the chapter. The system may be checked for nonlinearities using the Hilbert Transform technique (Tomlinson 1987). Otherwise the methods find the best linear model to fit the measured data. The effect of measurement noise on the algorithms must be considered.

Suppose a zero mean, uniform distribution of random variables was used to represent the measurement noise from the transducers and quantisation of analogue data. Figure 7.2 shows the effect of superimposing noise with a maximum peak to peak level of 10% (approximately 5.0 in absolute terms) of the maximum response on the frequency response function. Plotting the cost function against the value of the parameter a would give a graph very similar to figure 7.1. The added noise has raised the minimum value from zero to 0.217×10^4 kg^{-2} but has done nothing to the character of the cost function plot. The Newton-Raphson algorithm will again only work with accurate initial parameter estimates. The convergence of the parameter estimates obtained from the nonlinear recursive, equation error, instrumental

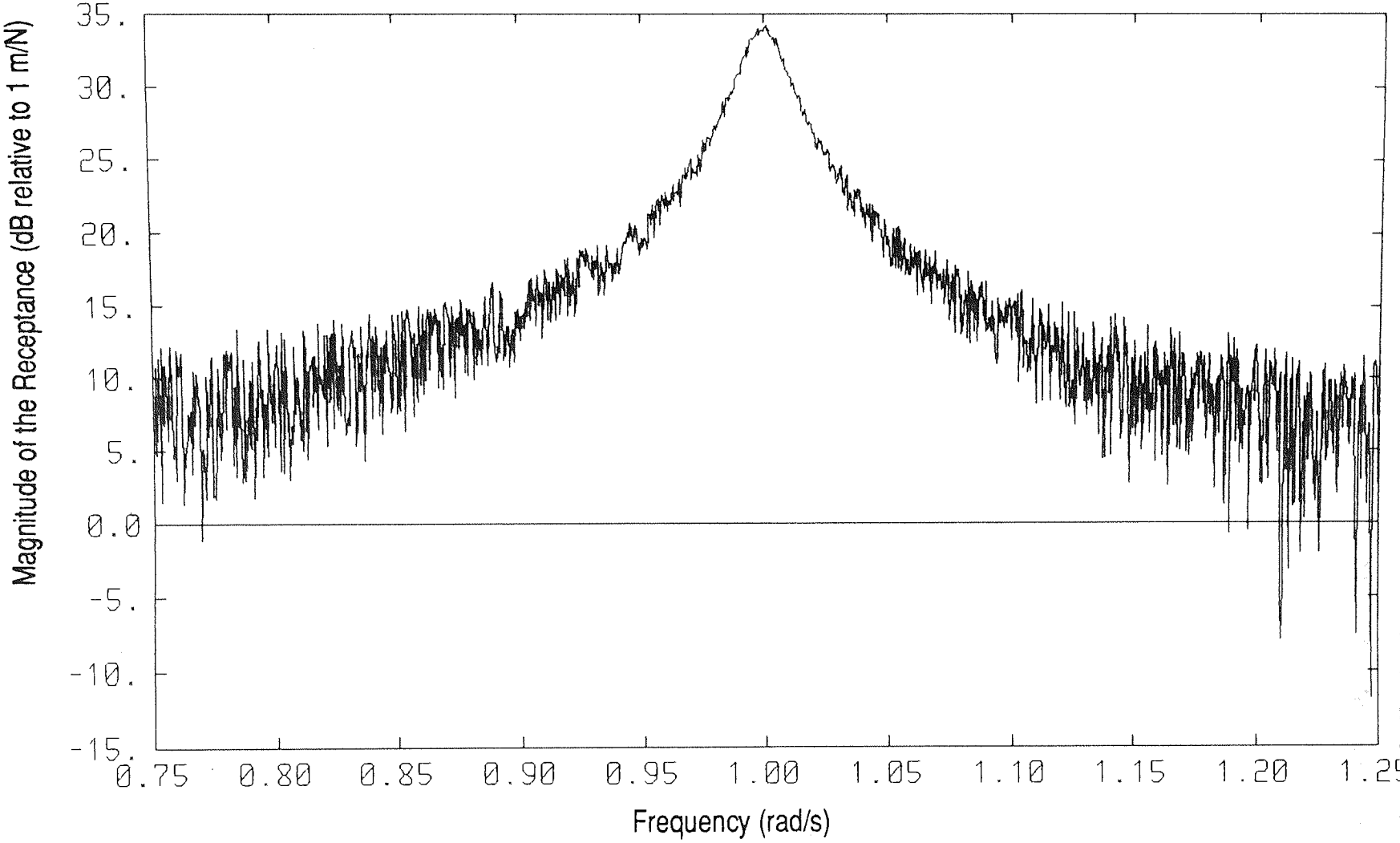

Figure 7.2 FRF for One Dimensional Example - 10% Noise Added

variable and Goyder algorithms starting with an initial parameter estimate of (0.9,0.0,1.1), are given in figure 7.3. Also shown in figure 7.3 is the reduction in the output error cost function for the three algorithms. An iteration for the recursive algorithm is taken to be one sweep through the parameters and the equation error algorithm is not iterative. All the algorithms estimate the natural frequency, or equivalently parameter a, accurately. The nonlinear recursive algorithm estimates the modal participation factor and damping, parameters b and c, most accurately and the equation error algorithm estimates them least accurately. Although the parameters obtained by the instrumental variable method are more accurate than those obtained by the equation error method, their quality is much worst than the parameters obtained from the nonlinear recursive and Goyder algorithms. Table 7.1 shows the absolute parameter values and percentage errors on convergence for the four algorithms.

Parameter	a	a	b	b	c	c
	value	% error	value	% error	value	% error
Algorithm						
Nonlinear Recursive	1.000	0.00	0.02001	0.06	0.999	0.10
Goyder	1.000	0.00	0.01994	0.31	0.997	0.30
Equation Error	1.000	0.04	0.01936	3.20	0.985	1.51
Instrumental Variable	1.000	0.00	0.01965	1.73	0.987	1.43

Table 7.1 Parameter values after convergence - 10% noise added

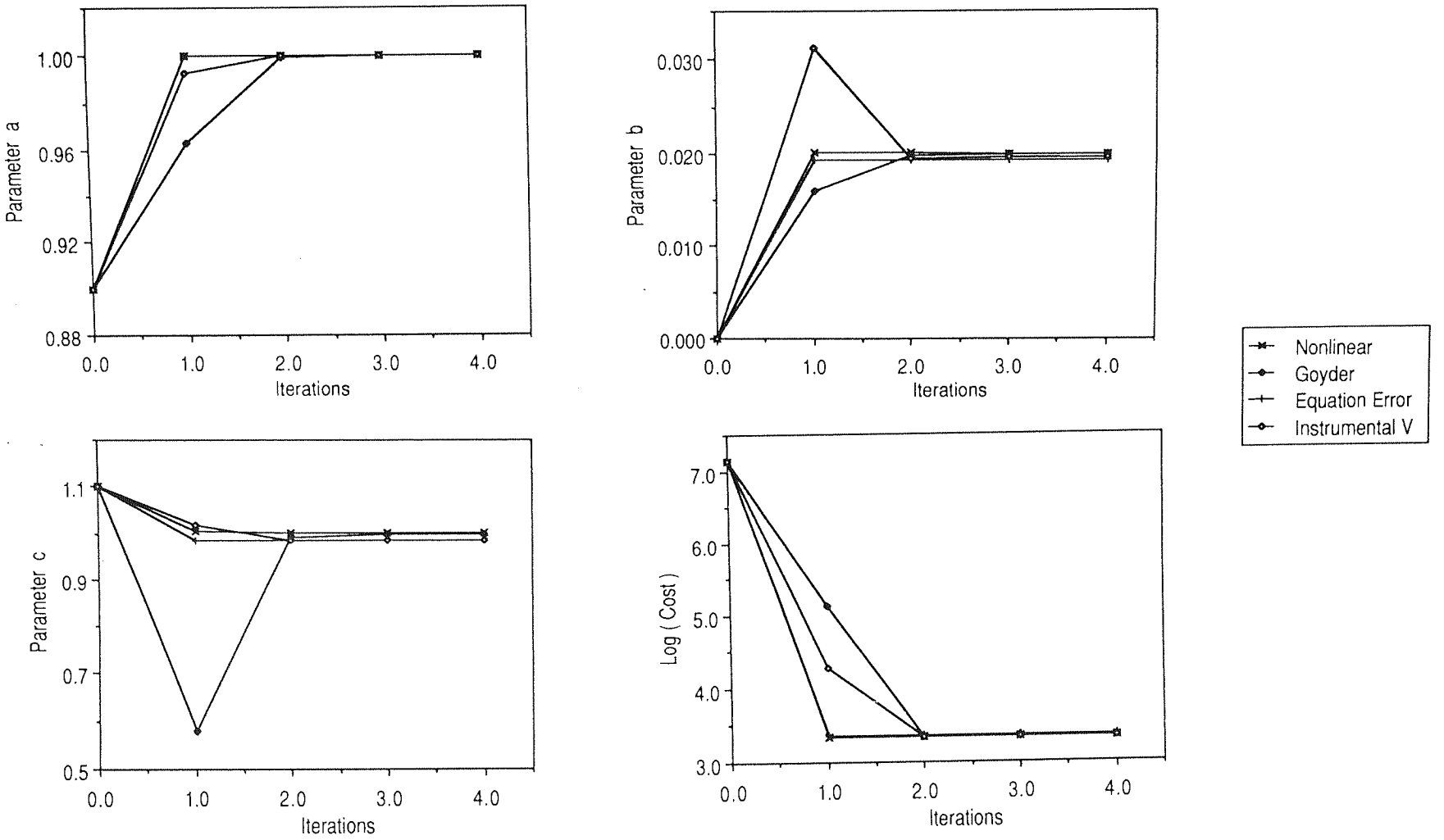

Figure 7.3 Convergence of Parameters - 10 % Noise Added, No Bias Errors

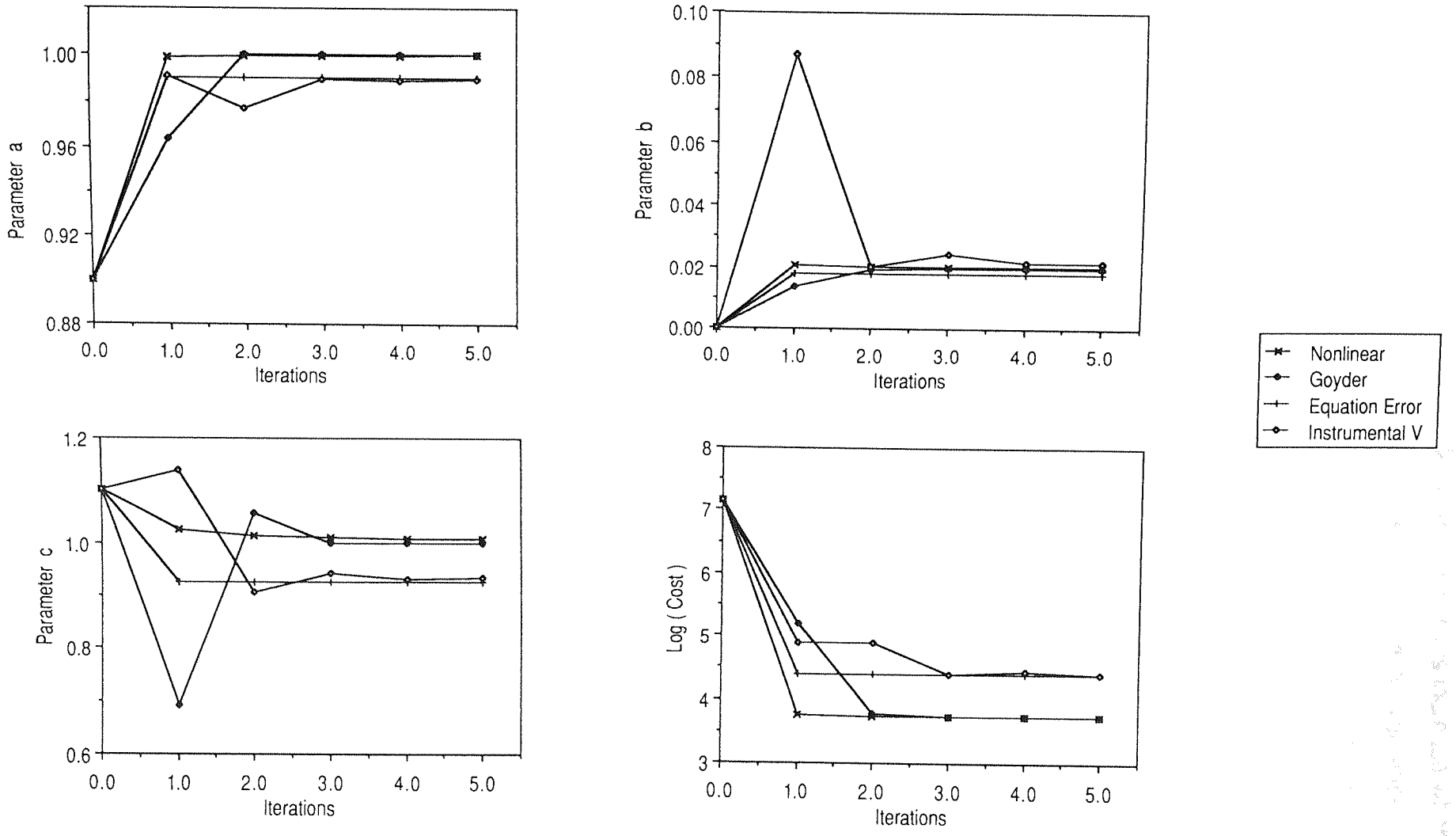

Figure 7.4 Convergence of Parameters - 10 % Noise Added, with Bias Errors

The problems with the quality of the parameter estimates increase when the noise does not have zero mean. Figure 7.4 shows the convergence of the unknown parameters when the mean of the noise is 10% of its peak to peak value. This example is not supposed to represent any particular physical situation but is merely an example of a systematic error which could arise in practice. The Goyder algorithm gives the best results although the nonlinear recursive algorithm also gives good results. The errors in the estimates obtained from the equation error and instrumental variable algorithms have increased substantially and even the natural frequency estimation has suffered. Once again the instrumental variable method is slightly better than the equation error method. Table 7.2 shows the absolute parameter values and percentage errors on convergence for the four algorithms. The large errors in computing the parameters b and c shows the difficulty in estimating both the modal participation factor and damping coefficient. For the equation error algorithm the ratio of parameter c to parameter b, which is approximately the maximum value of the frequency response function, is

Parameter	a	a	b	b	c	c
	value	% error	value	% error	value	% error
Algorithm						
Nonlinear Recursive	1.000	0.00	0.02015	0.75	1.005	0.53
Goyder	1.000	0.00	0.01995	0.24	1.000	0.03
Equation Error	0.990	0.97	0.01808	9.60	0.925	7.55
Instrumental Variable	0.989	1.07	0.02170	8.48	0.933	6.66

Table 7.2 **Parameter values after convergence - 10% noise with bias added**

estimated with an error of only 2.27%. The natural frequency is estimated only moderately accurately by the equation error and instrumental variable algorithms and the modal participation factor and damping are poorly estimated. Problems may have been expected since the noise, from a uniform distribution, is added to the output equation and not the state equation thus increasing the likelihood of biased estimates. Because the improvement with the instrumental variable method over the equation error method, compared to the Goyder method, is not very large the instrumental variable method will not be considered further.

7.3 Parameter Estimation in Real Systems

The last section considered the estimation of the parameters of a one dimensional system. Some of the problems in extending the methods to real systems were briefly mentioned and will be enlarged upon now.

In general, real systems are not one dimensional. Most systems are continuous structures and so in theory have infinite dimension. Over a finite frequency range even a continuous structure will appear finite dimensional. The actual dimension will depend on many variables, for example the frequency range of interest, the values of the structure's natural frequencies and the measurement noise from the instrumentation. It may even be difficult to estimate the number of degrees of freedom required to model a particular system. Repeated and close eigenvalues, that is natural frequencies, make this task even more difficult. These problems may be overcome by modelling the system with more degrees of freedom than are strictly necessary. The methods of parameter estimation may be extended to multiple degree of freedom systems. Except for Goyder's method, this is straightforward. Goyder (1980) extended his method to multiple degree of freedom systems by an iterative process considering one mode at a time. Some of these extensions and other new methods are given in the following

sections.

The major curse of increasing the dimension is the computational burden imposed. This burden may be minimised by choosing the best estimation algorithm, applying model order reduction outlined in Chapter 6 and optimising the computing code. Even so increasing the modelled system dimension will substantially increase the computing time required.

Measurements made on real systems are contaminated with noise. The origin of the noise and its statistics are difficult to access. There may be truncation errors in the analogue to digital converters or slight nonlinearities in the transducer amplifiers. The accelerometers cannot measure the acceleration at a point because they are of finite size, the shaker attachment may cause local stiffening of the structure and so on. In general, noise is one of two types which generally occur simultaneously. Either the noise is random with zero mean and will cancel out if enough averages are taken, or the 'noise' is not random. Non random 'noise' could, perhaps more correctly, be called modelling error or model mismatch. Any parameter estimation algorithm should produce unbiased estimates of the parameters. That is, if enough data is obtained there will be no error in the parameter estimates due to the random noise. Additionally the algorithms should not be sensitive to the non-random or structured noise. Thus the difference in parameter estimates derived from two slightly different data sets should be small. One particular type of structured noise or error is model mismatch. Here the assumed model is structurally different from the system generating the data. Perhaps the system is slightly nonlinear. The number of degrees of freedom in the model might be different from that of the system. Or maybe a parameter is not updated because its value is assumed to be known accurately when in fact its value is wrong. Structured noise is the most difficult to account for and so is considered in detail in this chapter.

7.4 Systems with a Large Number of Measurements

7.4.1 State Estimator

This section outlines a method to determine the physical parameters of a system when the number of measurements exceeds twice the number of modes present in the frequency range of interest. Should the modes be real, that is the system has proportional or negligible damping, then the number of measurements only needs to exceed the number of real modes. Only the general case will be considered in detail, the extension to problems with only real modes being straightforward. Since estimating the number of modes present in measured data can be difficult the method works best if there are many more measurements than identifiable modes. The errors from the model order reduction algorithms may then also be minimised. The practical difficulty with equation error estimation algorithms is the requirement to estimate the state vector. With a large number of measurements the analytical model may be reduced to a model with r degrees of freedom such that $2r \leq m$, where m is the number of response measurements. Then the state estimation problem becomes overdetermined and can be solved in the least squares sense. The equation error algorithm may then be applied to the reduced order model using this state estimate. Notice that the possibility $2r < m$ is allowed and in some circumstances positively encouraged. If $2r = m$ then the state and measurement vectors are of equal dimensions. In this case state vector may be found, formally, by matrix inversion. In practical problems this matrix inversion may be ill-conditioned. The condition of the problem may be improved by using a reduced model with a lower order, providing there are sufficient degrees of freedom to model all of the measured modes. Remember from Section 6.3 that the accuracy of the zeroth order reduction algorithm improves as order of the reduced model increases.

Mathematically the linearised equations of motion in the frequency domain are, from equations 6.1 and 6.2,

$$\left.\begin{aligned} &\left\{ \left[\mathbf{M}_0 + \delta\theta_1 \mathbf{M}_1 + .. + \delta\theta_p \mathbf{M}_p\right] j\omega \; + \right. \\ &\qquad \left. \left[\mathbf{K}_0 + \delta\theta_1 \mathbf{K}_1 + .. + \delta\theta_p \mathbf{K}_p\right] \right\} \mathbf{X}(\omega) = \mathbf{B}\,\mathbf{U}(\omega) + o\left(\delta\theta^2\right) \\ &\mathbf{Y}(\omega) \;=\; \mathbf{C}\,\mathbf{X}(\omega) \end{aligned}\right\} \quad (7.10)$$

where $\mathbf{X}(\omega)$, $\mathbf{Y}(\omega)$ and $\mathbf{U}(\omega)$ are the transforms of the state, output and input vectors respectively and the matrices are defined in Chapter 6.

Reducing this equation to one with r degrees of freedom using the zeroth order transformation gives, by analogy with equation 6.7,

$$\left.\begin{aligned} &\left\{ \left[\mathbf{I}_{2r} + \delta\theta_1 \mathbf{M}_{z1} + .. + \delta\theta_p \mathbf{M}_{zp}\right] j\omega \; + \right. \\ &\qquad \left. \left[\Lambda_0 + \delta\theta_1 \mathbf{K}_{z1} + .. + \delta\theta_p \mathbf{K}_{zp}\right] \right\} \mathbf{W}(\omega) \;=\; \mathbf{B}_z \mathbf{U}(\omega) + o\left(\delta\theta^2\right) \\ &\mathbf{Y}_z(\omega) \;=\; \mathbf{C}_z\,\mathbf{W}(\omega) \end{aligned}\right\} \quad (7.11)$$

where $\mathbf{W}(\omega)$ and $\mathbf{Y}_z(\omega)$ are the transforms of the reduced order state and its theoretical output and the matrices are again defined in Chapter 6.

The transform of the reduced state vector $\mathbf{W}(\omega)$ has to be estimated from the measured output $\mathbf{Y}_m(\omega)$. Assuming that $2r \leq m$ and $\mathbf{C}_z$ has rank equal to 2r then the least squares estimate of the frequency response function based

on the reduced state given by $W_m(\omega)$, is

$$F_{Rm}(\omega) = \frac{W_m}{U_m}(\omega) = (C_z^T C_z)^{-1} C_z^T F_m(\omega) \quad . \tag{7.12}$$

What happens if the inversion of $C_z^T C_z$ is ill-conditioned? This matrix may be written as

$$C_z^T C_z = \Phi_0^T C^T C \Phi_0 \quad . \tag{7.13}$$

As Φ_0 is of rank 2r to obtain the inverse of $C_z^T C_z$ then C must be of at least rank 2r. Hence r must be chosen so that $2r \leq \text{rank}(C)$. Usually the rank of C is the same as the dimension of the measurement vector. The largest possible r should be tried initially so that the inaccuracies in the analytical frequency response functions due to the reduction process are minimised, as described in Section 6.3. The order of the reduced model is then reduced until the matrix inversion is well conditioned. This is accomplished by neglecting rows and columns of $C_z^T C_z$. The elements of the matrix defined by equation 7.13 may be written as

$$(C_z^T C_z)_{ik} = {}_0\Phi_i^T C^T C \, {}_0\Phi_k \quad . \tag{7.14}$$

Thus reducing the degrees of freedom of the reduced model by one involves removing the last two rows and columns from $C_z^T C_z$.

7.4.2 Equation Error Algorithm

Once the frequency response functions in terms of the reduced state vectors have been estimated then the unknown parameters may be updated by minimising the following cost function.

$$J(\delta\theta) = \sum_{k=1}^{N} \sum_{i=1}^{2r} \sum_{h=1}^{q} \left| \left[\mathbf{D}(\omega_k, \delta\theta)\, \mathbf{F}_{Rm}(\omega_k) - \mathbf{B}_z \right]_{ih} \right|^2 \qquad (7.15)$$

where $\mathbf{D}(\omega_k, \delta\theta) = \left[\mathbf{I}_{2r} + \delta\theta_1 \mathbf{M}_{z1} + .. + \delta\theta_p \mathbf{M}_{zp} \right] j\omega_k + \left[\Lambda_0 + \delta\theta_1 \mathbf{K}_{z1} + .. + \delta\theta_p \mathbf{K}_{zp} \right].$

This effectively minimises the force or equation error for the system. Figure 7.5 shows the flow chart of the estimation algorithm. Equation 7.15 represents the simplest least squares estimation. As the simulated example in section 7.4.4 will show, this type of equation error algorithm has serious drawbacks. A slight extension to equation 7.15 is the weighted least squares algorithm which involves minimising

$$J(\delta\theta) = \sum_{k=1}^{N} \sum_{i=1}^{2r} \sum_{h=1}^{q} W_k \left| \left[\mathbf{D}(\omega_k, \delta\theta)\, \mathbf{F}_{Rm}(\omega_k) - \mathbf{B}_z \right]_{ih} \right|^2 \qquad (7.16)$$

where $\mathbf{D}(\omega_k, \delta\theta)$ is defined in equation 7.15 and W_k is a weighting function which may change throughout the frequency range of interest. For example W_k could be 1 for ω_k near to resonances of the measured system and zero elsewhere. Minimising equation 7.16 would then provide more weight to the areas of the frequency response function close to resonance. Goyder's method may be considered to be a particular case for this weighting function.

Equations 7.15 and 7.16 represent unconstrained least squares optimisation problem which is easily solved. In practical problems it is desirable to set constraints on the unknown physical parameters so that, for example, the length of an element does not become negative. Adding a term to penalise parameter deviations from the original analytic parameter values is the most easily implemented, although indirect, method to introduce these constraints.

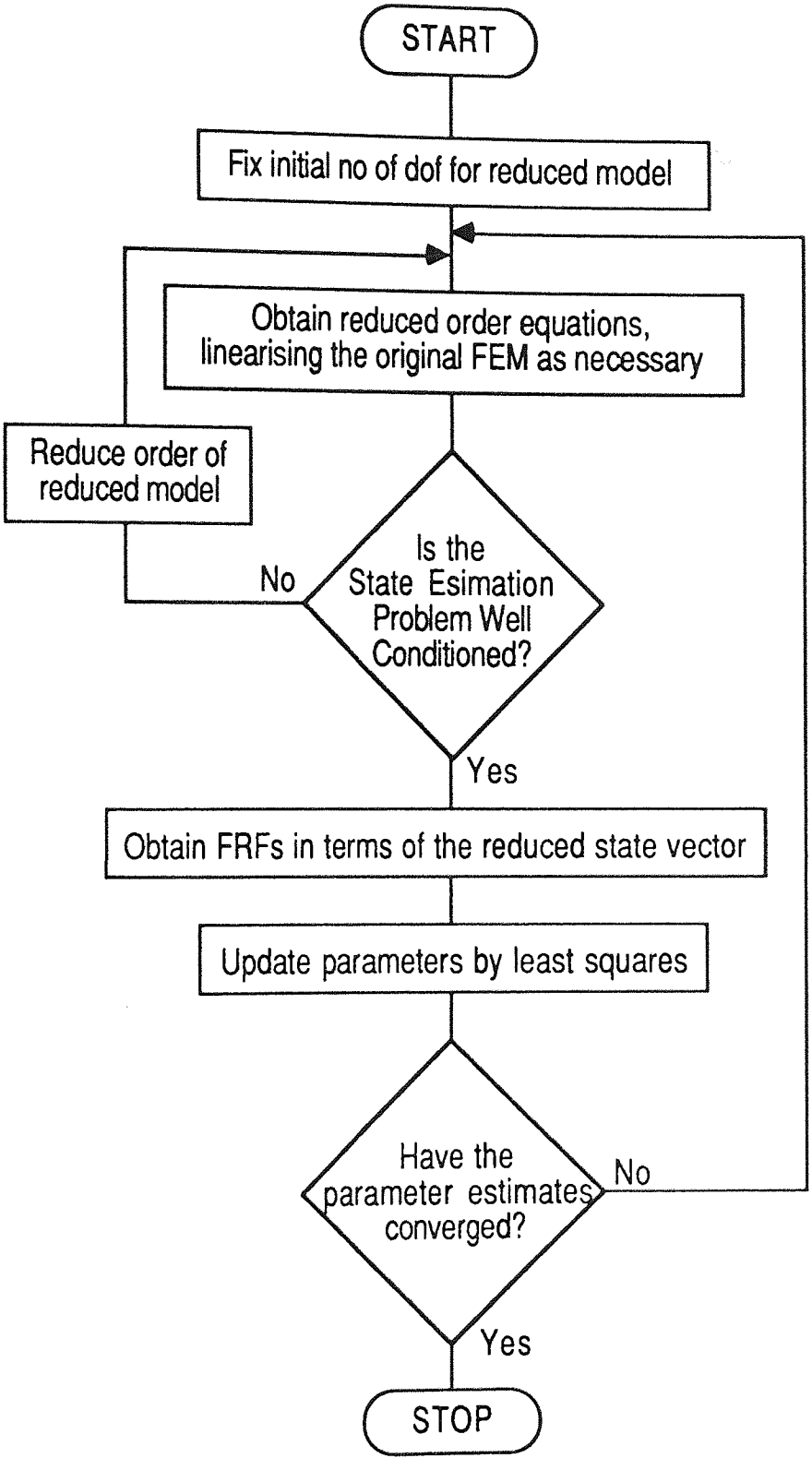

Figure 7.5 Flow Chart of Parameter Estimation Scheme

Mathematically a term

$$J_1(\delta\theta) = \left(\theta_e - \theta_a + \delta\theta\right)^T \mathbf{W}_\theta \left(\theta_e - \theta_a + \delta\theta\right) \qquad (7.17)$$

is added to equations 7.15 and 7.16, where θ_a is the original analytically derived parameter vector and $\mathbf{W}_\theta$ is a weighting matrix which is generally diagonal but is certainly positive definite. The weighted least squares algorithms given by equations 7.16 and 7.17 may be incorporated into the estimation scheme whose flow chart is given in figure 7.5.

7.4.3 An Extension of Goyder's Method

Suppose that the state estimator given in section 7.4.1 has already been used to obtain the frequency response function in terms of the reduced state vector, $\mathbf{F}_{Rm}(\omega)$. Then, based on these frequency response functions, an output error algorithm would minimise

$$J(\delta\theta) = \sum_{k=1}^{N} \sum_{i=1}^{2r} \sum_{h=1}^{q} \left| \left[\mathbf{F}_{Rm}(\omega_k) - \left[\mathbf{D}(\omega_k, \delta\theta)\right]^{-1} \mathbf{B}_z \right]_{ih} \right|^2 \qquad (7.18)$$

where $\mathbf{D}(\omega_k, \delta\theta)$ is given in equation 7.15.

$[\mathbf{D}(\omega_k, \delta\theta)]^{-1}$ is a highly nonlinear function of $\delta\theta$ and the direct minimisation of equation 7.18 would be very computer intensive. Direct minimisation may also give the problems experienced by the Newton Raphson technique in the minimisation of the one dimensional system in section 7.2. Goyder [1980] suggested a method for one dimensional systems, described in section 7.2, to overcome these difficulties. This method may be extended to the current problem by minimising

$$J(\delta\theta) = \sum_{k=1}^{N} \sum_{i=1}^{2r} \sum_{h=1}^{q} \left| \left[\mathbf{E}\left(\omega_k, \delta\theta \right) \right]_{ih} \right|^2 \qquad (7.19)$$

where $\mathbf{E}\left(\omega_k, \delta\theta \right) = \left[\mathbf{D}_0 (\omega_k) \right]^{-1} \left(\mathbf{D} (\omega_k, \delta\theta)\, \mathbf{F}_{Rm}(\omega_k) - \mathbf{B}_z \right)$

$\mathbf{D} (\omega_k, \delta\theta)$ is given in equation 7.15 and

$\mathbf{D}_0\left(\omega_k \right) = \mathbf{I}_{2r}\ j\omega_k + \Lambda_0$.

Note that $\mathbf{D}_0(\omega_k)$ is diagonal so that the inversion in equation 7.19 is particularly simple. On convergence minimising equation 7.19 is the same as minimising the output error based on the frequency response functions of the estimated state vector. Convergence to an output error more closely associated with the true output error is obtained by minimising

$$J(\delta\theta) = \sum_{k=1}^{N} \sum_{i=1}^{m} \sum_{h=1}^{q} \left| \left[\mathbf{E}\left(\omega_k, \delta\theta \right) \right]_{ih} \right|^2 \qquad (7.20)$$

where $\mathbf{E}\left(\omega_k, \delta\theta \right) = \mathbf{C}_z \left[\mathbf{D}_0 (\omega_k) \right]^{-1} \left(\mathbf{D} (\omega_k, \delta\theta)\, \mathbf{F}_{Rm}(\omega_k) - \mathbf{B}_z \right)$

and $\mathbf{D}(\omega_k,\delta\theta)$ and $\mathbf{D}_0(\omega_k)$ are defined in equations 7.15 and 7.19 respectively.

Minimising equation 7.20 will only result, on convergence, in minimising the output error if $\mathbf{C}_z$ is square. Often it is possible to meet this condition. The rank of $\mathbf{C}_z$ and the choice of the number of degrees of freedom in the reduced model have been discussed in section 7.4.1. This method requires that the number of degrees of freedom in the reduced model be as large as possible so that

$$C_z \left(C_z^T C_z \right)^{-1} C_z^T$$

is as close to the identity matrix as possible. In fact the above matrix will have 2r unity eigenvalues and the remaining eigenvalues will be zero.

Weight may also be given to the initial analytically estimated parameters in a similar way to the equation error method. In this case the term given in equation 7.17 is added to the cost function given by equation 7.19 or 7.20.

7.4.4 Simulated Example of a H Frame

The algorithms suggested in this section were tested using the undamped, simulated free-free frequency response of a H frame. The dimensions of the H

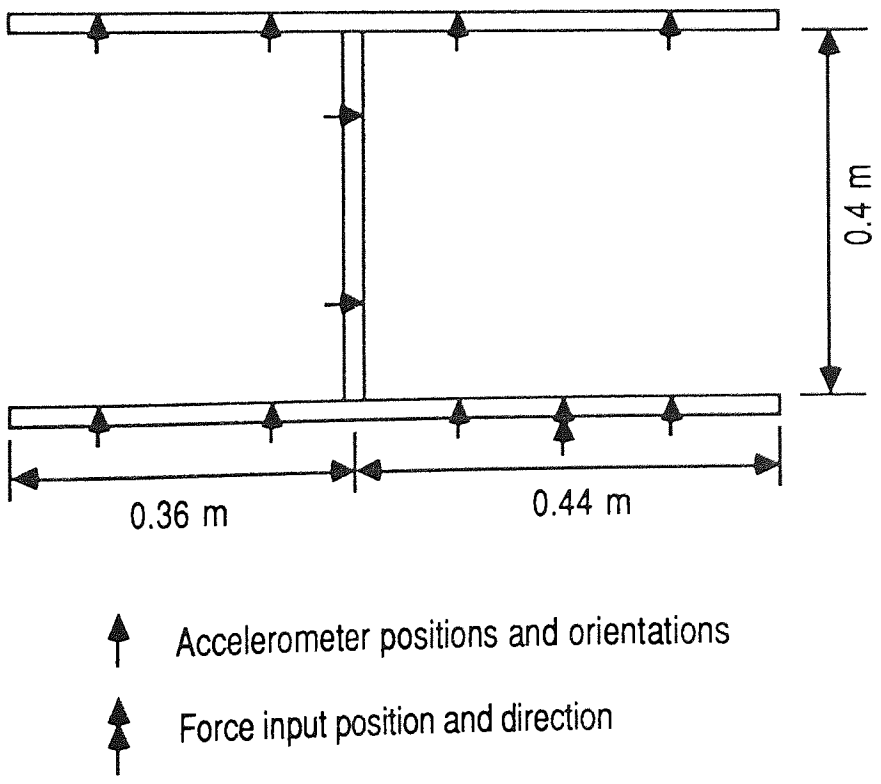

Figure 7.6 Dimensions of the H Frame Used in the Simulated Example

frame are shown in figure 7.6. Only motions in the plane of the frame are modelled. Thus each node is modelled using three degrees of freedom (two displacements and one rotation). Also shown in figure 7.6 are the accelerometer positions and orientations for the ten transducers and the position and direction of the single force input. Appendix D outlines the derivation of the finite element model for this system.

Four cases will be used to demonstrate the algorithm. No random noise has been added to the simulated data since it would present little trouble to the least squares algorithms. Cases III and IV demonstrate model mismatch which is a more difficult error to deal with. In all cases the reduced model order is nine. In cases I and II the frame is both simulated and modelled using 20 elements, which produces a 63 degree of freedom model. Each leg consists of eight elements and the cross beam has four elements. For case I there are three unknown parameters, the flexural rigidity of different groups of elements, defined in table 7.3. In this case the mass and stiffness matrices are linear functions of the unknown parameters. Case II has the length of the outer cross beam elements as an additional unknown parameter. The mass and stiffness matrices are highly nonlinear functions of this length. Case I is designed to show purely the effect of the model order reduction process. With no reduction the algorithm would produce the parameters in one iteration. Case II shows the effect of the mass and stiffness matrices being nonlinear functions of the physical parameters. The first two cases do not include the term, given in equation 7.17, to penalise deviations from the initial value of the parameters. Cases III and IV use a model with 40 elements, that is 123 degrees of freedom, to simulate the experimental data. The parameter updating algorithm tries to fit the data to a 20 element, or 63 degree of freedom, model. Thus the simulated data has errors with significant structure when compared to the model used for updating. This is more representative of the difficult errors encountered in fitting models to experimental data than adding random noise to the simulated data of case I and II. Cases II and IV update the same parameters as cases I and II respectively and these are

Parameter Number	Description	Simulation Value		Assumed Analytically Derived Value			
		63 dof	123 dof	case I	case II	case III	case IV
1	Flexural rigidity of elements away from joints	4500	4500	4300	4300	4300	4300
2	Flexural rigidity of elements on legs next to joints	4650	4800	4300	4300	4300	4300
3	Flexural rigidity of elements on cross beam next to joints	4650	4800	4300	4300	4300	4300
4	Length of cross beam elements next to joint	0.105	0.055	0.105 (fixed)	0.1	0.105 (fixed)	0.1

Table 7.3 Description and Values for the Unknown Parameters

given in table 7.3. Because of the model mismatch, the application of the equation error algorithms in cases III and IV requires the addition of the term given in equation 7.17 to limit the parameter deviations.

The simulated frequency response functions have a frequency range of 20 to 550 Hz in 0.5 Hz steps. Figure 7.7 shows the five elastic modes whose frequencies lie within this range. The frequencies and mode shapes given in figure 7.7 are those of the 123 degree of freedom simulation. Table 7.4 compares the computed natural frequencies for the first five elastic modes from the 63 and the 123 degree of freedom simulations. These differences

Elastic Mode Number	Simulated Natural Frequency (Hz) 123 dof Model	63 dof Model	Percentage Difference
1	54.64	54.62	0.0478
2	118.67	118.28	0.3247
3	135.46	135.22	0.1763
4	188.71	188.50	0.1098
5	494.56	495.25	0.1394

Table 7.4 Comparison of Natural Frequencies from the 63 dof and the 123 dof Simulations

in frequency and the similar small differences in frequency response functions show that the difference in input data between cases I and III and cases II and IV is also small. Assuming the input data contains enough information

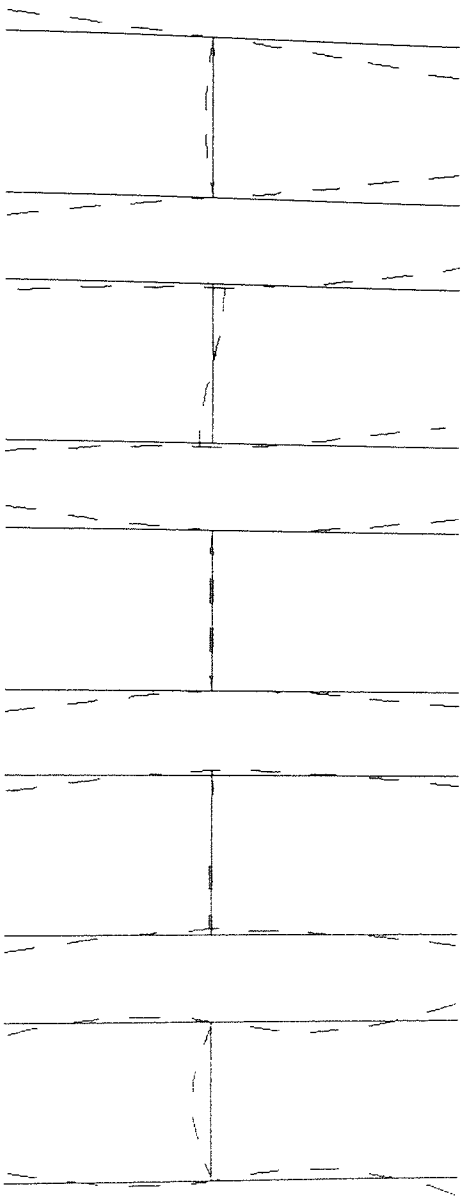

Natural Frequency = 54.6 Hz

Natural Frequency = 118.7 Hz

Natural Frequency = 135.5 Hz

Natural Frequency = 188.7 Hz

Natural Frequency = 494.6 Hz

Figure 7.7 Simulated Data Mode Shapes

about the parameters any parameter estimation algorithm would hopefully produce 'close' parameter estimates for cases I and III and for cases II and IV. The definitions of the unknown parameters, their values for the simulated data and their assumed analytically derived values for the four cases are given in table 7.3.

Figure 7.8 shows a typical simulated frequency response function, derived from the 123 degree of freedom model. Also shown is the corresponding frequency response function based on the 63 degree of freedom analytical model given by the parameter vector (4300,4300,4300,0.1), that is the initial parameters for cases II and IV. Table 7.5 compares the natural frequencies of the 123 dof simulation and the natural frequencies of the 63

Elastic Mode Number	Natural Frequency (Hz)		Percentage Difference
	Simulated 123 dof Model	Analytically Derived Model	
1	54.64	53.45	2.179
2	118.67	116.47	1.854
3	135.46	130.80	3.439
4	188.71	183.01	3.018
5	494.56	488.77	1.169

Table 7.5 Comparison of Natural Frequencies from the 123 dof Simulation and the Initial Analytical Model

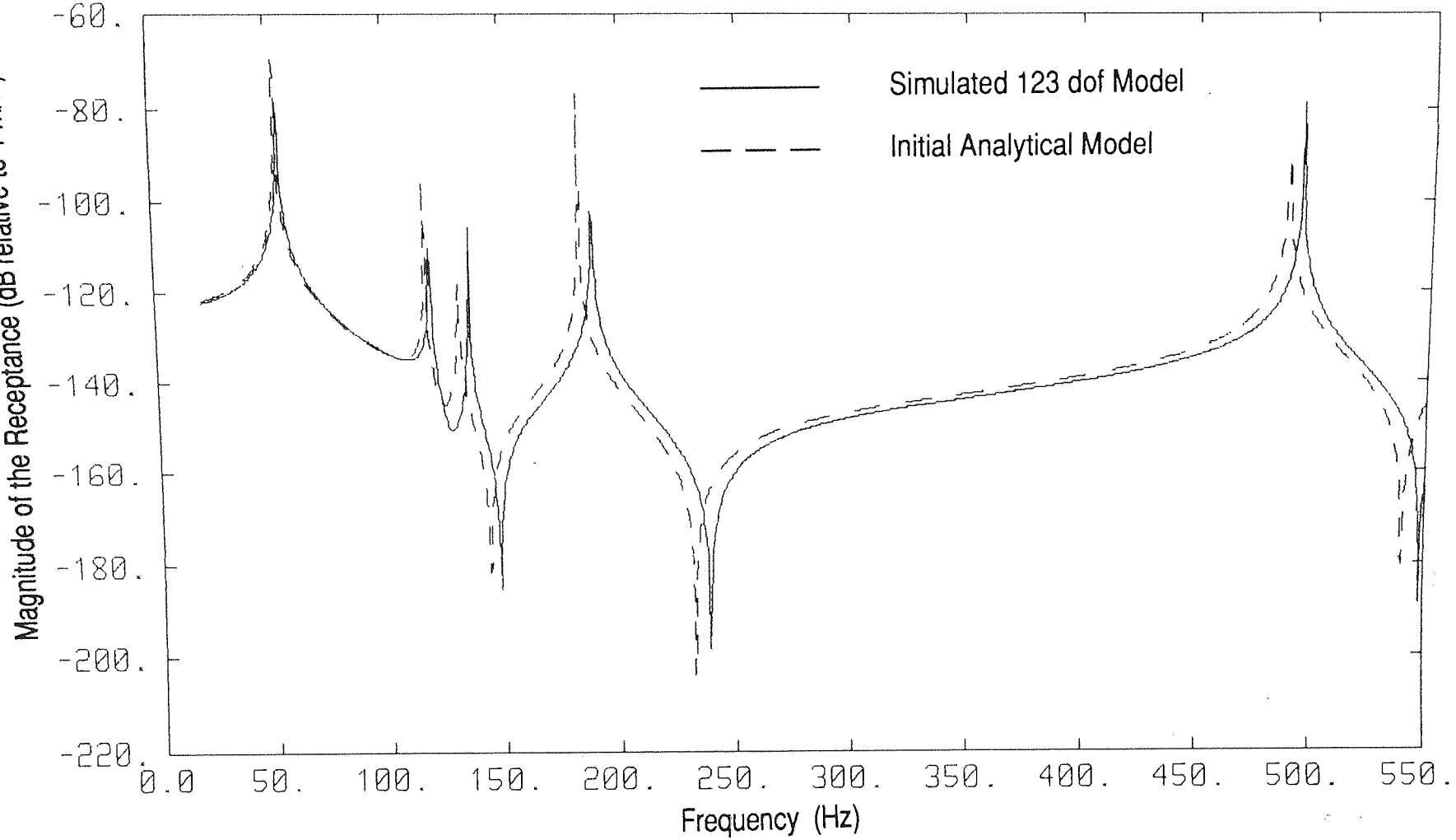

Figure 7.8 Comparison of Typical FRFs from the Simulated 123 dof Model and the Initial Analytical Model

dof model based on the above parameter values. Figure 7.8 and table 7.5 show that there is a small but significant difference between the simulated system and the assumed analytically derived model.

How do the algorithms given earlier cope with this simulated example? There are essentially four algorithms that will be tested. The first, called the Equation Error Algorithm, minimises the ordinary least square equation error given by equation 7.15. In cases III and IV the additional term to weight the initial analytical parameters given in equation 7.17 is used. The value of the weighting matrix W_θ is, for case IV,

$$W_\theta = 10\ \mathrm{diag}\left(0.1^2\ \ 0.1^2\ \ 0.1^2\ \ 4300^2 \right) \qquad (7.21)$$

where the terms are simply related to the magnitude of the elements of the parameter vector. For case III, where there are three unknown parameters, only the top left (3,3) submatrix of equation 7.21 is used. The second method, called the Weighted Equation Error Algorithm, is similar to the Equation Error Algorithm but includes a frequency dependent weighting function, given in equation 7.16. For this simulated example this weighting function is one for frequencies within 15 Hz of the simulated natural frequencies, and zero otherwise. Cases III and IV again need the additional term given by equation 7.17. The value of the weighting matrix is the same as given in equation 7.21 multiplied by the ratio of the number of frequency points used.

The third method, called the Extended Goyder Algorithm, minimises the cost function given by equation 7.19. A fourth method, called the Weighted Extended Goyder Algorithm, is obtained by minimising equation 7.20. This method is not considered further as in this particular example the results are so close to the Extended Goyder Algorithm that the plots of parameter convergence cannot be distinguished.

Consider case I first. Here the mass and stiffness matrices are linear functions of the unknown parameters and the structure of the updated analytical model and the model used to obtain the simulated data are the same. Figure 7.9 shows the convergence of the parameters using the Equation Error and Weighted Equation Error Algorithms, which yield results that produce indistinguishable plots. The parameters converge rapidly, after one or two iterations, and the updated parameters are correct to four significant figures after three iterations. Figure 7.10 shows the convergence of the parameters using the Extended Goyder Method, convergence to four significant figures occurring after two iterations. All the algorithms perform well.

Case II shows the effect of nonlinearities in the updating procedure. The mass and stiffness matrices are highly nonlinear functions of a fourth parameter, an element length, that is introduced. There is still no model structure mismatch so this is a purely nonlinear optimisation problem. Figure 7.11 shows the convergence of the parameter estimates for the first 24 iterations using the Equation Error and Weighted Equation Error Algorithms. Convergence is very slow although eventually the algorithms produce the correct parameter values. Figure 7.12 shows the convergence of the parameter estimates for the Extended Goyder Method. Convergence is now rapid and the result is correct to four significant figures after three iterations.

Case III is the first of the more realistic, and interesting, simulations. Here model mismatch means that there are no correct parameters for the algorithms to converge to. The quality of the algorithms has to gauged from the 'closeness' of the FRFs of the updated model and the simulated data. An alternative is to compare the natural frequencies of the updated model and the simulated system. Figure 7.13 shows the convergence of the parameter estimates using the Equation Error Algorithm. Convergence is rapid in this case, and also for case IV, because of the weighting term required to limit the deviations from the initial analytical estimates. The Weighted Equation Error

Algorithm is similar. Figure 7.14 shows the reduction in cost function for the parameter convergence shown in figure 7.13. Everything looks fine until the frequency response functions for the updated model are compared to those of the simulated data. Figure 7.15 compares typical FRFs and should be compared to figure 7.8. Table 7.6 compares the natural frequencies of the simulated data and the updated model. It is quite obvious that the updated model is worst. The updated natural frequencies are further away from the simulated values than the initial natural frequencies. How is this reconciled with the supposed improvement shown by the reduction in cost function in figure 7.14? The problem is that equation error, not output error, is being minimised. Thus the weight that would naturally apply to resonances in an output error minimisation, because of the increased amplitude, is not present. One possible method to overcome this drawback is to only include frequency values close to the resonances, that is use the Weighted Equation Error Algorithm. Figure 7.16 shows the convergence of the parameter estimates using this algorithm. Table 7.6 shows that the resulting natural frequencies are even worst that those estimated by the Equation Error Algorithm. Figure 7.17 shows the convergence of the parameter estimates using the Extended Goyder Method. Convergence is reasonably rapid, although slow compared to cases I and II. Table 7.6 shows that the updated model accurately reproduces the natural frequencies of the simulated data.

Case IV is similar to case III expect that now the mass and stiffness matrices are nonlinear functions of a fourth parameter. Figures 7.18 and 7.19 show the convergence of the parameter estimates using the Equation Error and Weighted Equation Error Algorithms respectively. The natural frequencies of the updated models and the simulated data are compared in table 7.7, showing that again the algorithms performance is abysmal. The reasons are the same as for case III. Figure 7.20 shows the convergence of the parameter estimates using the Extended Goyder Algorithm. Table 7.7 shows that the natural frequencies of the simulated data are accurately reproduced. Studying figure 7.20 shows that the convergence of the

parameters is quite slow. Figure 7.21 shows the convergence of the natural frequencies of the updated model and shows that some of these frequencies converge extremely rapidly whilst others only converge sluggishly.

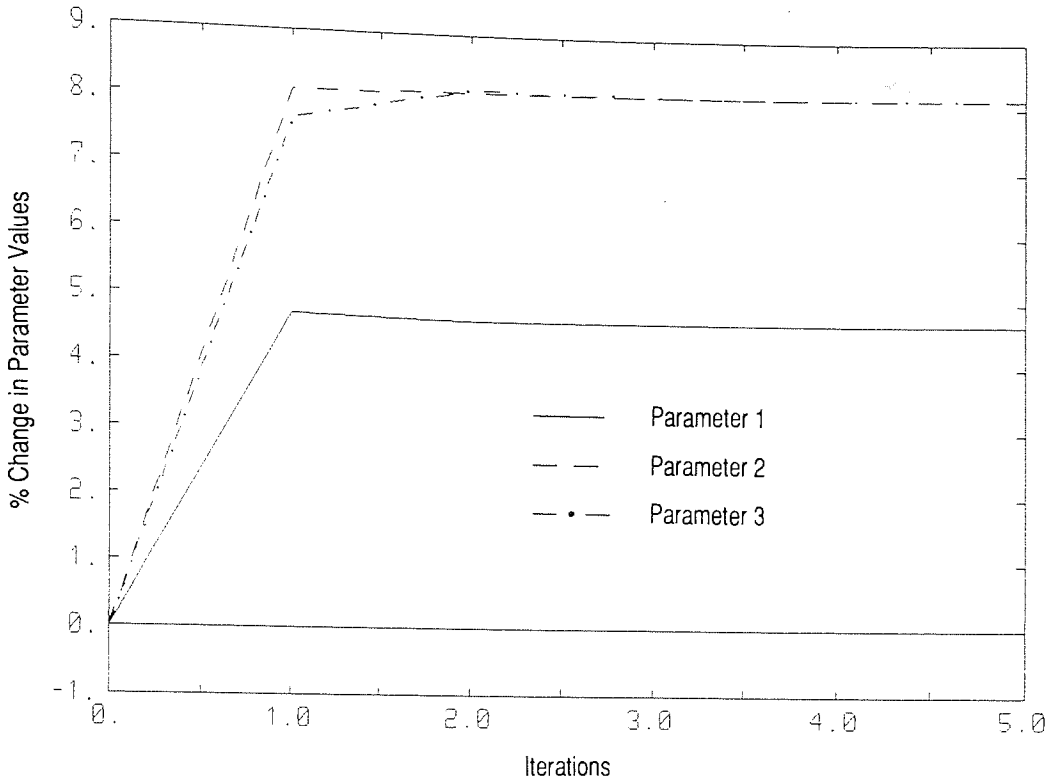

Figure 7.9 Convergence of Parameter Estimates for Case I - Equation Error and Weighted Equation Error Algorithms

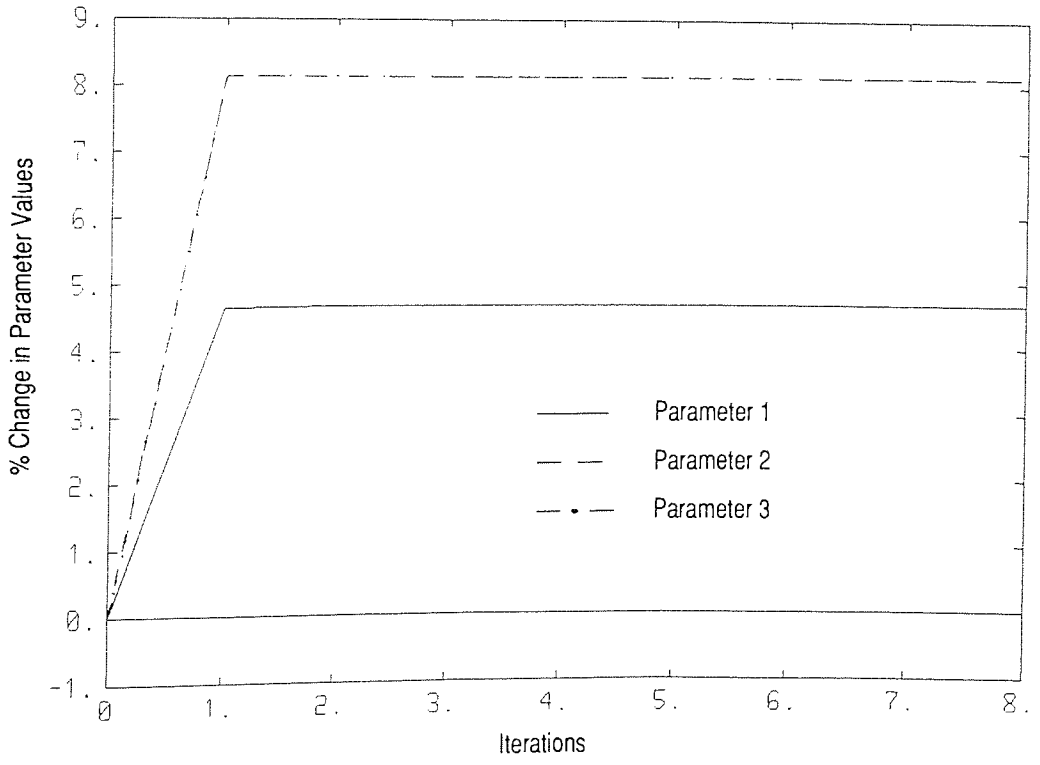

Figure 7.10 Convergence of Parameter Estimates for Case I - Goyder Algorithm

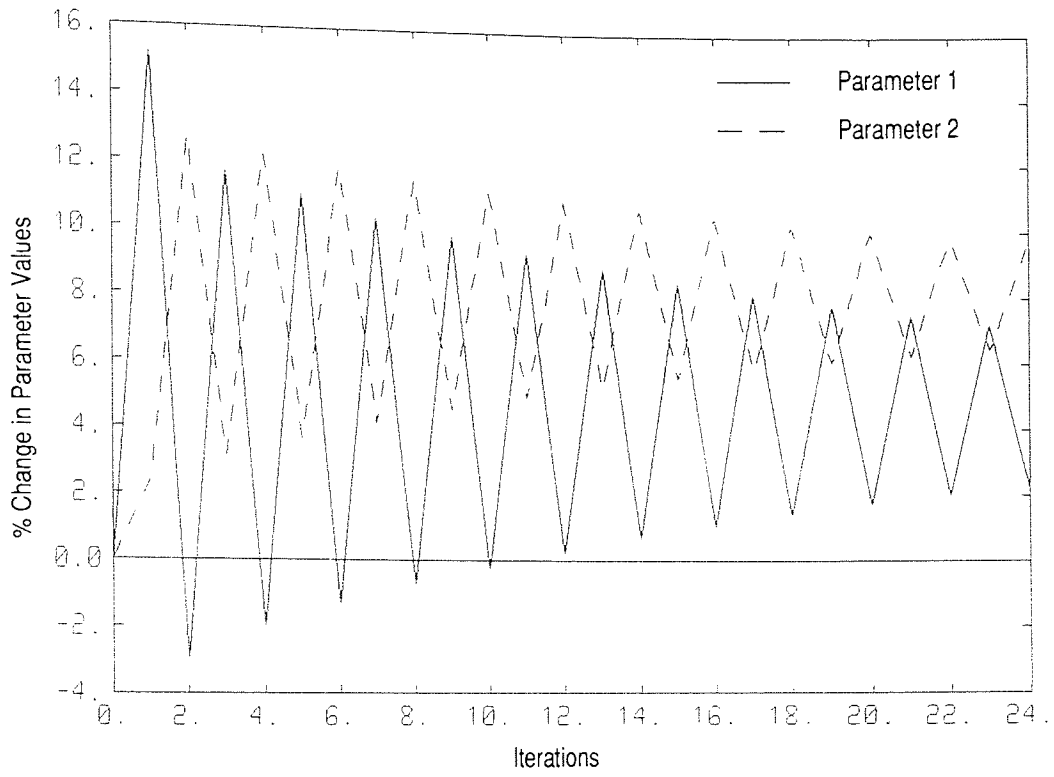

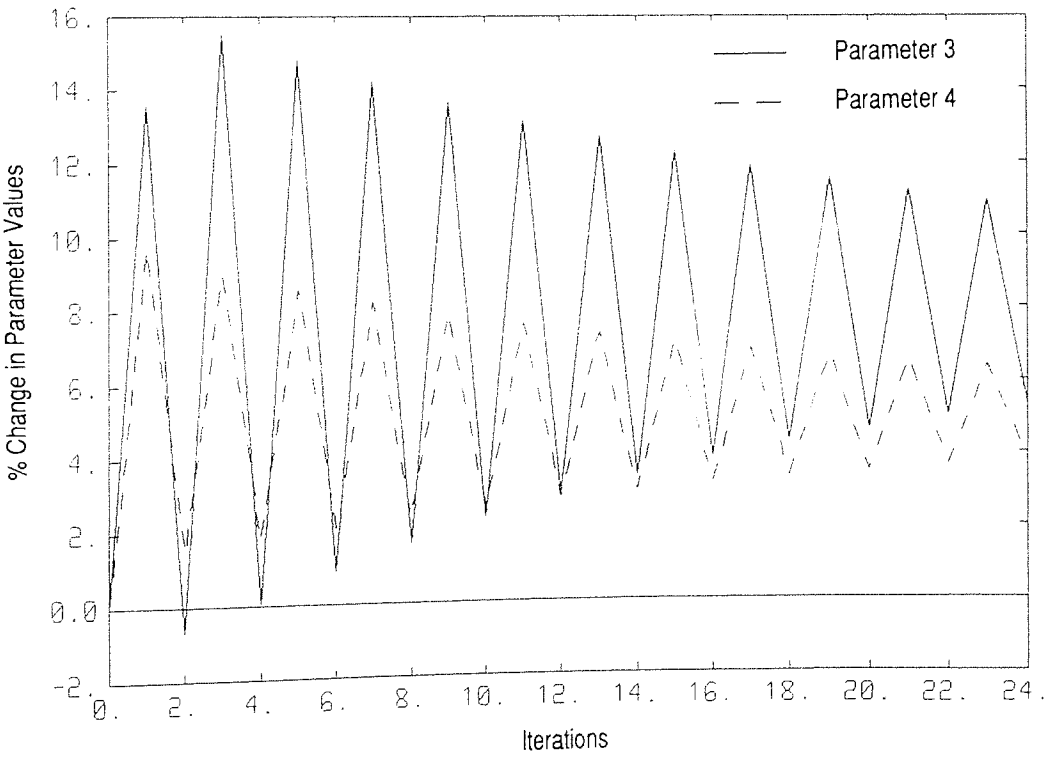

Figure 7.11 Convergence of Parameter Estimates for Case II - Equation Error and Weighted Equation Error Algorithms

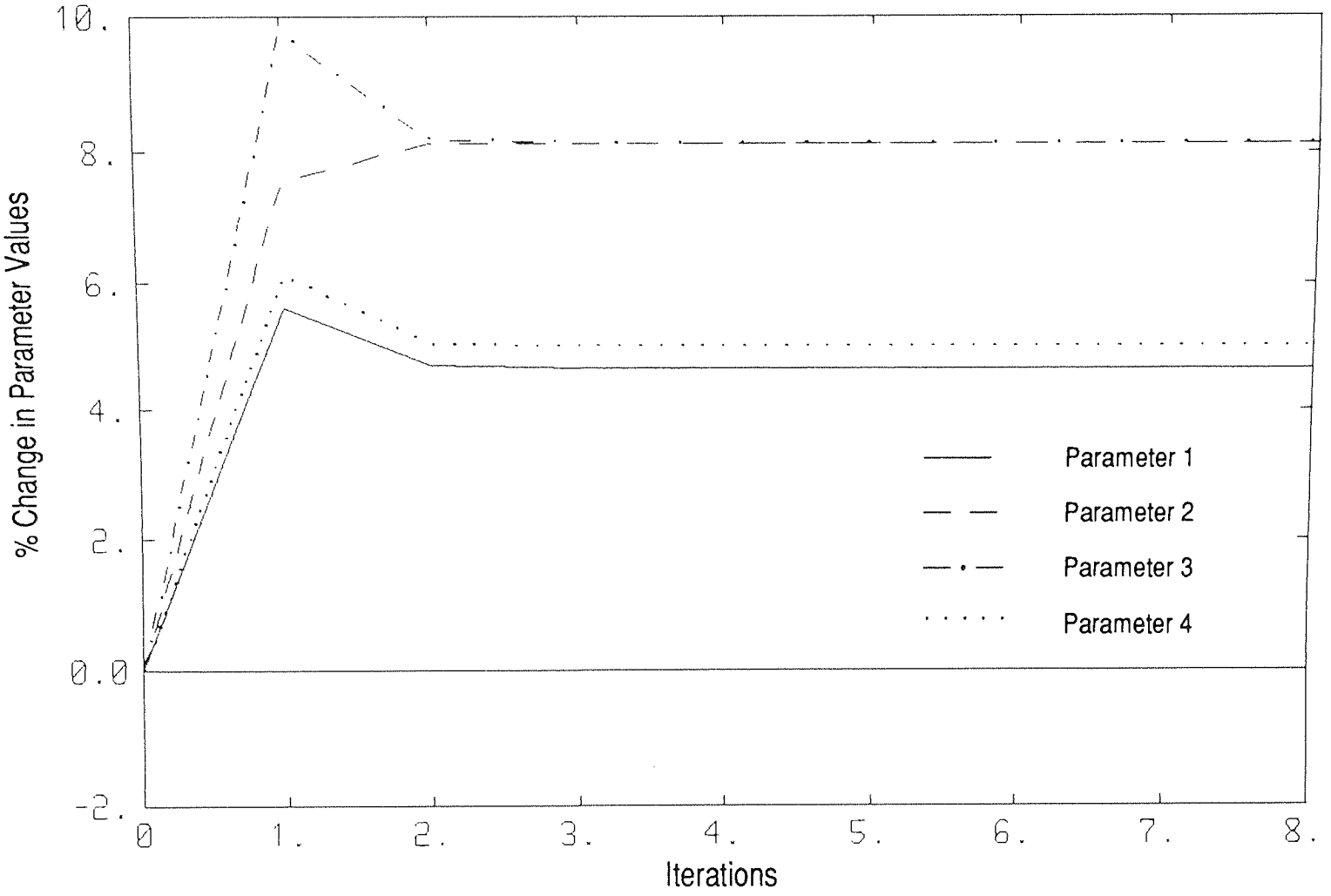

Figure 7.12 Convergence of Parameter Estimates for Case II - Goyder Algorithm

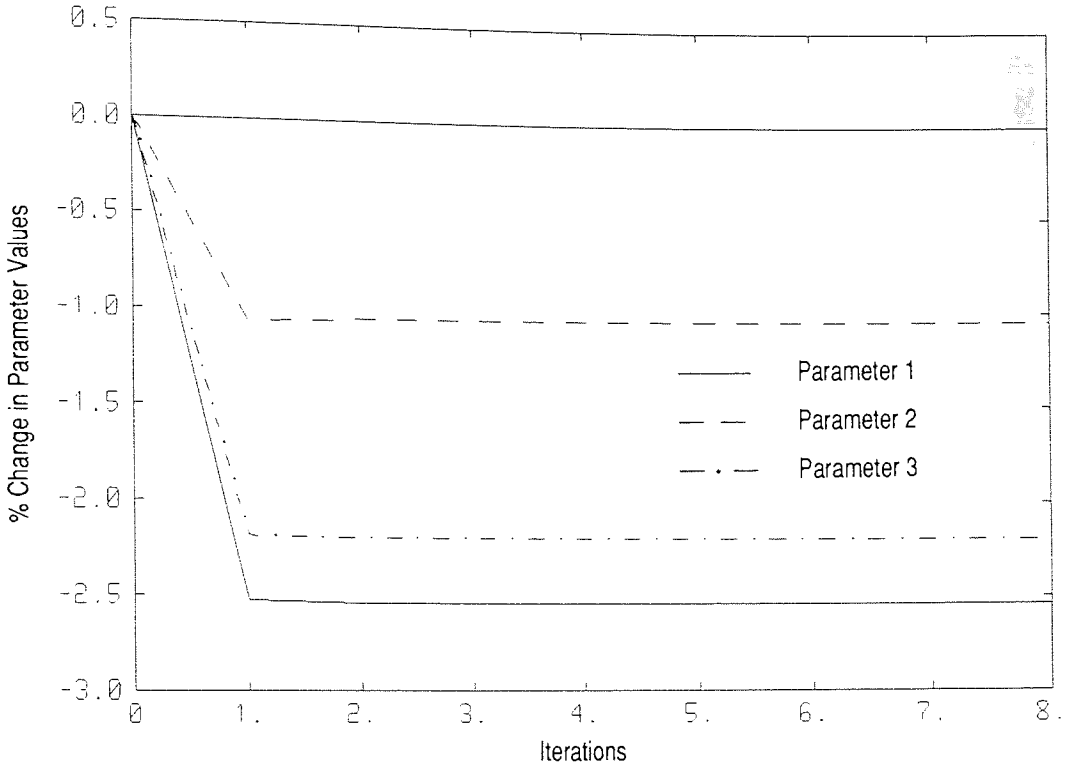

Figure 7.13 Convergence of Parameter Estimates for Case III - Equation Error Algorithm

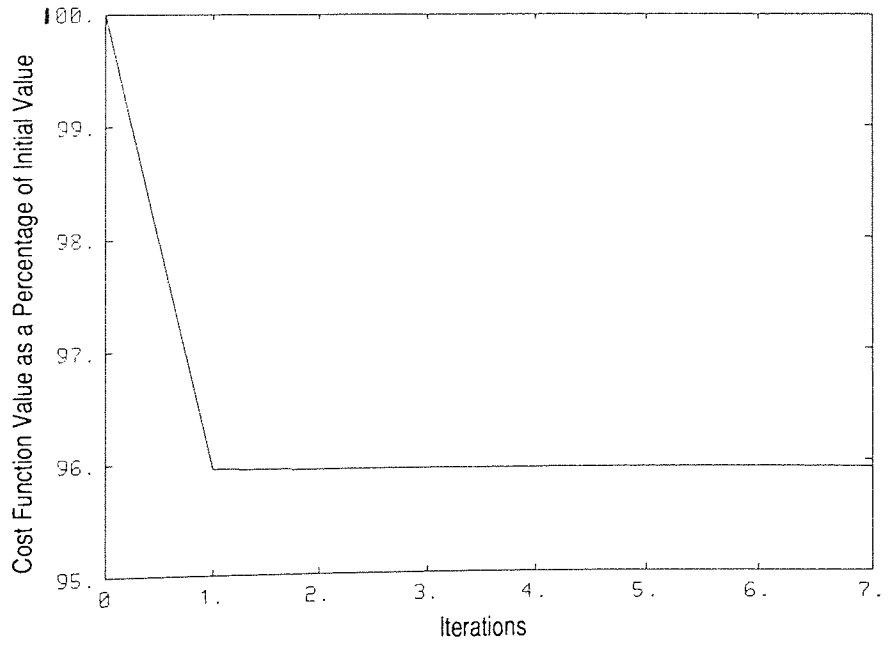

Figure 7.14 Cost Function for Case III - Equation Error Algorithm

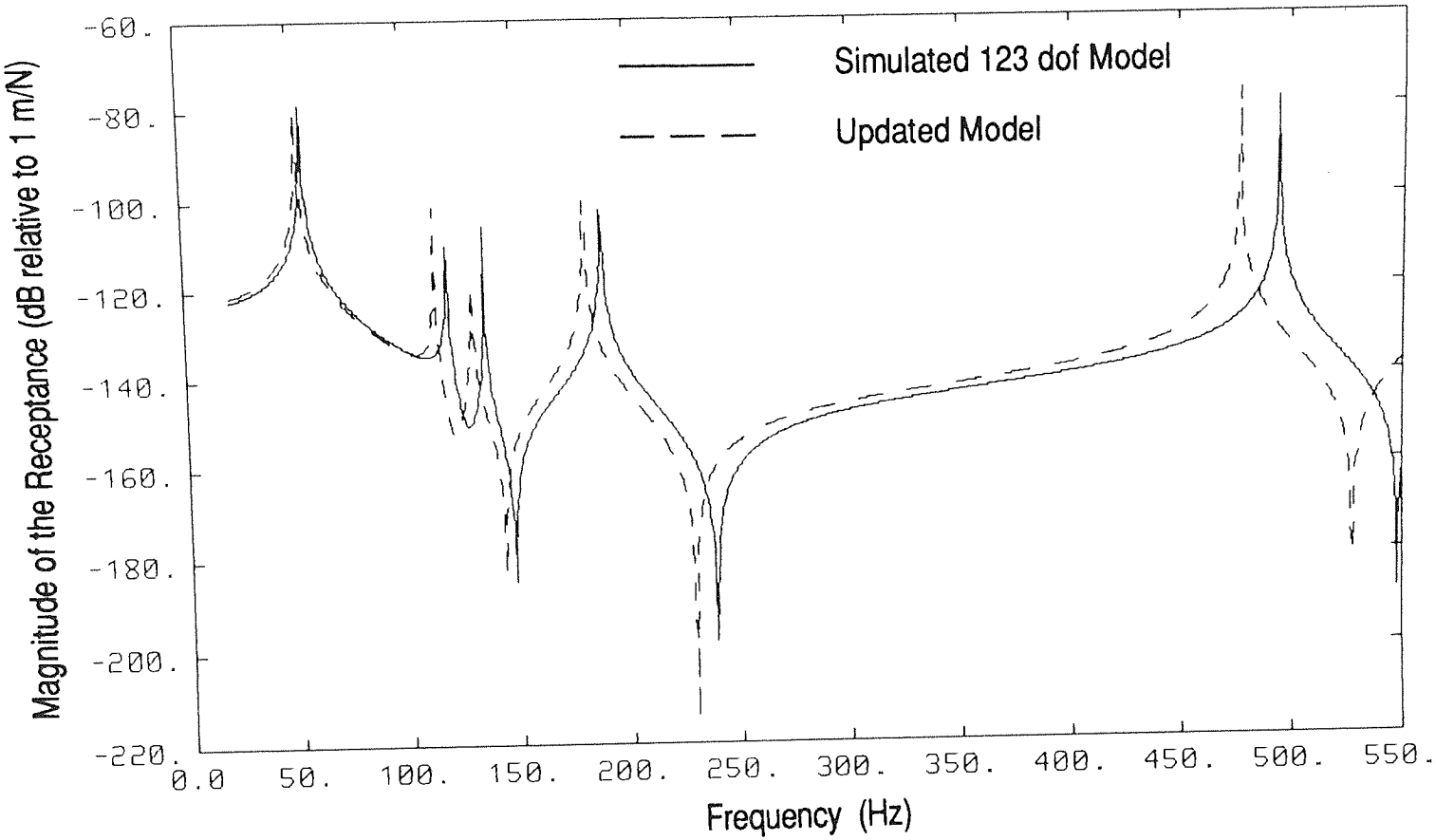

Figure 7.15 Comparison of Typical FRFs from the Simulated Model and the Model Obtained by the Equation Error Algorithm - Case III

Method	Parameter Value on Convergence				Natural Frequencies		Percentage Difference
	1	2	3	4	Simulated	Estimated	
Equation Error	4191	4255	4205	0.105	54.64 118.67 135.46 188.71 494.56	52.33 113.06 129.72 180.83 477.05	4.23 4.73 4.24 4.17 3.54
Weighted Equation Error	3938	4145	3947	0.105	54.64 118.67 135.46 188.71 494.56	50.86 110.20 127.26 177.12 464.00	6.93 7.14 6.05 6.14 6.18
Goyder	4476	4687	4672	0.105	54.64 118.67 135.46 188.71 494.56	54.63 118.49 135.46 188.76 494.59	0.02 0.15 0.00 0.03 0.01

Table 7.6 Summary of Results - Case III

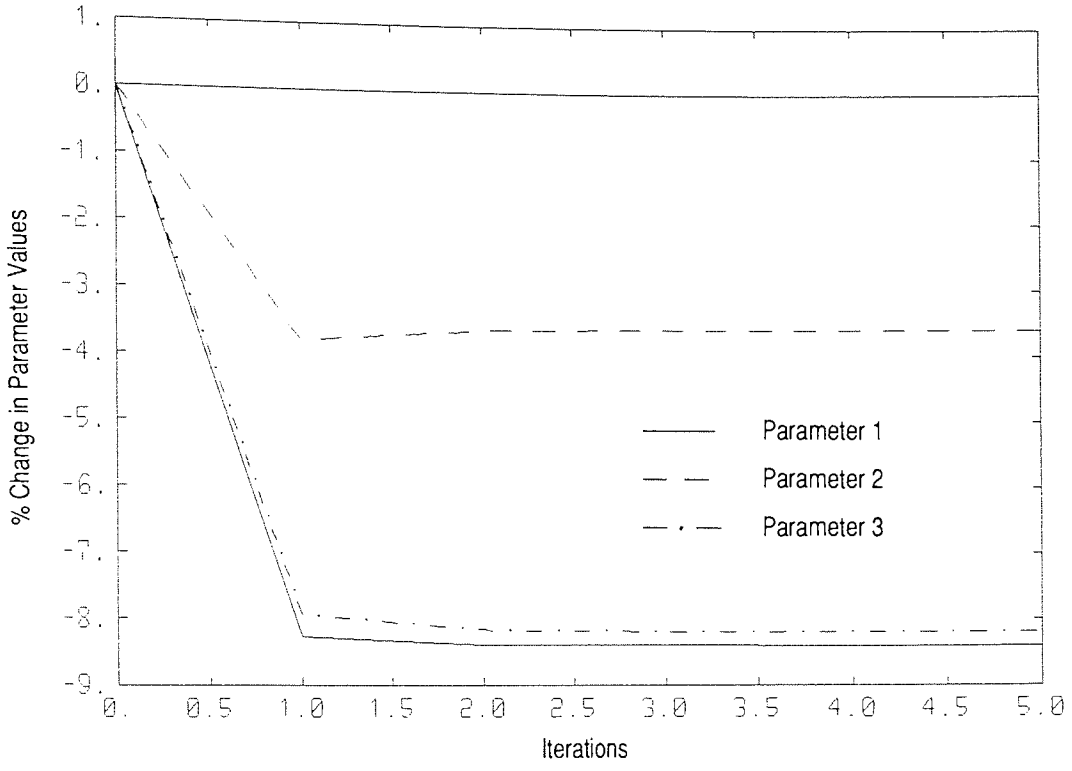

Figure 7.16 Convergence of Parameter Estimates for Case III - Weighted Equation Error Algorithm

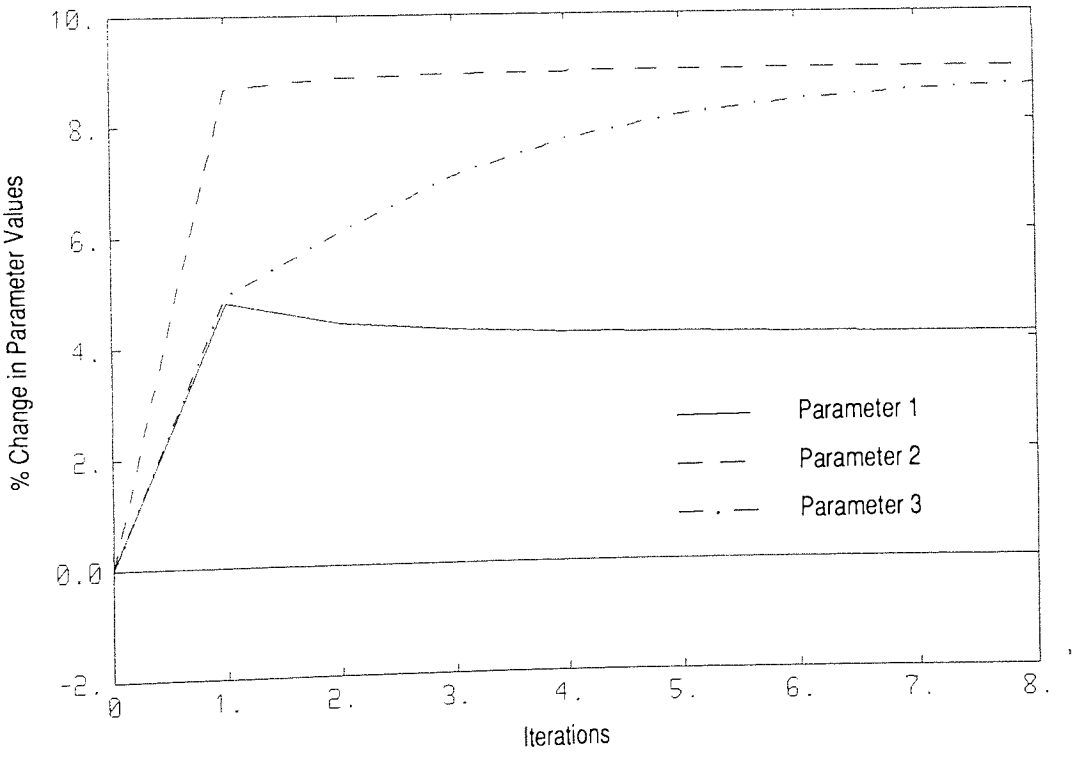

Figure 7.17 Convergence of Parameter Estimates for Case III - Goyder Algorithm

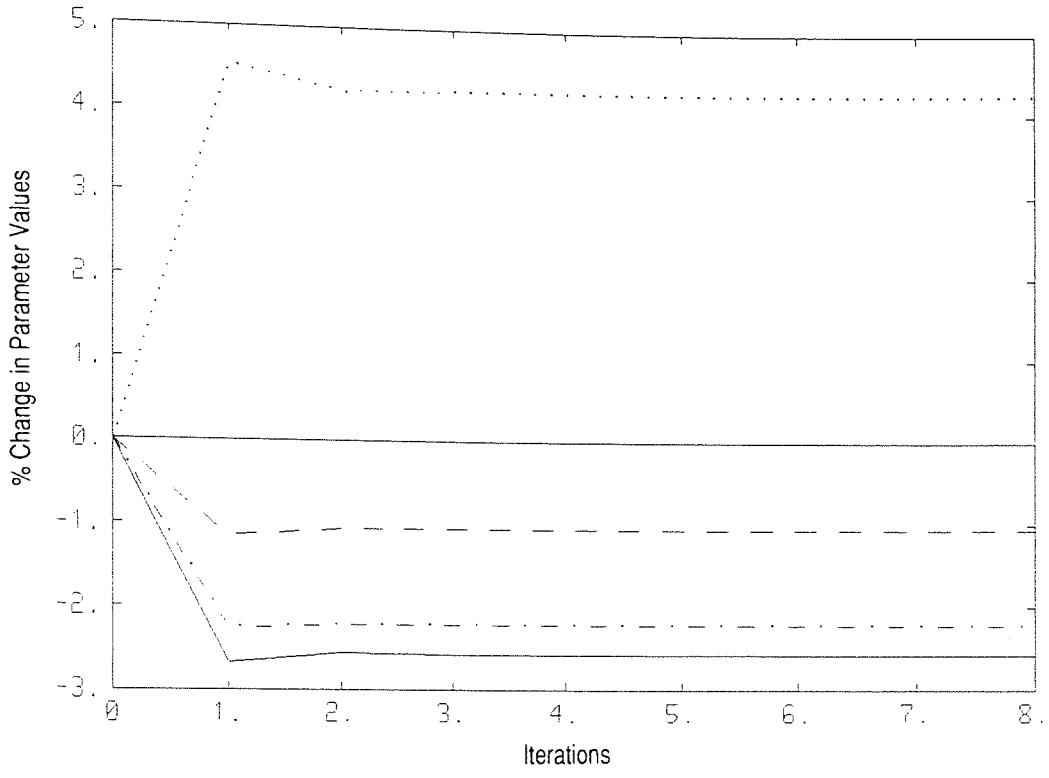

Figure 7.18 Convergence of Parameter Estimates for Case IV - Equation Error Algorithm

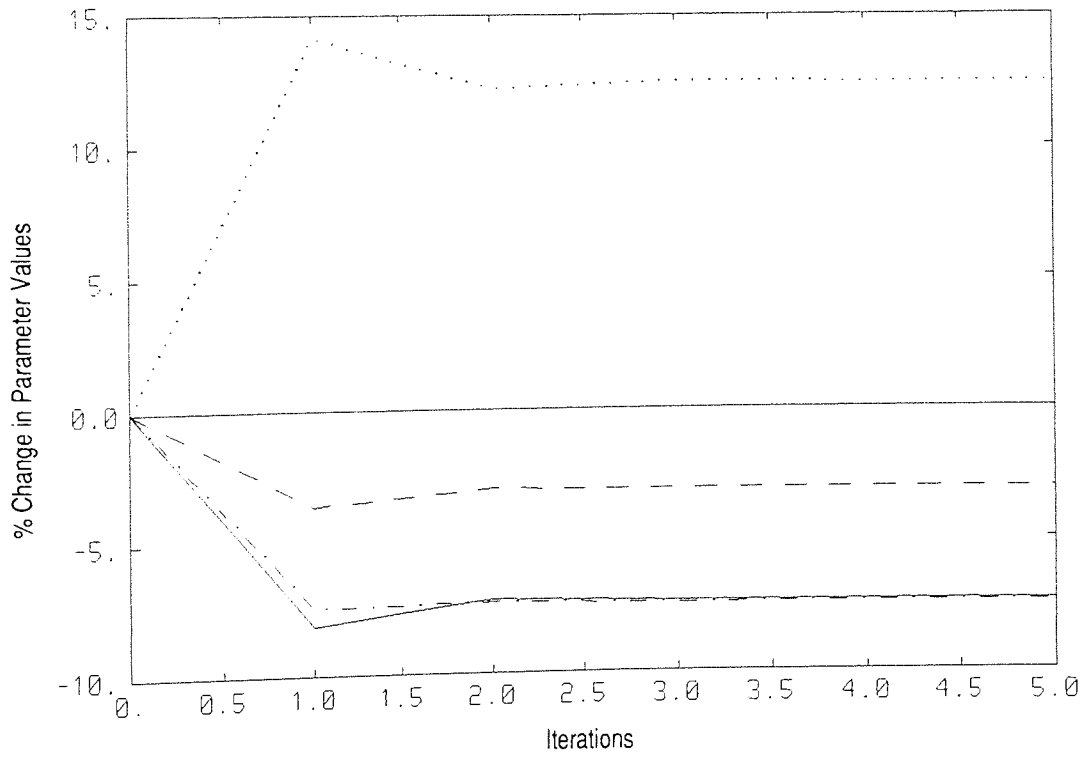

Figure 7.19 Convergence of Parameter Estimates for Case IV - Weighted Equation Error Algorithm

Method	Parameter Value on Convergence				Natural Frequencies		Percentage Difference
	1	2	3	4	Simulated	Estimated	
Equation Error	4189	4254	4204	0.1043	54.64	52.40	4.09
					118.67	113.38	4.45
					135.46	129.71	4.24
					188.71	180.91	4.13
					494.56	477.93	3.36
Weighted Equation Error	3983	4168	3980	0.1124	54.64	50.34	7.87
					118.67	107.49	9.42
					135.46	127.63	5.78
					188.71	176.93	6.24
					494.56	456.50	7.69
Goyder	4462	4693	4674	0.1046	54.64	54.64	0.01
					118.67	118.69	0.01
					135.46	135.46	0.00
					188.71	188.78	0.04
					494.56	494.57	0.00

Table 7.7 Summary of Results - Case IV

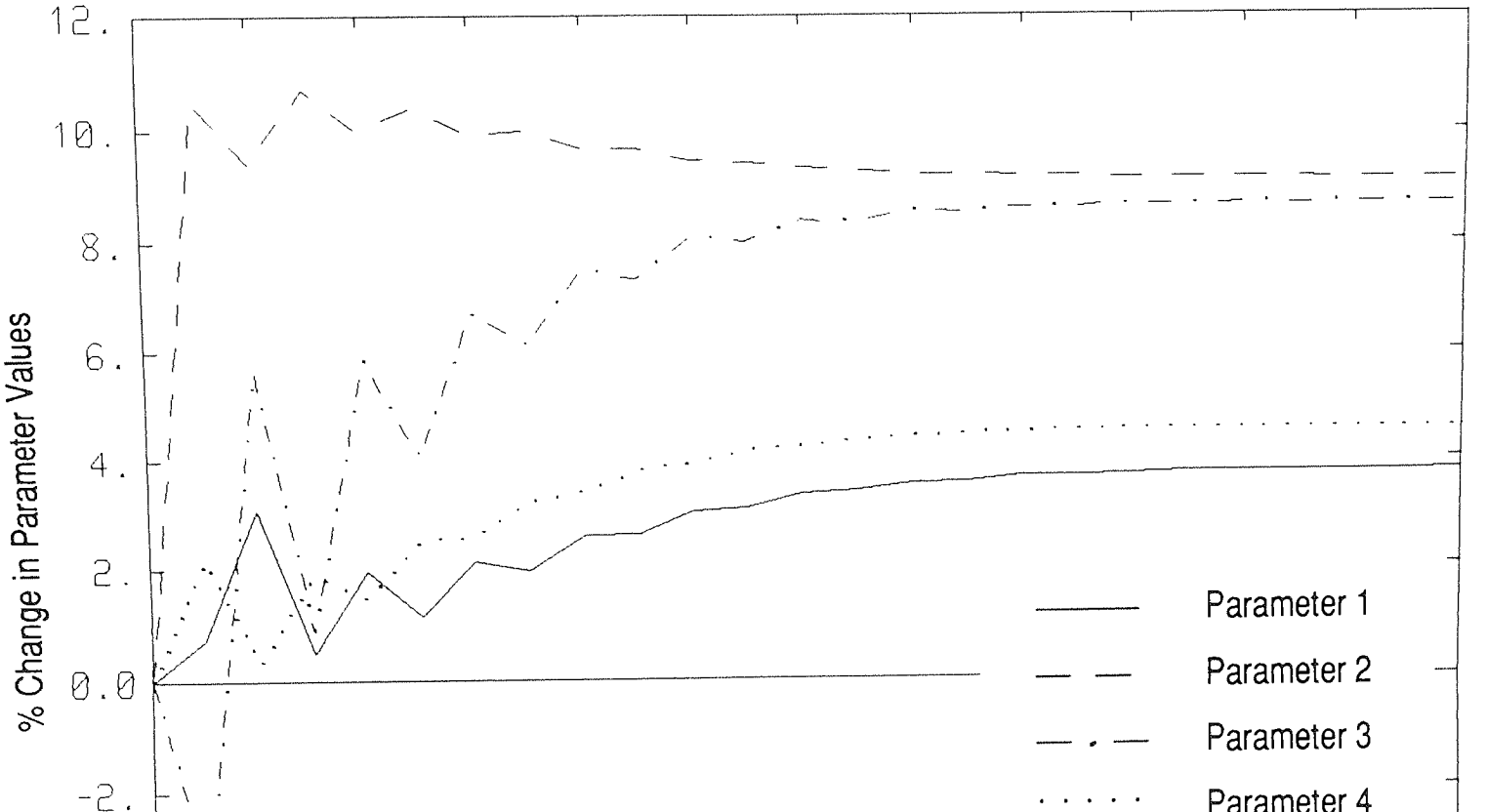

Figure 7.20 Convergence of Parameter Estimates for Case IV - Goyder Algorithm

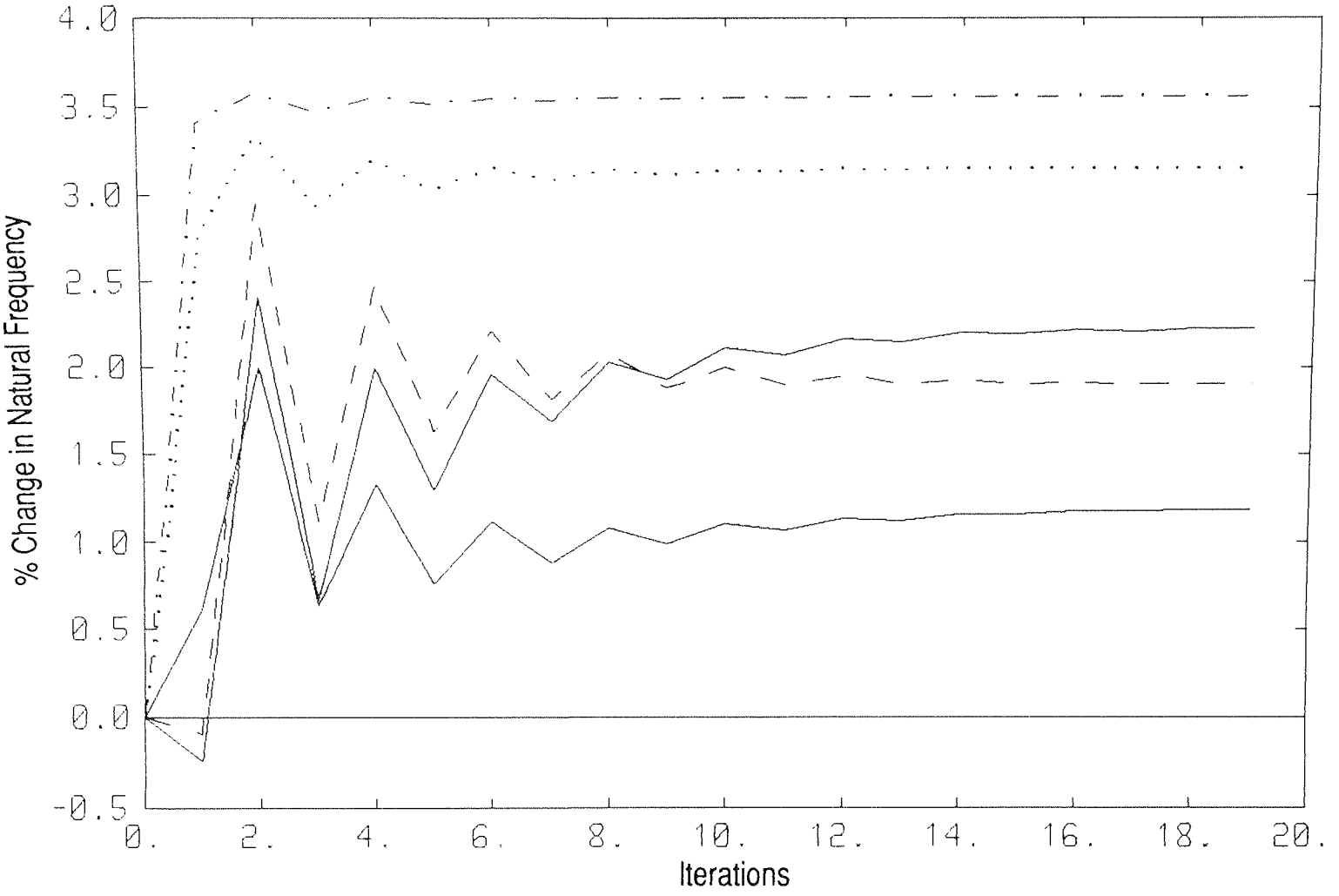

Figure 7.21 Convergence of the Updated Model Natural Frequencies for Case IV - Goyder Algorithm

Chapter 8

Experimental Example

8.1 Chapter Summary

This chapter describes the experimental work performed to demonstrate the algorithms derived in this thesis. The actual hardware and choice of techniques to derive FRFs and the modal model are, in many ways, arbitrary. Different methods and excitation signals may produce slightly different results. All the algorithms in this thesis attempt to find the best physical parameters to reproduce the measured data, allowing for the weighting of the initial analytical parameters. The basic principle that the better the measured data the more accurate the updated parameters therefore applies. Chapter 2 gives more detail on experimental techniques and the general methods used.

The experiments described in this chapter were performed on a H frame structure similar to the one used in the simulated exercise of Section 7.4.4. The algorithms used to update the parameters are the extension to Goyder's method (described in Section 7.4.3) and the corrected minimum variance algorithm (described in Chapter 5).

8.2 Measurement Hardware and Software

The experiments were performed using stepped sine excitation. The excitation signals were generated and the signals correlated to produce the FRF coefficients by a Solartron 1170 two channel Frequency Response Analyser. Although this analyser automates the frequency sweep through the required range it does not record the FRF coefficients automatically. Therefore the analyser is controlled by an IBM PC/AT via a GPIB interface. An 'in house' computer program allows the analyser to be set up from the computer, performs the experiment and records the FRF data on disc. For further analysis using the extension to Goyder's method the data was transferred to the University VAX Cluster using the Kermit file transfer protocol. To apply

the corrected minimum variance algorithm a modal model had to be generated which was obtained using the SMS STAR software package. The modal model was then transferred to the VAX Cluster. The structure is excited using a Derritron 100W shaker and associated amplifier. Brüel and Kjaer force transducer (type 8200), accelerometer (type 4333) and signal conditioning amplifiers (type 2626) were used.

The calibration of the transducers was performed using the method of section 2.7.2. In this case calibration of the transducers could be viewed as verifying the calibration constants quoted by the manufacturers. Figures 8.1 and 8.2 shows the inertance for the calibration tests before and after the experimental results were taken. Taking the average values of the FRFs produces measured masses of 9.30 kg and 8.99 kg from the dynamic tests which compare favourably with the static mass measurement of 9.36 kg. Although the difference may seem high, the discrepancy is, in fact, less than 3.6%. Notice that the FRFs are not constant although, referring to the scale, the change is relatively small. In fact the system does contain resonances at low frequencies due to the elastic supports of the mass and the pendulum action of the mass. The FRFs in figures 8.1 and 8.2 show the high frequency properties of these resonances. Taking the asymptotic value of the FRFs at high frequencies give measured masses of 9.54 kg and 9.30 kg. This produces a difference compared to the static mass measurement of 1.9%. Because the calibration results were so close to those expected the calibration constants quoted by Brüel and Kjaer were used throughout the experiment.

8.3 The Tested Structure

Figure 8.3 shows the structure used to demonstrate the algorithms derived in this thesis. The frame is made of aluminium alloy and has a rectangular cross section measuring 50 x 25 mm. Each joint is made using two bolts. Also

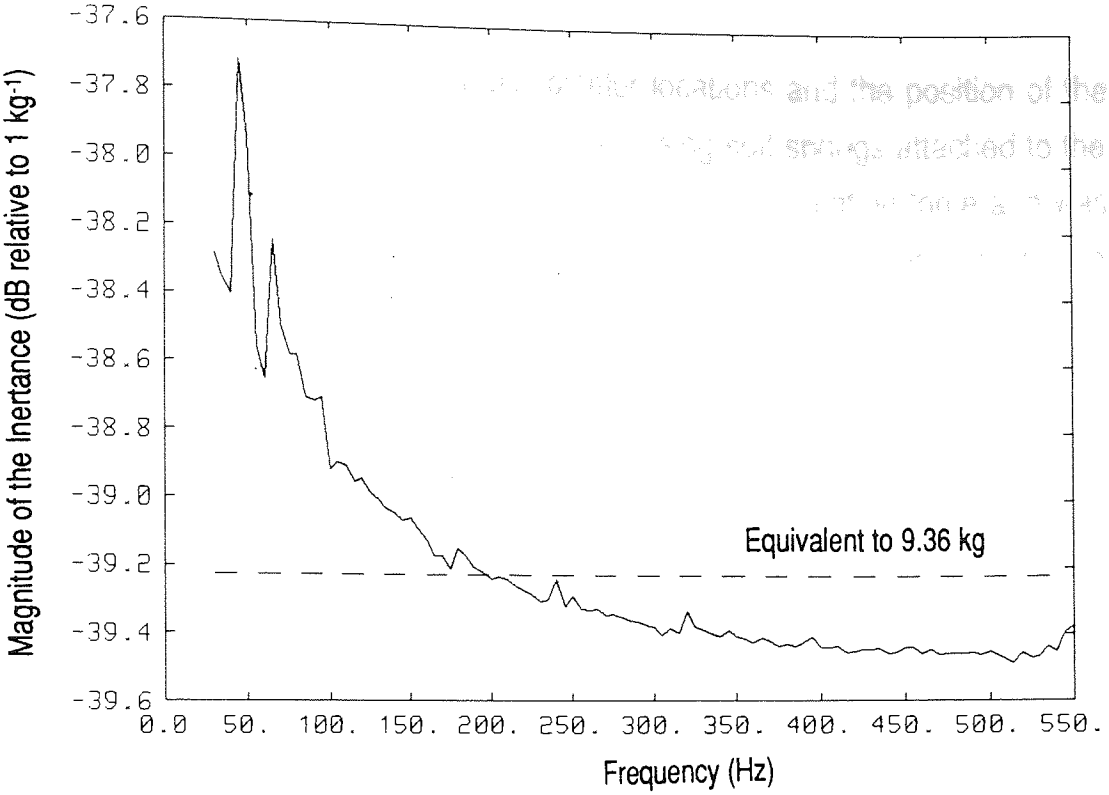

Figure 8.1 Calibration Inertance Obtained Prior to Experiment

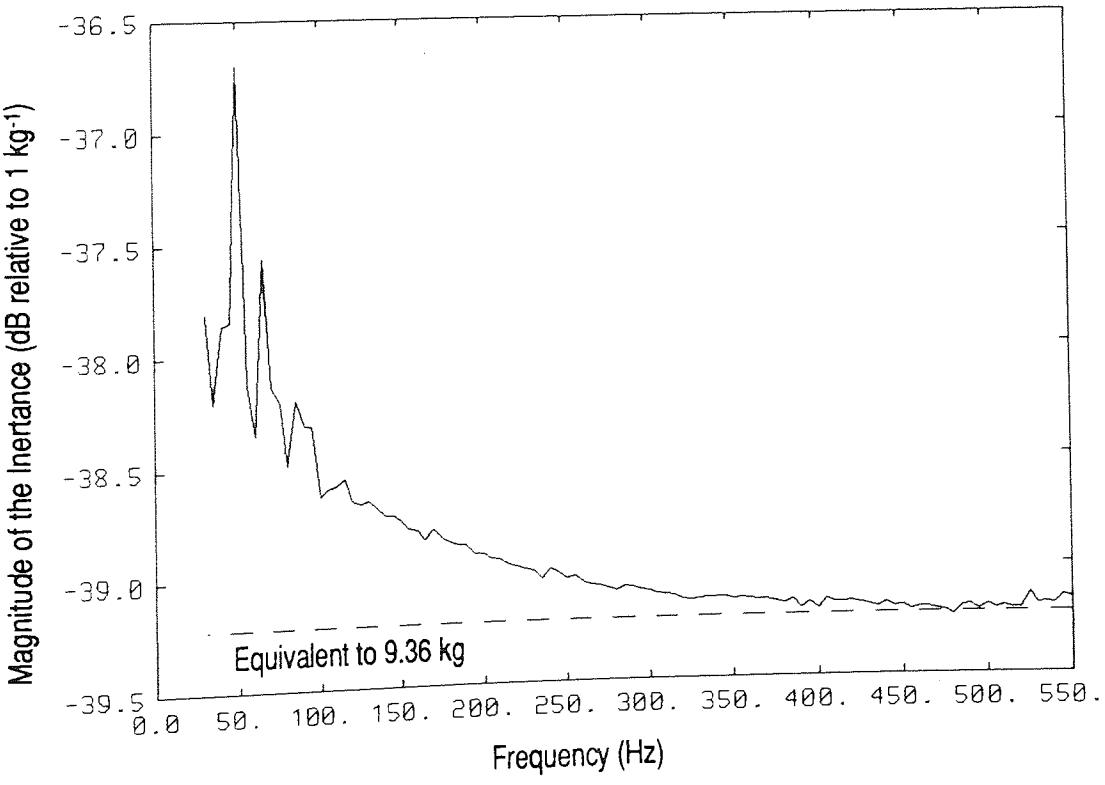

Figure 8.2 Calibration Inertance Obtained after Experiment

shown on figure 8.3 are the accelerometer locations and the position of the force excitation. The H Frame is supported using soft springs attached to the suspension points indicated. A shaker provided the excitation force and was attached to the H Frame by a push rod or stinger. The frequency response functions were measured, using the stepped sine excitation and a single roving accelerometer, in the range 30 to 550 Hz at 0.5 Hz intervals.

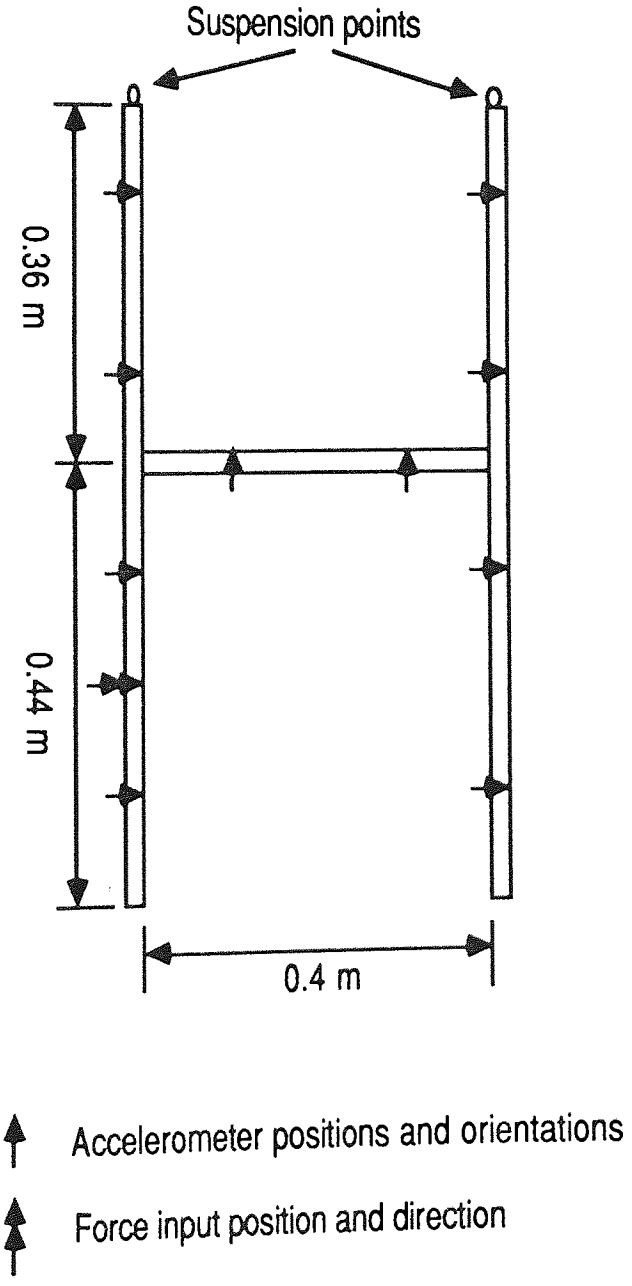

Figure 8.3 **Dimensions of the H Frame and the Experimental Transducer Locations**

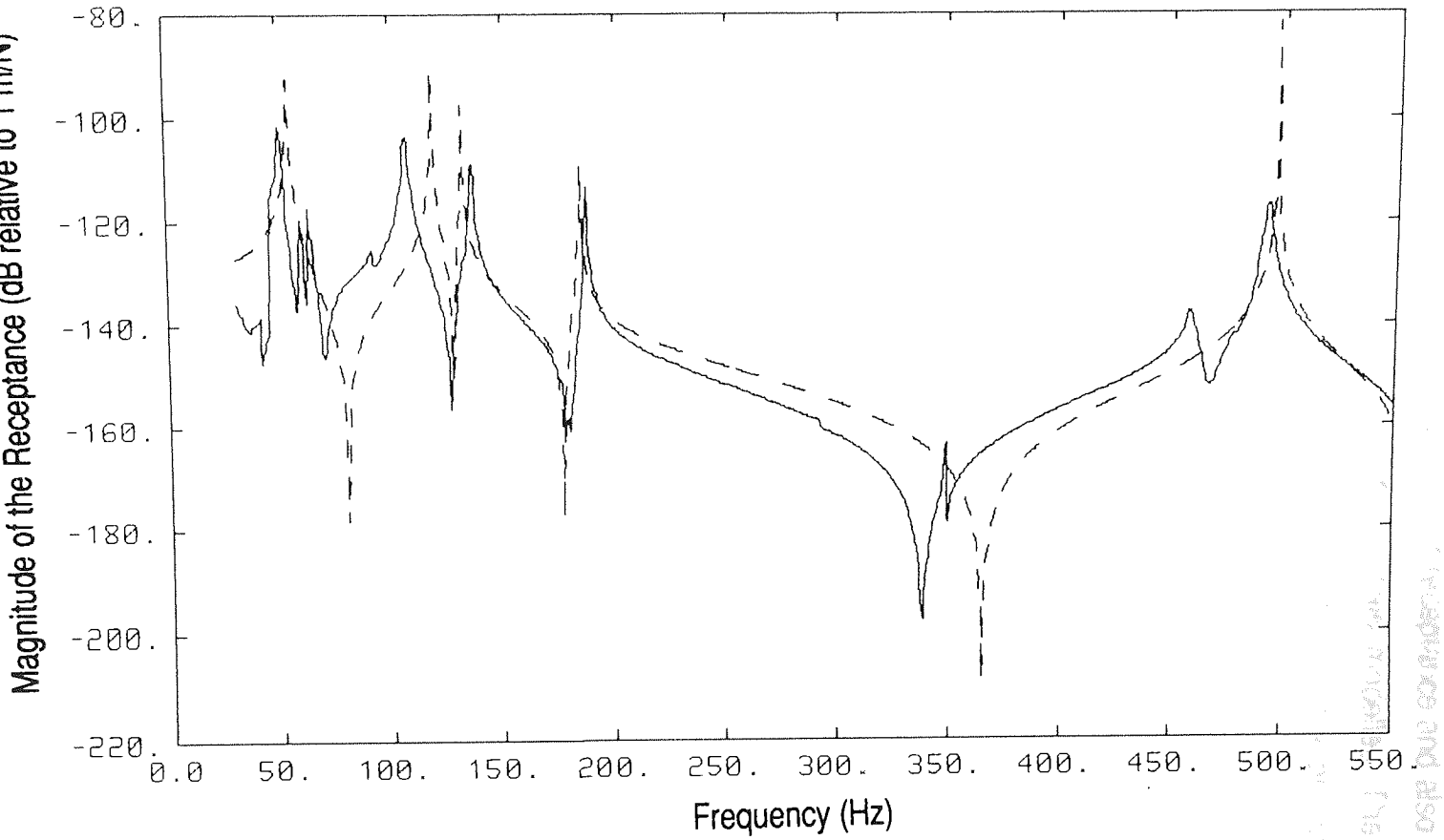

Figure 8.4 Comparis on of Typical Experimental FRF and Modelled FRF

——— Experimental Data - - - - Initial Model

Figure 8.4 shows a typical measured transfer receptance and also shows the equivalent theoretical response function as initially modelled. The measured response seems to have extra resonances, particular at approximately 460 Hz and in the range 50 to 70 Hz. These modes arise due to interactions of the frame with the mounting arrangement. Using the Modal Assurance Criterion they do not correlate well with the theoretical modes and will not be considered further. The five main resonances may be easily identified in the test data and related to the corresponding theoretical modes, shown in figure 7.7. This correspondence will be checked in section 8.5 using the Modal Assurance Criterion.

The choice of parameters to update is a difficult one. In order to demonstrate the algorithm presented in this paper six parameters are updated. These are described in table 8.1 along with the estimated analytical values but are in no way an optimal parameter set. The parameters consist of three flexural rigidities, an element length and two parameters to model proportional damping.

Parameter Number	Description	Estimated Value in Initial Model
1	Flexural rigidity of elements away from joints	4560
2	Flexural rigidity of elements on legs next to joints	4560
3	Flexural rigidity of elements on cross beam next to joints	4560
4	Length of cross beam elements next to joint	0.1
5	Multiplier of the mass matrix for proportional damping	0
6	Multiplier of the stiffness matrix for proportional damping	0

Table 8.1 Description and Initial Values for the Unknown Parameters

8.4 Parameter Updating Directly from the FRFs

The parameters of the structure were first estimated from the FRF data using the extension to Goyder's method derived in section 7.4.3. This example is similar to the simulated one given in section 7.4.4 but where the simulated data has been replaced by experimental data. The FRF measurements were first converted from inertances to receptances by dividing by minus frequency squared.

Figures 8.5 and 8.6 show the convergence of the updated parameters. Figure 8.7 shows the value of the cost function given by equation 7.14. Note that there is no weight given to the initial parameter estimates as described by equation 7.12. Initially there is a large reduction in cost. Subsequent changes in the cost are small and the parameters converge very slowly. This slow convergence occurs because similar modelled receptances may be obtained from many different parameter values. The natural frequencies of the updated model are plotted in figure 8.8 and show that three frequencies converge reasonable quickly. The last natural frequency is not reproduced accurately. This is mainly because the resonance associated with this natural frequency has a low magnitude because the exciter location chosen means that the mode is poorly excited. The fit to the fifth mode would be improved by altering the force input location or by using multi-input forces.

Figures 8.9 and 8.10 show the convergence of the six parameters with a weighting matrix given by

$$W_\theta = 10^{-8} \ \text{diag}\left(0.1^2 , 0 , 0 , 4560^2 , 0 , 0 \right)$$

This weighting matrix implies that parameters 1 and 4 have been analytically estimated most accurately. As expected the parameters now convergence much more quickly. Parameters 1 and 4 change very little from their analytically derived values. Figure 8.11 shows the frequency response function

for the analytical model using the updated parameters with the lowest cost value. The first four resonances have been accurately fitted. The high frequency part of the response and the anti-resonances are a poor fit to the experimental data, again because the magnitude of the responses is small in these areas. Anti-resonances will also be difficult to match because they depend critically on the position of the transducers. The high frequency response of the structure may be given increased weight, if desired, by using mobility or inertance in the updating procedures rather than receptance.

Table 8.2 gives the natural frequencies of the experimental structure, the initial model and the updated models. As stated earlier the first four frequencies are successfully updated.

	Natural Frequencies (Hz)			
	Experi-mental	Initial Model	Updated Model, Not Weighted	Updated Model, Weighted
1	52.6	54.3	51.2	50.0
2	106.7	118.6	106.3	108.5
3	135.7	131.9	135.5	135.4
4	187.7	184.7	183.0	187.7
5	492.4	496.5	358.5	497.9

Table 8.2 **Natural Frequencies from Experiment, Initial Model and Updated Model**

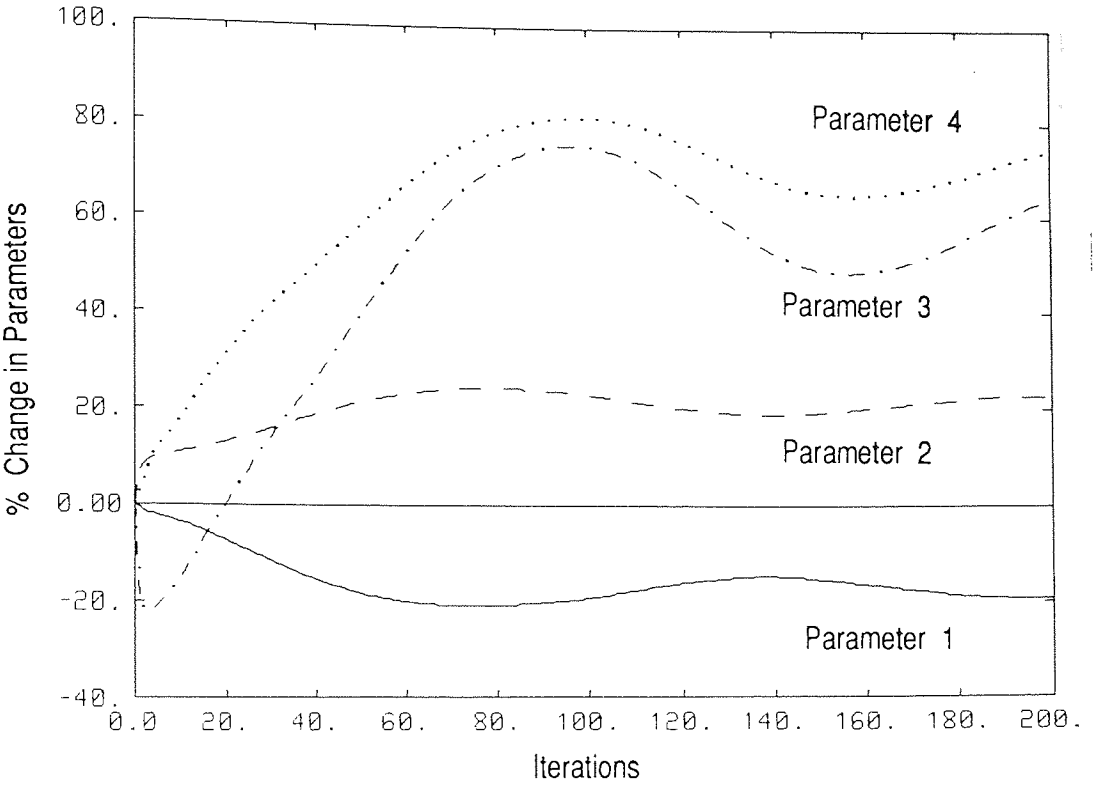

Figure 8.5 Convergence of Parameters 1 to 4. No Weight for Initial Values.

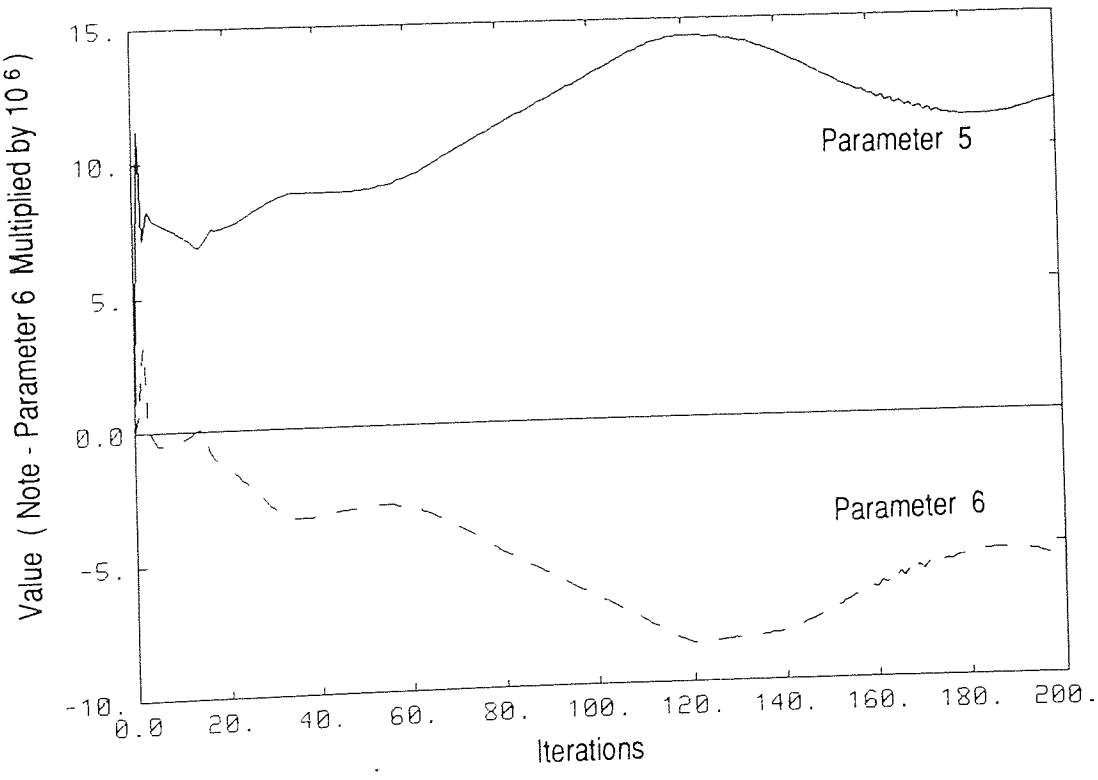

Figure 8.6 Convergence of Parameters 5 & 6. No Weight for Initial Values.

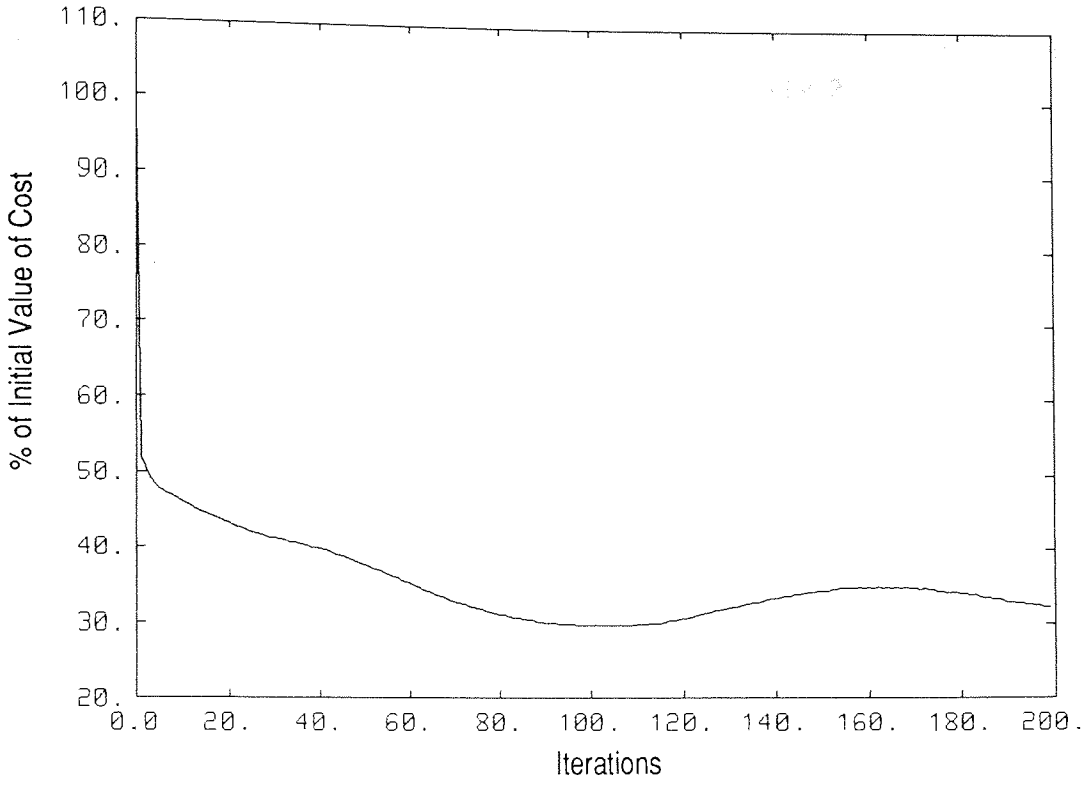

Figure 8.7 Cost Variation During Updating. No Weight for Initial Parameter Values.

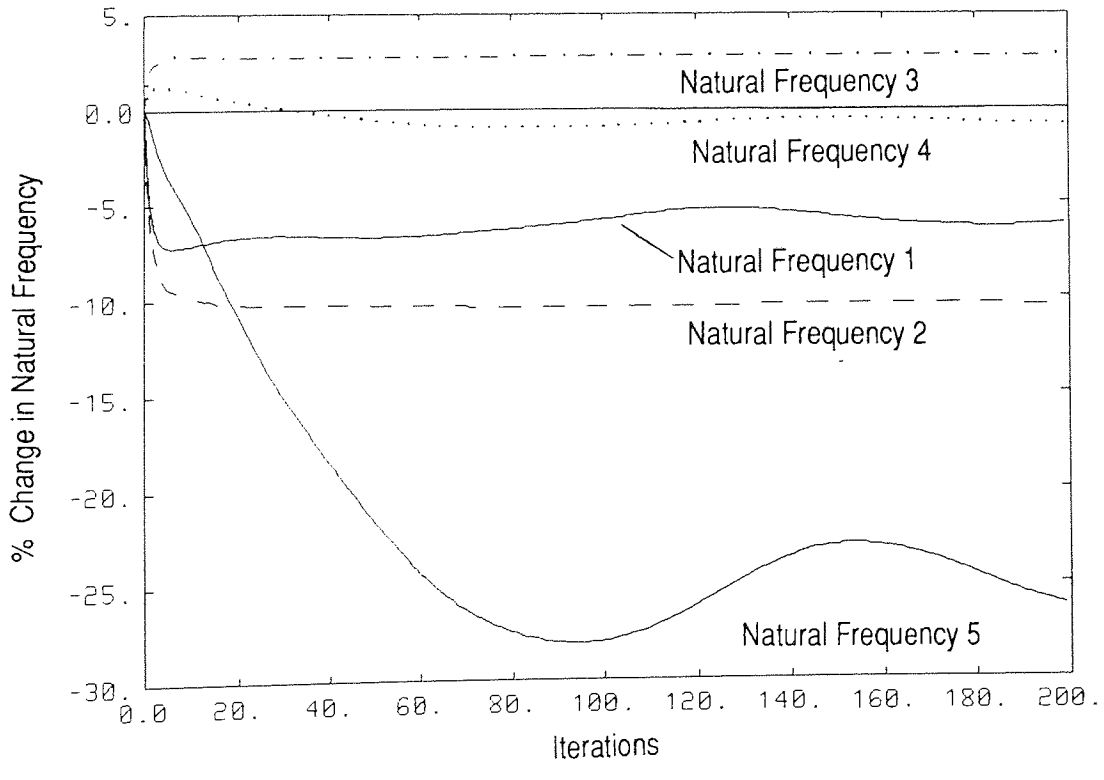

Figure 8.8 Convergence of Natural Frequencies. No Weight for Initial Parameter Values.

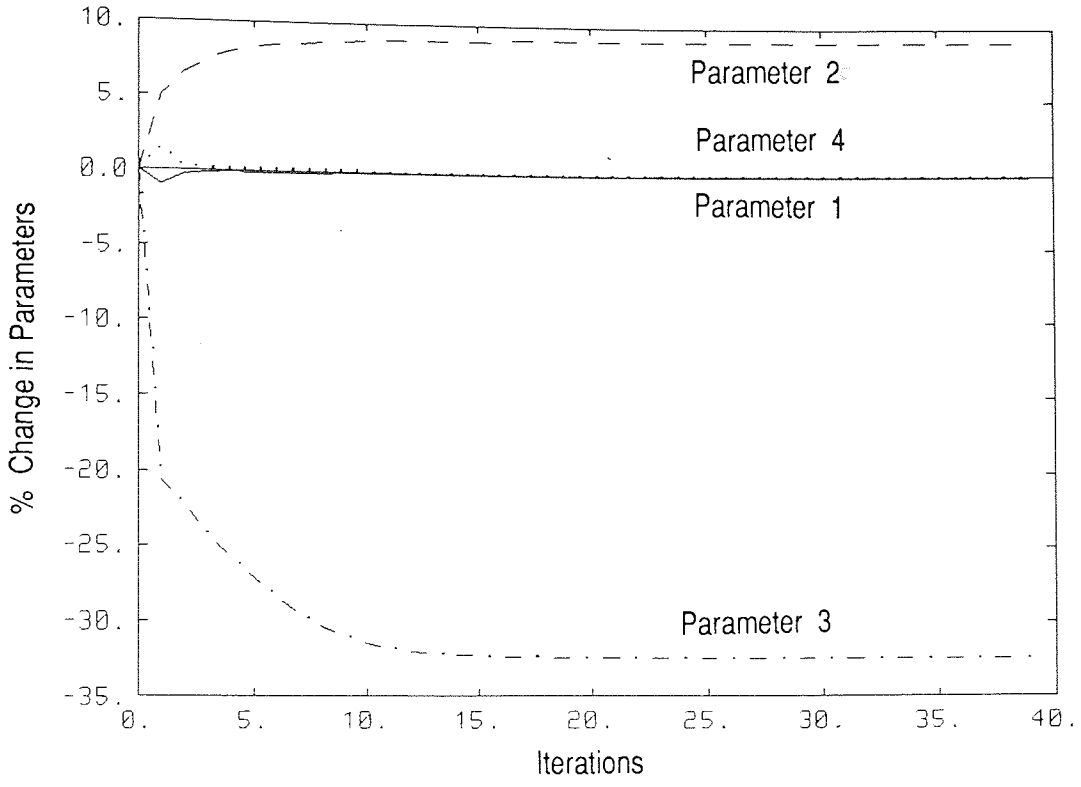

Figure 8.9 Convergence of Parameters 1 to 4. Weight Given to Initial Values.

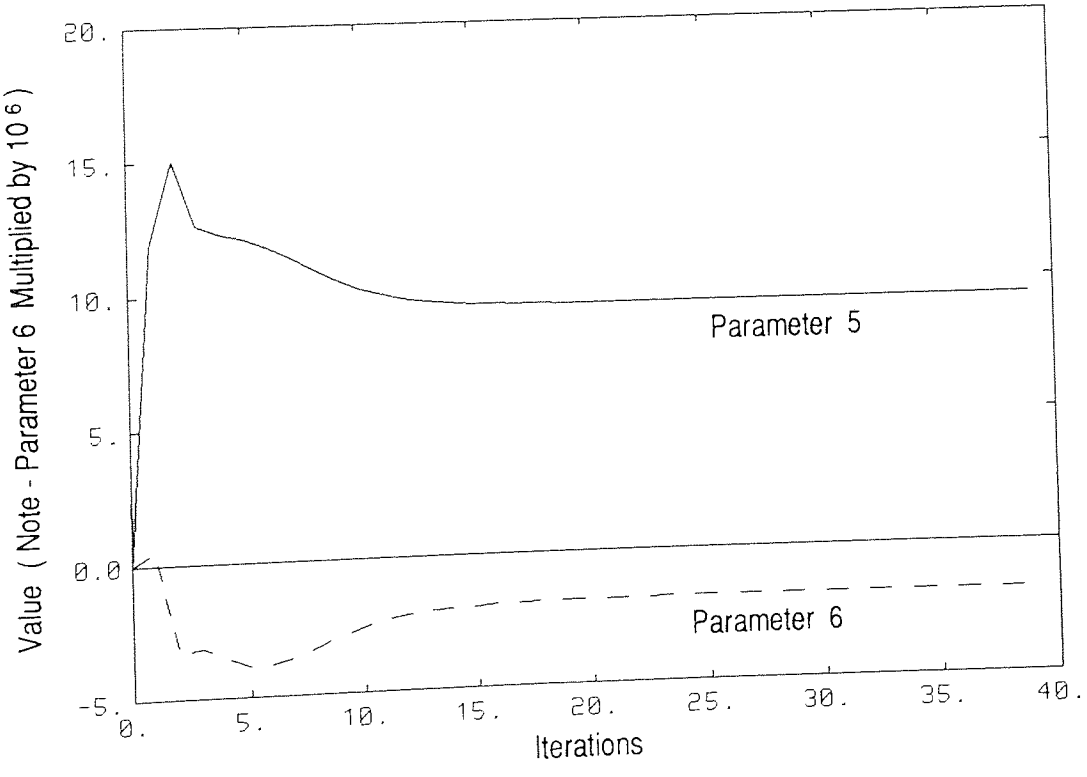

Figure 8.10 Convergence of Parameters 5 & 6. Weight Given to Initial Values.

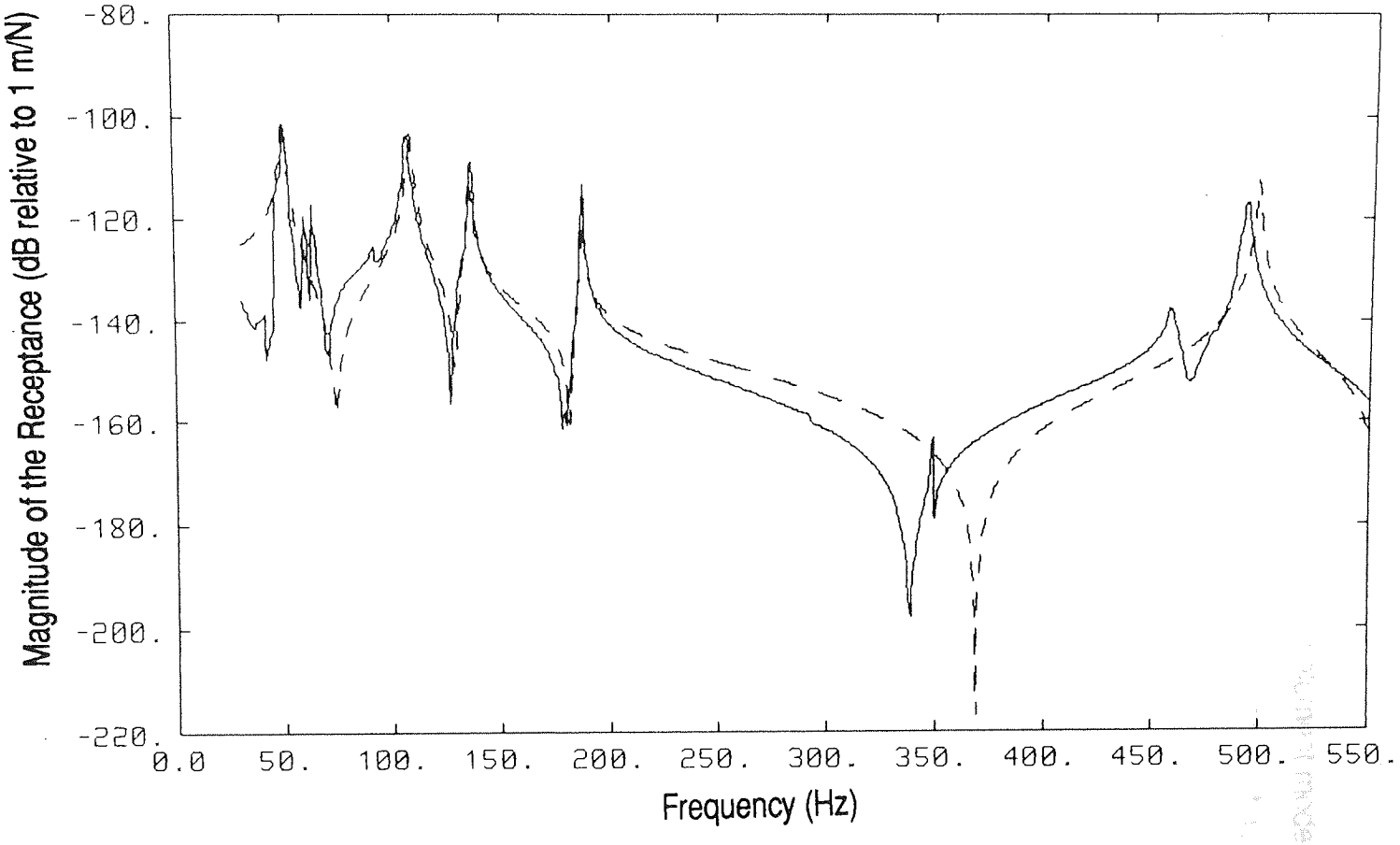

Figure 8.11 Comparis on of Typical Experimental FRF and Updated FRF

——— Experimental Data - - - - Updated Model

8.5 Parameter Updating from the Modal Model

The first stage in updating the parameters of a finite element model using the modal model is to generate the natural frequencies, damping ratios and mode shapes for the structure. The FRFs used in the last section, obtained from stepped sine excitation, form the basic data from which to compute the modal model. The five main resonances in the data may be identified visually. Using the SMS STAR computer package with the Global Polynomial or Rational Fraction Least Squares curve fitting algorithm (see the Orthogonal Polynomial Method, Section 2.6.3) gives the frequencies and damping ratios shown in table 8.3. Consider the same theoretical model and unknown parameters as in Section 8.4 but with an initial parameter vector of

$$(4560 , 4560 , 4560 , 0.105 , 0 , 0) \quad .$$

Mode Number	Natural Frequency (Hz)	Damping Ratio (%)
1	52.6	1.78
2	106.7	0.40
3	135.7	0.36
4	187.7	0.21
5	492.4	0.16

Table 8.3 Measured Natural Frequencies and Damping Ratios

The modal Assurance Criterion (MAC) between the measured mode shapes and those of the initial analytical model is

$$MAC = \begin{bmatrix} 0.970 & 0.000 & 0.007 & 0.005 & 0.020 \\ 0.014 & 0.986 & 0.000 & 0.006 & 0.000 \\ 0.014 & 0.002 & 0.995 & 0.025 & 0.009 \\ 0.009 & 0.017 & 0.000 & 0.922 & 0.001 \\ 0.022 & 0.000 & 0.002 & 0.000 & 0.989 \end{bmatrix} \quad (8.1)$$

The elements across the diagonal are all above 0.9 and this confirms that the five identified modes correspond with the five lowest frequency analytical mode shapes.

Because the damping is difficult to model only the natural frequencies will be used to update the parameters. Thus only the first four parameters of table 8.1 will be used as the final two parameters relate to proportional damping. Suppose that the measurement and initial parameter variances are given by

$$V_0 = \text{diag}(100 , 900 , 900 , 0.0001)$$

$$V_\varepsilon = \text{diag}(0.25 , 0.25 , 0.25 , 0.25 , 0.25) \quad . \quad (8.2)$$

In this case (case I), using the algorithm derived in Chapter 5, the parameters rapidly converge, as shown in figure 8.12, and the final analytical frequencies are given in table 8.4. Because the noise variance was assumed to be high the natural frequencies of the updated model reflect the measured frequencies only moderately accurately. The MAC matrix between the experimental and updated mode shapes is approximately the same as 8.1.

	Natural Frequencies (Hz)				
	Experi-mental	Initial Model	Updated Model, Case I	Updated Model, Case II	Updated Model, Case III
1	52.6	54.3	53.5	52.3	52.3
2	106.7	118.6	112.9	106.7	106.7
3	135.7	131.9	135.4	135.5	135.5
4	187.7	184.7	188.0	187.8	187.8
5	492.4	496.5	492.3	492.4	492.4

Table 8.4 Natural Frequencies from Experiment, Initial Model and Model Updated using Modal Data

Suppose we assume that the frequencies were measured exactly. In theory this would imply that the measurement noise variance was zero. From Chapter 5 this would imply that $\mathbf{D}_j = 0$ for all j. Because only four parameters are to be updated and there are five measured frequencies, $\mathbf{V}_{zj}$ is singular. Therefore the algorithm cannot be used to estimate the parameters with zero measurement noise, or $\mathbf{V}_\varepsilon = 0$. As a compromise assume (case II) that the measurement noise is given by

$$\mathbf{V}_\varepsilon = \text{diag}\,(10^{-6} , 10^{-6} , 10^{-6} , 10^{-6} , 10^{-6})$$

and the initial parameter variance is given by 8.2. Figure 8.13 shows the convergence of the parameters in this case and table 8.4 shows the natural frequencies on convergence. All the natural frequencies accurately reflect the measured quantities. With only four parameters and five frequencies it would be very fortuitous for all five natural frequencies to be reproduced exactly,

even with no measurement noise. Again the MAC matrix between the experimental and updated mode shapes is approximately the same as 8.1.

As a final example (case III), assume that the measurement noise and the initial parameter variances are given by 8.2, but assume that the updated parameters and measurement noise are uncorrelated. Thus $\mathbf{D}_j$ is zero for all j. This simulates the minimum variance method used by all previous authors. Figure 8.14 shows the convergence of the parameters in this case and table 8.4 shows the natural frequencies on apparent convergence. All the natural frequencies accurately reflect the measured quantities. Again, with only four parameters and five frequencies it would be very fortuitous for all five natural frequencies to be reproduced exactly. Effectively this method assumes zero measurement noise. The major difference between these results and those of case II is that when the correlation between the updated parameters and measurement noise is ignored, convergence is much slower. This experimental example confirms the simulated results of Chapter 5. The MAC matrix between the experimental and updated mode shapes is approximately the same as 8.1. One problem is the numerical stability of the algorithm with $\mathbf{D}_j = \mathbf{0}$ for all j. In figure 8.14 the rapid parameter change after about 40 iterations gives some indication of the sensitivity of the updating procedure to the parameter values. Although the algorithm seems to converge after this rapid change, in fact the parameter values start to diverge, and even become negative, after about 55 iterations. The reason the algorithm diverges is essentially the same as the reason why zero measurement noise could not be used in case II.

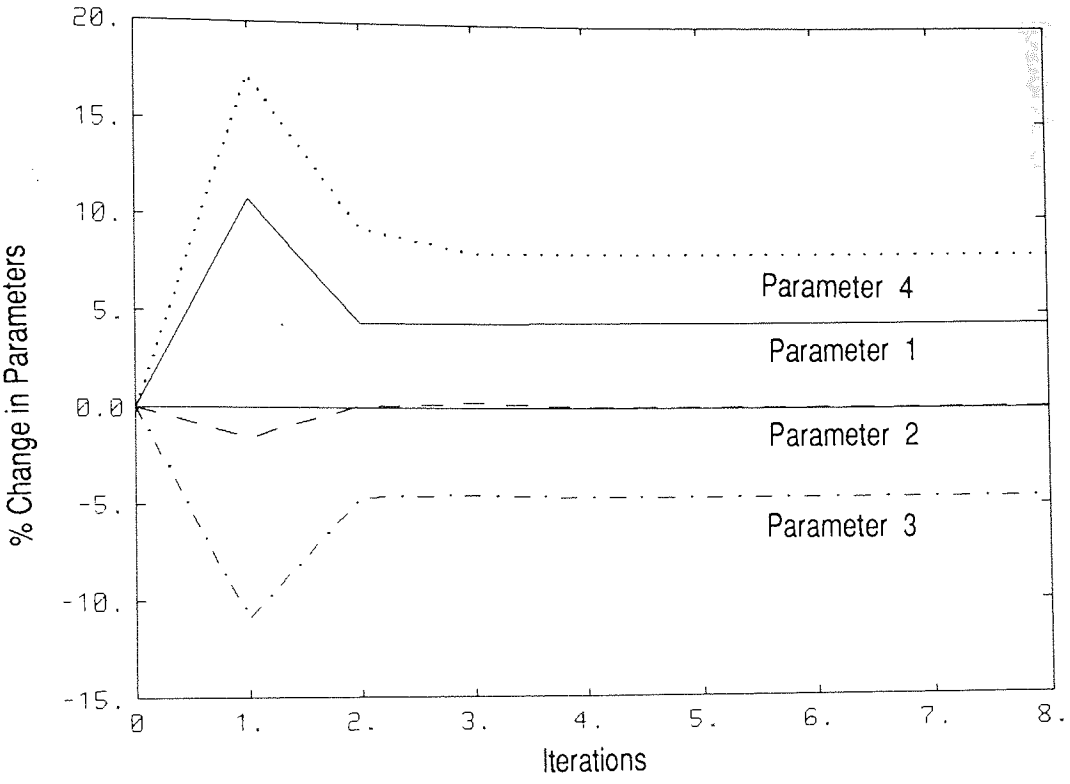

Figure 8.12 Convergence of Parameters using a Minimum Variance Estimator

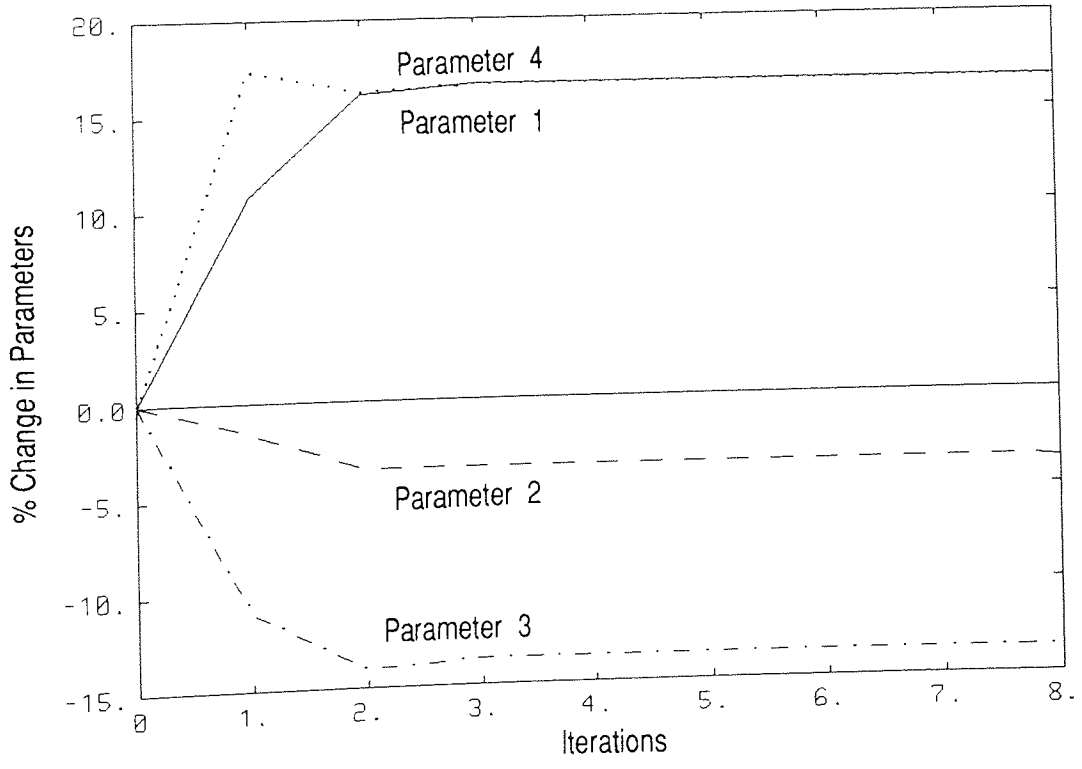

Figure 8.13 Parameter Convergence using a Minimum Variance Estimator, (negligible measurement noise)

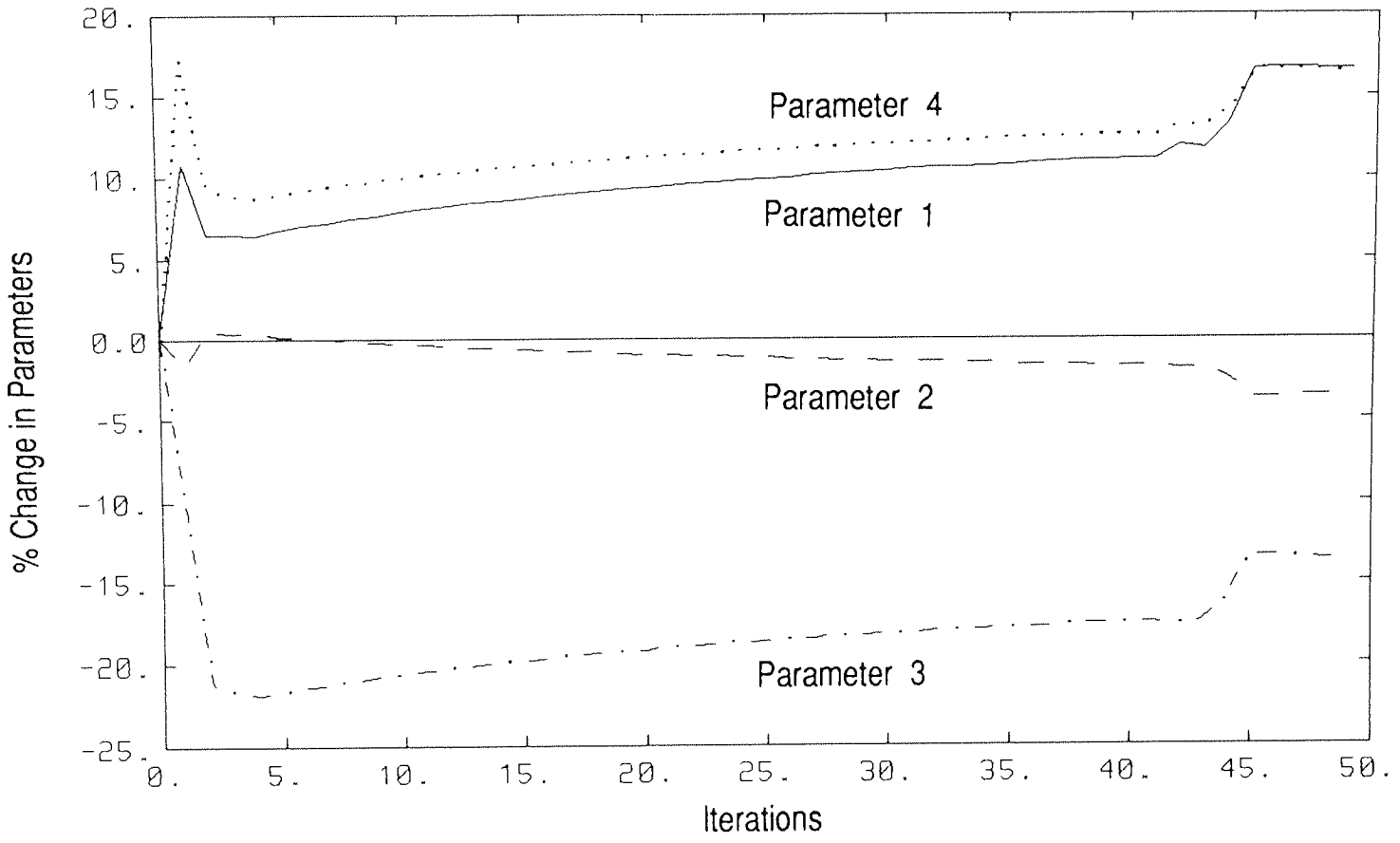

Figure 8.14 Parameter Convergence using a Minimum Variance Estimator, (Parameter to Noise Correlation Ignored)

Chapter 9

Discussion

This thesis has presented two new methods that may be used to update the unknown parameters of a finite element model. The properties of these methods and their application have been discussed in the relevant chapters. This chapter provides a summary of these properties in the context of practical model updating. Some suggestions for further work are given at the end. The first method updates the unknown parameters from the measured modal model by computing the parameter estimate that has minimum variance (Chapter 5). The second method updates the unknown parameters from the measured FRFs essentially using a weighted equation error approach applied to a reduced order model of the system (Section 7.4.3). These updating algorithms have been tested and compared to other existing algorithms using simulated and experimental data. The algorithms worked well in these examples but it must be realised that no algorithm is a panacea. The application of any parameter updating procedure requires a great deal of engineering insight and the idea of a 'black box' identification scheme, if it is possible or indeed even desirable, is a long way off.

Probably the most difficult decision is the choice of parameters to update. This must be determined for each structure individually and the parameters updated should be those with the greatest a priori uncertainty. Updating physical parameters helps the analyst to decide on the quality of the theoretical parameter estimates and also helps the interpretation of the resulting updated parameters. The alternative to updating physical parameters is to update the elements or submatrices of the mass, damping and stiffness matrices. Updating matrix elements involves a large number of measurements and/or the use of a condensed theoretical model. Although this may produce a good correlation between the measured and the updated theoretical results, interpreting and using the subsequent model is far more difficult. This thesis has been more concerned with the methods of updating parameters and has not considered the choice of parameters to update in any depth. Obviously the quality of the updated parameters will depend critically on this choice.

What are the advantages and disadvantages of the updating methods outlined? The minimum variance method, using the modal model, is a corrected version of a popular algorithm. Previous algorithms have ignored the correlation between the parameter estimates and the measurement noise. This oversight produces an algorithm which, given sufficient unknown parameters, always reproduces the measured quantities. Thus, these previous algorithms essentially assumed that the measurement noise was zero and so could be regarded as a pseudo inverse method with a particular weighting for the initial parameters. The new method, described in Chapter 5, converges much faster, and to more correct solutions than the previous methods. The amount of extra computation required is small. If the measurement noise variance is zero then all the algorithms will have problems fitting data to a model with fewer unknown parameters than measurements. Even with non-zero measurement noise variance the algorithms used previously will fail. These problems arise because the algorithms try to reproduce the measured quantities exactly but have too few parameters available to do so. The algorithm described in this thesis should find immediate application as an improved, direct replacement for the incorrect minimum variance updating algorithm.

The future of the updating algorithm using the FRFs directly is not so certain. The philosophy of using data that has undergone the least preprocessing, and to use as much data as possible to update the parameters is attractive. Where the modal model is difficult to extract, because of high damping or closely coupled modes, the method should be useful. Indeed the modal model could be obtained subsequently from the updated finite element model. If the modal model can be extracted satisfactorily then the ability to check the adequacy of the modes before model updating has advantages. The most promising method, based on an extension of Goyder's algorithm, worked reasonably well although it has problems fitting modes which have a low magnitude. This situation arose in the examples used in this thesis because

the excitation location was such that one mode was hardly excited. The problem could possibly be solved by using more than one excitation location in order to excite all modes adequately. Incorporating such excitation forces would be relatively easy since the theory of Chapters 6 and 7 already allows for multiple excitation points. The equation error and instrumental variable methods performed poorly. These methods minimise the errors in the equations of motion and give insufficient weight to the frequencies around resonance where the data is most accurate. Nonlinear curve fitting algorithms were not considered in depth as the computational burden is too great.

As an intermediate step in the calculation of the unknown parameters directly from the FRFs, a reduced order model was produced (Chapter 6). This reduced model is unusual in that some dependence on the unknown parameters is retained. Alternative parameter estimation algorithms, either time or frequency domain, may be able to use this form of the theoretical model to advantage.

The scope for further work in the updating of the parameters of finite element models is large. The following are six suggestions arising naturally from this thesis. They are certainly not exhaustive and range from mere developments to further research projects.

- Test the performance of the minimum variance updating algorithm on more realistic and complex examples.

- Try the extended Goyder method on a structure using FRFs obtained from more than one excitation location. Establish guidelines to determine when the modes of a system have been sufficiently excited.

- Test the performance of the extended Goyder method on large scale structures and structures with highly damped or closely coupled modes.

- Consider the use of other time and frequency parameter updating methods using the reduced order model of Chapter 6.

- Design and build an 'environment' for implementing parameter updating algorithms. A commercial package is available which uses an incorrect minimum variance updating procedure and provides links to a finite element program. A research tool along similar lines but with the capability to change updating algorithms at will would be very useful.

- Determine guidelines to decide which parameters of a finite element model to update, to decide on the most suitable updating algorithm and to assess the quality of the updated parameters. Trying to reduce the operator interaction in this way could make use of expert system technology.

References

Allemang, R.J., Rost, R.W. and Brown, D.L., 1983, 'Multiple Input Estimation of Frequency Response Functions: Excitation Considerations',American Society of Mechanical Engineers, Paper No 83-DET-73. Presented at the Design and Production Engineering Technical Conference, Dearborn, Michigan, September 11-14, 1983.

Allemang, R.J., Brown, D.L. and Rost, R.W., 1987, 'Experimental Modal Analysis and Dynamic Component Synthesis', AFWAL-TR-87-3069, Volumes I, II, III and IV, Flight Dynamics Laboratory, Wright-Patterson Air Force Base.

Allemang, R.J. and Brown, D.L., 1982, 'A Correlation Coefficient for Modal Vector Analysis', Proceedings of the 1st International Modal Analysis Conference, Orlando, Florida, November 1982, pp 110-116.

Andrew, A.L., 1978, 'Convergence of an Iterative Method for Derivatives of Eigensystems', Journal of Computational Physics, Vol 26, pp 107-112.

Avitabile, P., O'Callahan, J. and Pan, E.D., 1989, 'Effects of Various Model Reduction Techniques on Computed System Response', Proceedings of the 7th International Modal Analysis Conference, Las Vegas, Nevada, February 1989, pp 777-785.

Baruch, M., 1978, 'Optimisation Procedure to Correct Stiffness and Flexibility Matrices using Vibration Tests', AIAA Journal, Vol 16, No 11, pp 1208-1210.

Baruch, M., 1979, 'Selected Optimal Orthogonalization of Measured Modes', AIAA Journal, Vol 17, No 1, pp 120-121.

Baruch, M. and Bar Itzhack, I.Y., 1978, 'Optimal Weighted Orthogonalization of Measured Modes', AIAA Journal, Vol 16, No 4, pp 346-351.

Berman, A., 1979, 'Comment on "Optimal Weighted Orthogonalization of Measured Modes" ', AIAA Journal, Vol 17, No 8, pp 927-928.

Berman, A. and Nagy, E.J., 1983, 'Improvement of a Large Analytical Model Using Test Data', AIAA Journal, Vol 21, No 8, pp 1168-1173.

Berman, A. and Flannelly, W.G., 1971, 'Theory of Incomplete Models of Dynamic Structures', AIAA Journal, Vol 9, No 8, pp 1481-1487.

Brown, D., Allemang, R., Zimmerman, R. and Mergeay, M., 1979, 'Parameter Estimation Techniques for Modal Analysis', Society of Automotive Engineers Paper No 790221. Also SAE Transactions, Vol 88, No 1, pp 828-846.

Brown, T.A., 1988, 'A Matrix Cursor for Dynamic Model Improvement using Experimental Modes of Vibration', GEC Journal of Research, Vol 6, No 3, pp 139-146.

Caesar, B., 1986, 'Update and Identification of Dynamic Mathematical Models', Proceedings of the 4th International Modal Analysis Conference, Los Angeles, California, February 1986, pp 394-401.

Chen, J.C. and Garba, J.A., 1980, 'Analytical Model Improvement Using Modal Test Results', AIAA Journal, Vol 18, No 6, pp 684-690.

Chu, D.F., DeBroy, J.M. and Yang, J., 1989, 'Pitfalls of Mass Orthogonality Check', Proceedings of the 7th International Modal Analysis Conference, Las Vegas, Nevada, February 1989, pp 822-829.

Collins, J.D., Hart, G.C., Hasselman, T.K., and Kennedy, B., 1974, 'Statistical Identification of Structures', AIAA Journal, Vol 12, No 2, pp 185-190.

Collins, J.D., Young, J., and Kiefling, L., 1972, 'Methods and Applications of System Identification in Shock and Vibration', in 'System Identification of Vibrating Structures presented at the 1972 Winter Annual Meeting of the ASME', pp 45-71.

Cottin, N., Felgenhauer, H.P. and Natke, H.G., 1984, 'On the Parameter Identification of Elastomechanical Systems Using Input and Output Residuals', Ingenieur Archiv (Archive of Applied Mechanics), Vol 54, No 5, pp 378-387.

Detchmendy, D.M. and Sridhar, R., 1966, 'Sequential Estimation of States and Parameters in Noisy Nonlinear Dynamical Systems', ASME Journal of Basic Engineering, Vol 88D, pp 362-368.

Dobson, B.J., 1987, 'A Straight Line Technique for Extracting Modal Properties from Frequency Response Data', Journal of Mechanical Systems and Signal Processing, Vol 1, No 1, pp 29-40.

Ewins, D.J., 1984, 'Modal Testing: Theory and Practice', Research Studies Press Limited.

Ewins, D.J. and Gleeson, P.T., 1982, 'A Method for Modal Identification of Lightly Damped Structures', Journal of Sound and Vibration, Vol 84, No 1, pp 57-79.

Fox, R.L. and Kapoor, M.P., 1968, 'Rates of change of Eigenvalues and Eigenvectors', AIAA Journal, Vol 6, pp 2426-2429.

Friswell, M.I., 1989a, 'The Adjustment of Structural Parameters using a Minimum Variance Estimator', Journal of Mechanical Systems and Signal Processing, Vol 3, No 2, pp 143-155.

Friswell, M.I., 1989b, 'Updating Physical Parameters from Frequency Response Function Data', Proceedings of the 12th Biennial ASME Conference on Mechanical Vibration and Noise, Montreal, Canada, September 1989.

Friswell, M.I., 1990, 'Candidate Reduced Order Models for Structural Parameter Estimation', ASME Journal of Vibration and Acoustics, Vol 112, No 1, pp 93-97.

Friswell, M.I. and Penny J.E.T., 1990a, 'Updating Model Parameters Directly from Frequency Response Function Data', Proceedings of the 8th International Modal Analysis Conference, Kissimmee, Florida, January 1990, pp 843-849.

Friswell, M.I. and Penny J.E.T., 1990b, 'Stepped Multisine Modal Testing using Phased Components', Journal of Mechanical Systems and Signal Processing, Vol 4, No 2, April 1990, pp 145-156.

Friswell, M.I. and Penny, J.E.T., 1990c, 'Updating Model Parameters from Frequency Domain Data via Reduced Order Models', to be published in the Journal of Mechanical Systems and Signal Processing, Vol 4, 1990.

Fritzen, C-P., 1986, 'Identification of Mass, Damping and Stiffness Matrices of Mechanical Systems', ASME Journal of Vibration, Acoustics, Stress and Reliability in Design, Vol 108, No 1, pp 9-16.

Gaukroger, D.R., Skingle, C.W. and Heron, K.H., 1973, 'Numerical Analysis of Vector Response Loci', Journal of Sound and Vibration, Vol 29, No 3, pp 341-353.

Glover, K., 1984, 'All Optimal Hankel-norm Approximations of Linear Multivariable Systems and their L^{∞}-error Bounds', International Journal of Control, Vol 39, No 6, pp 1115-1193.

Gourlay, A.R. and Watson, G.A., 1973, 'Computational Methods for Matrix Eigenproblems', John Wiley & Sons.

Goyder, H.G.D., 1980, 'Methods and Application of Structural Modelling from Measured Structural Frequency Response Data', Journal of Sound and Vibration, Vol 68, No 2, pp 209-230.

Gravitz, S., 1958, 'An Analytical Procedure for Orthogonalization of Experimentally Measured Modes', Journal of Aerospace Sciences, Vol 25, pp 721-722.

Guyan, R.J., 1965, 'Reduction of Stiffness and Mass Matrices', AIAA Journal, Vol 3, No 2, pp 380.

Hart, G.C. and Martinez, D.R., 1982, 'Improving Analytical Dynamic Models using Frequency Response Data - Application', Proceedings of the 23rd AIAA/ASME/ASCE/AHS Structures, Structural Dynamics and Materials Conference, May 1982, Part 2, pp 46-55. Also AIAA paper 82-0637.

Heylen, W., 1982, 'Optimization of Model Matrices by Means of Experimentally Obtained Dynamic Data', Proceedings of the 1st International Modal Analysis Conference, Orlando, Florida, November 1982, pp 32-38

Heylen, W., 1987, 'Optimisation of Model Matrices of Mechanical Structures using Experimental Modal Data', PhD Dissertation 87D05, Mechanical Engineering Department, Katholieke Universteit Leuven, Belgium.

Hoff, C. and Natke, H.G., 1989, 'Correction of a Finite Element Model by Input-Output Measurements with Application to a Radar Tower', The International Journal of Analytical and Experimental Modal Analysis, Vol 2, No 3, pp 1-7.

Ibrahim, S.R., Stavrinidis, C., Fissette, E. and Brunner, O., 1989, 'A Direct Two Response Approach for Updating Analytical Dynamic Models of Structures with Emphasis on Uniqueness', Proceedings of the 7th International Modal Analysis Conference, Las Vegas, Nevada, January 1989, pp 340-346.

Irons, B., 1965, 'Structural Eigenvalue Problems: Elimination of Unwanted Variables', AIAA Journal, Vol 3, No 5, pp 961-962.

Irons, B. and Shrive, N., 1983, 'Finite Element Primer', Ellis Horwood Limited.

Janter, T., Heylen, W. and Sas, P., 1988, 'QA-Updating', Proceedings of the 13th International Seminar on Modal Analysis, Katholieke Universiteit Leuven, Leuven, Belgium, September 1988, paper C-13.

Jennings, A., 1981, 'Eigenvalue Methods and the Analysis of Structural Vibration', in 'Sparse Matrices and their Uses', edited by I.S. Duff, Academic Press.

Kalaba, R. and Spingarn, K., 1982, 'Control, Identification and Input Optimisation', Plenum Press.

Laub, A.J., 1980, 'Computation of 'Balancing' Transformations', Proceedings of the 1980 Joint Automatic Control Conference, San Francisco, California, Vol 1, paper FA8-E.

Leuridan, J.M., Brown, D.L. and Allemang, R.J., 1986, 'Time Domain Parameter Identification Methods for Linear Modal Analysis: A Unifying Approach', ASME Journal of Vibration, Acoustics, Stress and Reliability in Design, Vol 108, pp 1-8.

Leuridan, J., Van der Auweraer, H. and Mergeay, M., 1988, 'Review of Parameter Identification Techniques', Proceedings of the 13th International Seminar on Modal Analysis, Katholieke Universiteit Leuven, Leuven, Belgium, September 1988, Basic Course Paper 12. Also Esprit Project 1561, Technical Report Task 6111.

Liefooghe, C., Janter, T. and Sas, P., 1988, 'Case Studies of the Application of the QA Model Updating Algorithm', Proceedings of the 13th International Seminar on Modal Analysis, Katholieke Universiteit Leuven, Leuven, Belgium, September 1988, Paper C-14.

Meirovitch, L., 1986, 'Elements of Vibration Analysis', McGraw-Hill.

Mickleborough, N.C. and Pi, Y.L., 1989, 'Modal Parameter Identification using Z-Transforms', International Journal for Numerical Methods in Engineering, Vol 28, pp 2307-2321.

Moore, B.C., 1981, 'Principal Component Analysis in Linear Systems: Controllability, Observability, and Model Reduction', IEEE Transactions on Automatic Control, Vol AC-26, pp 17-32.

Mottershead, J.E., 1988, 'A Unified Theory of Recursive, Frequency Domain Filters with Application to System Identification in Structural Dynamics', ASME Journal of Vibration, Acoustics, Stress and Reliability in Design, Vol 110, pp 360-365.

Mottershead, J.E., Lees, A.W., and Stanway, R., 1987, 'A Linear, Frequency Domain Filter for Parameter Identification of Vibrating Structures', ASME Journal of Vibration, Acoustics, Stress and Reliability in Design, Vol 109, pp 262-269.

Mottershead, J.E., and Stanway, R., 1986, 'Identification of Structural Vibration Parameters by using a Frequency Domain Filter', Journal of Sound and Vibration, Vol 109, No 3, pp 495-506.

Mottershead, J.E., Tee, T.K. and Lees, A.W., 1988, 'Identification of a Positive Definite Mass Matrix', ASME Journal of Vibration, Acoustics, Stress and Reliability in Design, Vol 110, pp 49-52.

Nalitolela, N., Penny, J.E.T., and Friswell, M.I., 1990, 'Updating Structural Parameters of a Finite Element Model by Adding Mass or Stiffness to the System', Proceedings of the 8th International Modal Analysis Conference, Kissimmee, Florida, January 1990, pp 836-842.

Natke, H.G., 1988, 'Updating Computational Models in the Frequency Domain Based on Measured Data: a Survey', Journal of Probabilistic Engineering Mechanics, Vol 3, No 1, pp 28-35.

Nelson, R.B., 1976, 'Simplified Calculation of Eigenvector Derivatives', AIAA Journal, Vol 14, No 9, pp 1201-1205.

O'Callahan, J., 1989, 'A Procedure for an Improved Reduced System (IRC) Model', Proceedings of the 7th International Modal Analysis Conference, Las Vegas, Nevada, January 1989, pp 17-21.

O'Callahan, J.C., Avitabile, P., Madden, R. and Lieu, I.W., 1986, 'An Efficient Method of Determining Rotational Degrees of Freedom from Analytical and Experimental Modal Data', Proceedings of the 4th International Modal Analysis Conference, Los Angeles, California, February 1986, pp 50-58.

O'Callahan, J.C., Avitabile, P. and Riemer, R., 1989, 'System Equivalent Reduction Expansion Process', Proceedings of the 7th International Modal Analysis Conference, Las Vegas, Nevada, January 1989, pp 29-37.

Olsen, N., 1983, 'Burst Random Excitation', Sound and Vibration, November, pp 20-23.

Paz, M., 1984, 'Dynamic Condensation', AIAA Journal, Vol 22, No 5, pp 724-727.

Przemieniecki, J.S., 1968, 'Theory of Matrix Structural Analysis', McGraw-Hill.

Richards, T.H., 1977, 'Energy Methods in Stress Analysis', Ellis Horwood Limited.

Robinson, J.C., 1982, 'Application of a Systematic Finite Element Model Modification Technique to Dynamic Analysis of Structures', Proceedings of the 23rd AIAA/ASME/ASCE/AHS Structures, Structural Dynamics and Materials Conference, May 1982, Part 2, pp 489-502. Also AIAA paper 82-0730.

Roemer, M.J. and Mook, D.J., 1990, 'Robust Time Domain Identification of Mass, Stiffness and Damping Matrices', Proceedings of the 8th International Modal Analysis Conference, Kissimmee, Florida, January 1990, pp 1271-1277.

Ross Jr, R.G., 1971, 'Synthesis of Stiffness and Mass Matrix from Experimental Vibration Modes', Society of Automotive Engineers Paper No 710787. Also SAE Transactions, Vol 80, pp 2627-2635.

Rudisill, C.S. and Chu, Y., 1975, 'Numerical Methods for Evaluating the Derivatives of Eigenvalues and Eigenvectors', AIAA Journal, Vol 13, No 6, pp 834-837.

Santos, J. and Arruda, J., 1990, 'Finite Element Model Updating using Frequency Response Functions and Component Mode Synthesis', Proceedings of the 8th International Modal Analysis Conference, Kissimmee, Florida, January 1990, pp 1195-1201.

Sestieri, A. and D'Ambrogio, W., 1989, 'Why be Modal: How to Avoid the Use of Modes in the Modification of Vibrating Systems', International Journal of Analytical and Experimental Modal Analysis, Vol 4, pp 25-30.

Shamash, Y., 1975, 'Model Reduction using the Routh Stability Criterion and the Padé Approximation Technique', International Journal of Control, Vol 21, No 3, pp 475-484.

Snoeys, R., Sas, P., Heylen, W. and Van Der Auweraer, H., 1987, 'Trends in Experimental Modal Analysis', Journal of Mechanical Systems and Signal Processing, Vol 1, No 1, pp 5-27.

Tan, R.C.E., 1987, 'Computing Derivatives of Eigensystems by the Vector ε-Algorithm', IMA Journal of Numerical Analysis, Vol 7, pp 485-494.

Tan, R.C.E. and Andrew, A.L., 1989, 'Computing Derivatives of Eigenvalues and Eigenvectors by Simultaneous Iteration', IMA Journal of Numerical Analysis, Vol 9, pp 111-122.

Thomas, D.L., 1982, 'Errors in Natural Frequency Calculations using Eigenvalue Economisation', International Journal of Numerical Methods in Engineering, Vol 18, pp 1521-1527.

Thomas, M., Massoud, M. and Beliveau, J., 1986, 'Identification of System Physical Parameters from Force Appropriation Technique', Proceedings of the 4th International Modal Analysis Conference, Los Angeles, California, February 1986, pp 1098-1103.

Tlusty, J., 1976, 'Experimental and Computational Identification of Dynamic Structural Models', Annals of the CIRP, Vol 25, No 2, pp 497-503.

Tlusty, J. and Ismail, F., 1980, 'Dynamic Structural Identification Tasks and Methods', Annals of the CIRP, Vol 29, No 1, pp 251-255.

Tomlinson, G.R., 1987, 'Developments in the use of the Hilbert Transform for Detecting and Quantifying Non-linearity Associated with Frequency Response Functions', Journal of Mechanical Systems and Signal Processing, Vol 1, No 2, April 1990.

Urgueira, A., Lieven, N.A.J. and Ewins, D.J., 1990, 'A Generalised Reduction Method for Modal Testing', Proceedings of the 8th International Modal Analysis Conference, Kissimmee, Florida, January 1990, pp 22-27.

Vold, H., Crowley, J. and Rocklin, G., 1985, 'A Comparision of H1, H2, Hv, Frequency Response Functions', Proceedings of the 3rd International Modal Analysis Conference, Orlando, Florida, January 1985, pp 272-278.

Wei, J.C., Zhang, Q., Allemang, R.J. and Wei, M.L., 1988, 'Correction of Finite Element Model via Selected Physical Parameters', Proceedings of the 13th International Seminar on Modal Analysis, Katholieke Universiteit Leuven, Leuven, Belgium, September 1988, paper C-12. Also presented at 7th International Modal Analysis Conference, pp 1231-1238.

Wilkinson, J.H., 1965, 'The Algebraic Eigenvalue Problem', Clarendon Press.

Zaveri, K., 1984, 'Modal Analysis of Large Structures - Multiple Exciter Systems', Brüel and Kjaer Publication.

Zienkiewicz, O.C., 1977, 'The Finite Element Method', 3rd Edition, McGraw-Hill.

Zienkiewicz, O.C. and Taylor, R.L., 1989, 'The Finite Element Method, Volume 1, Basic Formulation and Linear Problems', 4th Edition, McGraw-Hill.

Appendices

Appendix A Notation

a	Parameter in the one dimensional example. Equivalent to natural frequency squared, or stiffness / mass
$\hat{a}$	Current estimate of parameter a
${}_ia_{hk}$	Coefficients used to calculate eigenvector derivatives. Defined by equations 2.18 and 2.20
A	Cross sectional area of beam in one dimensional beam examples
$\mathbf{A}$	Coefficient matrix used in updating algorithms, Section 3.3
$\mathbf{A}_c$	Coefficient matrix with complex elements used in updating algorithms in Section 7.2
$\mathbf{A}_r$	Coefficient matrix with real elements used in updating algorithms in Section 7.2
${}_ib_{hk}$	Coefficients used to calculate eigenvector derivatives for the reduced model using the zeroth order transformation
b	Parameter in the one dimensional example. Equivalent to natural frequency times damping coefficient, or damping / mass
$\mathbf{b}$	Vector used in updating algorithms, Section 3.3
$\mathbf{b}_c$	Vector with complex elements used in updating algorithms in Section 7.2
$\mathbf{b}_r$	Vector with real elements used in updating algorithms in Section 7.2
$\hat{b}$	Current estimate of parameter b
$\mathbf{B}$	Matrix allocating the force input to the state vector in the full order model
$\mathbf{B}_{Fi}$	Coefficient of $\delta\theta_i$ in the expansion of the matrix allocating the force input to the state vector in the reduced order model resulting from first order transformation

B_{F0}	Constant term in the expansion of the matrix allocating the force input to the state vector in the reduced order model resulting from first order transformation
B_n	Matrix allocating the force input to the correct generalised coordinates
B_z	Matrix allocating the force input to the state vector in the reduced order model resulting from zeroth order transformation
c	Parameter in the one dimensional example. Equivalent to the modal constant
c_{ik}	Constant used in calculating eigenvector derivatives
C	Matrix linking the output vector to the state vector of the full order model. Note NOT damping
C_{Fi}	Coefficient of $\delta\theta_i$ in the expansion of the matrix linking the output vector to the state vector in the reduced order model resulting from first order transformation
C_{F0}	Constant term in the expansion of the matrix linking the output vector to the state vector in the reduced order model resulting from first order transformation
$C_n(\theta)$	The usual (n,n) damping matrix which is dependent on the parameter θ
C_z	Matrix linking the output vector to the state vector in the reduced order model resulting from zeroth order transformation
$C_n(\theta)$	The usual (n,n) viscous damping matrix which is dependent on the parameter vector θ
$D(\omega_k,\delta\theta)$	Dynamic matrix defined in equation 7.15
D_j	Correlation between measurement noise and j th parameter estimate, Chapter 5

$D_0(\omega_k)$	$= D(\omega_k,0) = I_{2r}\, j\, \omega_k + \Lambda_0$
E	Young's modulus
E[ ]	Expected value
$f(\omega,a,b,c)$	One dimensional theoretical frequency response function
$f_m(\omega)$	One dimensional measured frequency response function
$F(\omega)$	General theoretical frequency response function
$F_m(\omega)$	General measured frequency response function
$F_R(\omega)$	The theoretical frequency response function based on the reduced order state vector
$F_{Rm}(\omega)$	The estimated measured frequency response function based on the reduced order state vector
F_1	Force corresponding to the master dofs in condensation techniques, Section 4.4
G(s)	Example transfer function in reduced order model example, Section 4.3
H_j	Sensitivity matrix of the measured quantities with respect to the unknown parameters. Defined in equation 5.12 and Section 5.3
I_k	Identity matrix of dimension k
j	$\sqrt{(-1)}$
J(a,b,c)	Cost function for the one dimensional example in section 6.2
$J(\delta\theta)$	General cost function
$J_1(\delta\theta)$	Addition to cost function to weight original analytically derived parameter vector
$K(\theta)$	The parameter dependent extended stiffness matrix
K_a	Analytical stiffness matrix

K_{Fi}	Coefficient of $\delta\theta_i$ in the expansion of the extended stiffness matrix in the reduced order model resulting from first order transformation
K_i	Coefficient of $\delta\theta_i$ in the expansion of the extended stiffness matrix in the full order model
$K_n(\theta)$	The usual (n,n) stiffness matrix which is dependent on the parameter θ
K_R	Reduced stiffness matrix, Section 4.4
K_u	Updated stiffness matrix
K_{zi}	Coefficient of $\delta\theta_i$ in the expansion of the extended stiffness matrix in the reduced order model resulting from zeroth order transformation
K_0	The extended stiffness matrix evaluated at the parameter value $\theta = \theta_e$
K_{11}, K_{12}, K_{21}, K_{22}	Submatrices of the stiffness matrix. Used in the condensation techniques Section 4.4
m	Dimension of output vector
m(x)	mass / unit length of beam in simple examples
$M(\theta)$	The parameter dependent extended mass matrix
M_a	Analytical mass matrix
M_{Fi}	Coefficient of $\delta\theta_i$ in the expansion of the extended mass matrix in the reduced order model resulting from first order transformation
M_i	Coefficient of $\delta\theta_i$ in the expansion of the extended mass matrix in the full order model

$\mathbf{M}_n(\theta)$	The usual (n,n) mass matrix which is dependent on the parameter θ
$\mathbf{M}_R$	Reduced mass matrix, Section 4.4
$\mathbf{M}_u$	Updated mass matrix
$\mathbf{M}_{zi}$	Coefficient of $\delta\theta_i$ in the expansion of the extended mass matrix in the reduced order model resulting from zeroth order transformation
$\mathbf{M}_0$	The extended mass matrix evaluated at the parameter value $\theta = \theta_e$
$\mathbf{M}_{11}, \mathbf{M}_{12}, \mathbf{M}_{21}, \mathbf{M}_{22}$	Submatrices of the mass matrix. Used in the condensation techniques Section 4.4
n	Number of degrees of freedom in the full model
N	Number of frequencies at which the FRF is measured
p	Number of unknown parameters
q	Number of force inputs
$\mathbf{q}$	$= (q_1, q_2, \ldots, q_n)^T$. Generalised co-ordinate vector in finite element analysis
$\mathbf{Q}$	Generalised force vector in finite element analysis
r	Number of degrees of freedom in the reduced model. Also number of measured modes in Chapter 5
R(s)	Reduced transfer function in Section 4.3
$R_{yu}(\tau)$	Cross Correlation Function between y and u
$R_{yy}(\tau)$	Auto Correlation Function of y
s	Laplace Transform variable
$S_{yu}(\omega)$	Cross Spectral Density between y and u
$S_{yy}(\omega)$	Auto Spectral Density of y

$\mathbf{T}$	Transformation matrix, used in the condensation techniques Section 4.4. Also matrix used to update the parameters in Chapter 5
$\mathbf{u}$	Input or force vector
$\mathbf{U}(\omega)$	Fourier Transform of input vector
$\mathbf{U}_m(\omega)$	Fourier Transform of measured input vector
$\mathbf{u}_k$	Unit vector in the k th coordinate direction
$\mathbf{v}$	Reduced order state vector resulting from first order transformation
$\mathbf{v}_i$	Theoretical mode shape vector
$\mathbf{v}_{mi}$	Measured mode shape vector
$\mathbf{V}_{ik}$	Vector used in calculating eigenvector derivatives
V_j	Variance of the j th parameter estimate, Chapter 5
V_{zj}	Variance between the measurement vector and its current theoretical estimate, Chapter 5
V_0	Variance of the initial parameter estimate, Chapter 5
V_ε	Variance of the measurement noise, Chapter 5
$\mathbf{w}$	Reduced order state vector resulting from zeroth order transformation
W_k	Value of weighting function for one dimensional Goyder algorithm example, defined in equation 7.9 Also weight function for general equation error algorithm (equation 7.16)
$\mathbf{W}(\omega)$	Fourier Transform of reduced order state vector resulting from zeroth order transformation
$\mathbf{W}_m(\omega)$	Estimated Fourier Transform of reduced order state vector resulting from zeroth order transformation based on measured data

$\mathbf{W}_r$	Matrix used in the Instrumental Variable Method, Section 7.2
$\mathbf{W}_\varepsilon$	Matrix giving weight to the measurement noise in the least squares estimator, Chapter 5
$\mathbf{W}_\theta$	Weighting matrix to limit deviation from initial parameters, equation 6.12. Also matrix giving weight to the initial parameter values in the least squares estimator, Chapter 5
$\mathbf{x}$	State vector in full order model
$\mathbf{x}_1, \mathbf{x}_2$	Partition of the state vector $\mathbf{x}$ in the condensation techniques of Section 4.4
$\mathbf{X}(\omega)$	Fourier Transform of the state vector of the full order model
$\mathbf{y}$	Output vector
$\mathbf{y}_F$	Output vector for the reduced order model resulting from first order transformation
$\mathbf{y}_Z$	Output vector for the reduced order model resulting from zeroth order transformation
$\mathbf{Y}(\omega)$	Fourier Transform of output vector
$\mathbf{Y}_m(\omega)$	Measured Fourier Transform corresponding to the output vector
$\mathbf{Y}_z(\omega)$	Fourier Transform of output vectorbased on the reduced order model
$\mathbf{z}$	Transformed state vector. Also theoretical vector corresponding to measured quantities in Chapter 5.
$\mathbf{z}_m$	Measurement vector in Chapter 5.
$\mathbf{z}_j$	j th estimate of the measurement vector in Chapter 5.
α	Multiple of mass matrix in definition of proportional viscous damping matrix
β	Multiple of stiffness matrix in definition of proportional viscous damping matrix

$\delta\theta$ = $(\theta - \theta_e) = (\delta\theta_1, \delta\theta_2, \ldots, \delta\theta_p)$, variation of the parameters from the current estimate

ε Measurement noise vector

$\Phi(\theta)$ Matrix of the first 2r eigenvectors as a function of the unknown parameters

Φ_0 Matrix of the first 2r eigenvectors evaluated at the current parameter estimate

Φ_i Matrix coefficent of $\delta\theta_i$ in the Taylor series expansion of $\Phi(\theta)$

ϕ_a Typical analytical eigenvector

ϕ_m Typical measured eigenvector

$_0\phi_i$ Eigenvector corresponding to $_0\lambda_i$ at the current parameter estimate

$\phi_i(\theta)$ eigenvector corresponding to the i th eigenvalue of the full model as a function of the unknown parameters

$_0\lambda_i$ i th eigenvalue of the full model at the current parameter estimate in ascending order of natural frequency

$\lambda_i(\theta)$ i th eigenvalue of the full model as a function of the unknown parameters in ascending order of natural frequency

$\Lambda(\theta)$ Matrix consisting of 2r negative eigenvalues of the full model along the diagonal as a function of the unknown parameters

$= -\text{diag}(\lambda_1(\theta), \lambda_2(\theta), \ldots, \lambda_{2r}(\theta))$

Λ_0 Matrix consisting of 2r eigenvalues of the full model along the diagonal, evaluated at the current parameter estimate

Λ_i	Matrix coefficent of $\delta\theta_i$ in the Taylor series expansion of $\Lambda(\theta)$
μ_i	Minus the i th natural frequency squared
μ_{mi}	Minus the i th measured natural frequency squared
θ	Vector of the unknown parameters
θ_a	Original analytical estimate of the parameter vector
θ_e	Current estimate of the parameter vector
θ_j	j th estimate of the parameter vector, Chapter 5
θ_0	Initial analytical estimate of the parameter vector, Chapter 5
ω	Frequency of sinusoidal excitation and response
ω_k	k th measured frequency value
ψ_i	i th real eigenvector (proportional damping)

Glossary

ADC	Analogue to Digital Converter
ARMA	Auto Regressive Moving Average
DAC	Digital to Analogue Converter
dof	Degrees of freedom
FRF	Frequency response function
MAC	Modal Assurance Criterion
mdof	multi degree of freedom
MSF	Modal Scale Factor
sdof	single degree of freedom
SEREP	System Equivalent Reduction Expansion Process

Appendix B Pin Jointed Frame Example

This appendix derives the finite element model of a pin jointed frame used as a numerical example in section 5.5. The structure is shown in figure 5.10. As a consequence of the pin jointed assumption, the beams do not bend so that only the extension of the beams is considered. Each beam is assumed to be homogeneous, and of constant cross sectional area. Since the model is only really interested in the equivalent stiffness of the beams these restrictions could be relaxed. The model consists of ten elements, which are the individual beams. The equivalent stiffness of the beams are related to the cross sectional area A and length l_i of the beams by

$$k_i = \frac{(EA)_i}{l_i} \qquad (A1)$$

The model consists of three types of elements, or beams: horizontal beams, vertical beams and sloping beams. The element mass and stiffness matrices of these elements, obtained by small displacement theory, will now be given. All the stiffness matrices are based on the expression for strain energy in a beam, which is

$$\text{Strain Energy} = \frac{1}{2} k_{eff} e^2 \qquad (A2)$$

where e is the extension in the beam and k_{eff} is the effective spring constant for the beam. The mass matrix is obtained by assuming a constant mass per unit length along the beam and a linear displacement model between the two ends.

Horizontal beams. Figure A1 defines the local co-ordinates for the horizontal beam elements. The mass and stiffness matrices, $\mathbf{M}^i$ and $\mathbf{K}^i$, based on a co-ordinate vector of $(u_1, v_1, u_2, v_2)^T$ are given by

$$\mathbf{M}^i = \frac{m_i l_i}{6}\begin{bmatrix} 2 & 0 & 1 & 0 \\ 0 & 2 & 0 & 1 \\ 1 & 0 & 2 & 0 \\ 0 & 1 & 0 & 2 \end{bmatrix} \qquad \mathbf{K}^i = k_i\begin{bmatrix} 1 & 0 & -1 & 0 \\ 0 & 0 & 0 & 0 \\ -1 & 0 & 1 & 0 \\ 0 & 0 & 0 & 0 \end{bmatrix} \qquad \text{(A3)}$$

where m_i is the mass per unit length of the i th element.

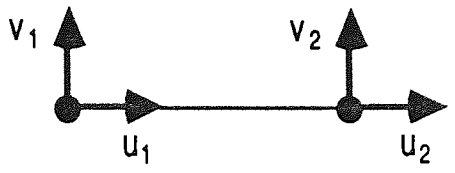

Figure A1 Local Co-ordinates for a Typical Horizontal Beam Element

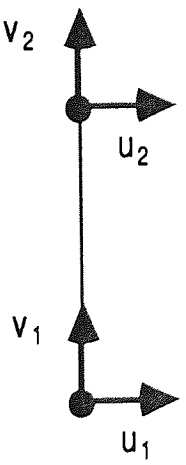

Figure A2 Local Co-ordinates for a Typical Vertical Beam Element

Vertical beams. Figure A2 defines the local co-ordinates for the horizontal beam elements. The mass and stiffness matrices, $\mathbf{M}^i$ and $\mathbf{K}^i$, based on a co-ordinate vector of $(u_1, v_1, u_2, v_2)^T$ are given by

$$\mathbf{M}^i = \frac{m_i l_i}{6}\begin{bmatrix} 2 & 0 & 1 & 0 \\ 0 & 2 & 0 & 1 \\ 1 & 0 & 2 & 0 \\ 0 & 1 & 0 & 2 \end{bmatrix} \qquad \mathbf{K}^i = k_i\begin{bmatrix} 0 & 0 & 0 & 0 \\ 0 & 1 & 0 & -1 \\ 0 & 0 & 0 & 0 \\ 0 & -1 & 0 & 1 \end{bmatrix} \qquad \text{(A4)}$$

Sloping beams. Figure A3 defines the local co-ordinates for the beam elements which slope at approximately 45 degrees. The mass and stiffness matrices, $\mathbf{M}^i$ and $\mathbf{K}^i$, based on a co-ordinate vector of $(u_1, v_1, u_2, v_2)^T$ are given by

$$\mathbf{M}^i = \frac{m_i l_i}{6}\begin{bmatrix} 2 & 0 & 1 & 0 \\ 0 & 2 & 0 & 1 \\ 1 & 0 & 2 & 0 \\ 0 & 1 & 0 & 2 \end{bmatrix} \qquad \mathbf{K}^i = \frac{k_i}{2}\begin{bmatrix} 1 & -1 & -1 & 1 \\ -1 & 1 & 1 & -1 \\ -1 & 1 & 1 & -1 \\ 1 & -1 & -1 & 1 \end{bmatrix} \qquad \text{(A5)}$$

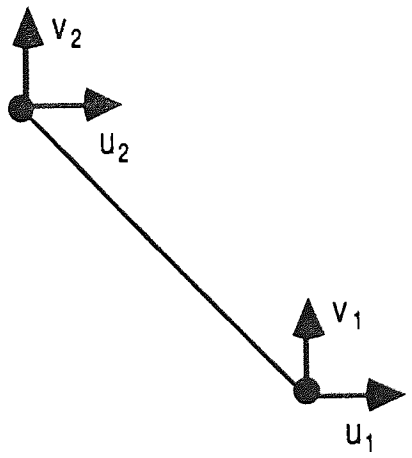

Figure A3 Local Co-ordinates for a Typical Sloping Beam Element

Given these mass and stiffness matrices for the individual elements the complete mass and stiffness matrices may be obtained by inspection using the structure defined by figure 5.10. The local co-ordinates are equated to the global, or generalised, co-ordinates to place the element matrices in the correct submatrices of the system mass and stiffness matrices.

Appendix C Model Order Reduction Example

This appendix gives the mass and stiffness matrices used as an example of model order reduction in Chapter 6. Although these matrices do not represent any particular structure they are closely related to model of the pin jointed frame outlined in Appendix B.

The mass matrix is assumed known and given by

$$\mathbf{M}_n(\theta) = \frac{1}{4}\begin{bmatrix} 18 & 0 & 2 & 0 & 2 & 0 & 3 & 0 & 0 & 0 \\ 0 & 18 & 0 & 2 & 0 & 2 & 0 & 3 & 0 & 0 \\ 2 & 0 & 14 & 0 & 0 & 0 & 2 & 0 & 3 & 0 \\ 0 & 2 & 0 & 14 & 0 & 0 & 0 & 2 & 0 & 3 \\ 2 & 0 & 0 & 0 & 18 & 0 & 2 & 0 & 0 & 0 \\ 0 & 2 & 0 & 0 & 0 & 18 & 0 & 2 & 0 & 0 \\ 3 & 0 & 2 & 0 & 2 & 0 & 18 & 0 & 2 & 0 \\ 0 & 3 & 0 & 2 & 0 & 2 & 0 & 18 & 0 & 2 \\ 0 & 0 & 3 & 0 & 0 & 0 & 2 & 0 & 10 & 0 \\ 0 & 0 & 0 & 3 & 0 & 0 & 0 & 2 & 0 & 10 \end{bmatrix}$$

The stiffness matrix is a function of θ_1 and is given by

$$K_n(\theta) = \begin{bmatrix} 12 & -3 & 0 & 0 & 0 & 0 & -3 & 3 & 0 & 0 \\ -3 & 3 & 0 & 0 & 0 & 0 & 3 & -3 & 0 & 0 \\ 0 & 0 & 3 & -3 & 0 & 0 & 0 & 0 & -3 & 3 \\ 0 & 0 & -3 & 3 & 0 & 0 & 0 & 0 & 3 & -3 \\ 0 & 0 & 0 & 0 & 21 & -3 & -9 & 0 & 0 & 0 \\ 0 & 0 & 0 & 0 & -3 & 3 & 0 & 0 & 0 & 0 \\ -3 & 3 & 0 & 0 & -9 & 0 & 21 & -3 & -9 & 0 \\ 3 & -3 & 0 & 0 & 0 & 0 & -3 & 3 & 0 & 0 \\ 0 & 0 & -3 & 3 & 0 & 0 & -9 & 0 & 12 & -3 \\ 0 & 0 & 3 & -3 & 0 & 0 & 0 & 0 & -3 & 3 \end{bmatrix}$$

$$+ \begin{bmatrix} 3 & 0 & -3 & 0 & 0 & 0 & 0 & 0 & 0 & 0 \\ 0 & 3 & 0 & 0 & 0 & -3 & 0 & 0 & 0 & 0 \\ -3 & 0 & 3 & 0 & 0 & 0 & 0 & 0 & 0 & 0 \\ 0 & 0 & 0 & 3 & 0 & 0 & 0 & -3 & 0 & 0 \\ 0 & 0 & 0 & 0 & 0 & 0 & 0 & 0 & 0 & 0 \\ 0 & -3 & 0 & 0 & 0 & 3 & 0 & 0 & 0 & 0 \\ 0 & 0 & 0 & 0 & 0 & 0 & 0 & 0 & 0 & 0 \\ 0 & 0 & 0 & -3 & 0 & 0 & 0 & 3 & 0 & 0 \\ 0 & 0 & 0 & 0 & 0 & 0 & 0 & 0 & 0 & 0 \\ 0 & 0 & 0 & 0 & 0 & 0 & 0 & 0 & 0 & 0 \end{bmatrix} \theta_2$$

As indicated in Chapter 6 the damping matrix is given by

$$C_n = \theta_1 M_n .$$

Appendix D H Frame Example

This appendix derives the finite element model of the H frame shown in figure 7.6. This structure was used as a simulated example in Chapter 7 and an experimental example in Chapter 8. The model is two dimensional only and consists of beam elements. These beams may bend perpendicular to the axis of the beam or extend along this axis. The displacement models for the elements are the most simple, that is a linear model for bar extension and a

Figure A4 Local Co-ordinates for a Typical Beam Element for the H Frame

cubic model for beam bending. Each element is assumed to have a constant cross sectional area and to be homogeneous. Figure A4 shows the local coordinates for a typical element. The mass and stiffness matrices for this element in terms of the local co-ordinate vector $(u_1, v_1, r_1, u_2, v_2, r_2)^T$ are given by

$$M^i = \frac{m_i l_i}{420} \begin{bmatrix} 140 & 0 & 0 & 70 & 0 & 0 \\ 0 & 156 & 22 l_i & 0 & 54 & -13 l_i \\ 0 & 22 l_i & 4 l_i^2 & 0 & 13 l_i & -3 l_i^2 \\ 70 & 0 & 0 & 140 & 0 & 0 \\ 0 & 54 & 13 l_i & 0 & 156 & -22 l_i \\ 0 & -13 l_i & -3 l_i^2 & 0 & -22 l_i & 4 l_i^2 \end{bmatrix}$$

$$K^i = \frac{E}{l_i^3} \begin{bmatrix} A_i l_i^2 & 0 & 0 & -A_i l_i^2 & 0 & 0 \\ 0 & 12 I_i & 6 I_i l_i & 0 & -12 I_i & 6 I_i l_i \\ 0 & 6 I_i l_i & 4 I_i l_i^2 & 0 & -6 I_i l_i & 2 I_i l_i^2 \\ -A_i l_i^2 & 0 & 0 & A_i l_i^2 & 0 & 0 \\ 0 & -12 I_i & -6 I_i l_i & 0 & 12 I_i & -6 I_i l_i \\ 0 & 6 I_i l_i & 2 I_i l_i^2 & 0 & -6 I_i l_i & 4 I_i l_i^2 \end{bmatrix}$$

where m_i is the mass per unit length, l_i is the length, A_i is the cross sectional area and I_i is the second moment of area, all for the i th element. E is the Young's modulus for the elements.

The H frame is modelled by a finite element model with either 20 or 40 elements. This corresponds to 21 or 41 nodes respectively. Since the motion of the frame is considered in the vertical plane only, each node has 3 degrees of freedom. Thus the dimension of the displacement vector for the 20 and 40 element models are 63 and 123 respectively. Table A1 shows these dimensions and also the number of elements in the individual beams.

Total No of Elements	No Elements in Long Beams	No Elements in Cross Beams	No of Nodes	DOF
20	8	4	21	63
40	16	8	41	123

Table A1 Details of the Two Finite Element Models of the H Frame

The element mass and stiffness matrices are positioned in the system matrices using the compatibility conditions between the generalised co-ordinates and the local co-ordinates. The unknown parameters are either bending stiffnesses (flexural rigidities) or element lengths, given by EI_i or l_i in the above expressions. The initial values of the flexural rigidities are estimated from the theoretical values for a rectangular cross section beam. The different values for parameters 2 and 3 in the 63 dof and the 123 dof simulations (see table 7.3) should be noted. The elements for the 63 dof simulation cover two elements of the 123 dof simulation. Thus when the values of flexural rigidity in two adjacent elements in the 123 dof simulation are different, the value of flexural rigidity for the combined element in the 63 dof simulation must be an average value.

This model of the H frame is a gross simplification. For example, the joints are assumed to be perfectly rigid, when in fact they are bolted and so will have complex dynamics. No allowance is made for elemental shear. Given the simple nature of the model it reproduces the experimental dynamics remarkably well.

Appendix E Derivation of Equations in Chapter 5

Chapter 5 derived an algorithm to update the parameters of a finite element model using a minimum variance estimator. This appendix contains the derivation of some of the equations used in Chapter 5. The equation numbers in brackets at the end of the following equations refer to the basic equations and properties (from Chapter 5) used to obtain the given expression.

Equation 5.15. This equation is derived by writing the expected value of the parameter estimate at the j+1 th iteration in terms of the previous parameter estimate and the measurement noise. Thus

$$E[\theta_{j+1}] = E[\theta_j + T(z_m - z_j)] \quad \text{(Equation 5.14)}$$

$$= E[\theta_j] + T\,E[z_m - z_j] \quad \text{(T constant)}$$

$$= E[\theta_j] + T\,E[z - z_j + \varepsilon^T] \quad \text{(Equation 5.8)}$$

$$= E[\theta_j] + T\,H_j\,E[\theta - \theta_j] + T\,E[\varepsilon^T] \quad \text{(Equation 5.11)}$$

$$= \theta \quad \text{(Equations 5.9 \& 5.10)}$$

Equation 5.16. The covariance of the new parameter estimate is obtained by writing the parameter estimate at the j+1 th iteration in terms of the previous parameter estimate. Hence

$$V_{j+1} = E\left[\left(\theta_{j+1} - \theta\right)\left(\theta_{j+1} - \theta\right)^T\right]$$

$$= E\left[\left(\theta_j - \theta + T\left(z_m - z_j\right)\right)\left(\theta_j - \theta + T\left(z_m - z_j\right)\right)^T\right]$$

(Equation 5.14)

$$= E\left[\left(\theta_j - \theta\right)\left(\theta_j - \theta\right)^T\right] + E\left[\left(\theta_j - \theta\right)\left(z_m - z_j\right)^T\right]T^T$$

$$+ T\,E\left[\left(z_m - z_j\right)\left(\theta_j - \theta\right)^T\right] + T\,E\left[\left(z_m - z_j\right)\left(z_m - z_j\right)^T\right]T^T$$

$$= V_j + \left(D_j - V_j H_j^T\right)T^T + T\left(D_j^T - H_j V_j\right) + T\,V_{zj}T^T$$

since

$$E\left[\left(z_m - z_j\right)\left(\theta_j - \theta\right)^T\right]$$

$$= E\left[\left(z_m - z\right)\left(\theta_j - \theta\right)^T + \left(z - z_j\right)\left(\theta_j - \theta\right)^T\right]$$

$$= E\left[\varepsilon^T\left(\theta_j - \theta\right)^T - H_j\left(\theta_j - \theta\right)\left(\theta_j - \theta\right)^T\right]$$

(Equations 5.8 & 5.11)

$$= E\left[\left(\theta_j\,\varepsilon\right)^T\right] - H_j E\left[\left(\theta_j - \theta\right)\left(\theta_j - \theta\right)^T\right] \quad \text{(Equation 5.9)}$$

$$= D_j^T - H_j V_j$$

and where (equation 5.17)

$$V_{zj} = E\left[(z_m - z_j)(z_m - z_j)^T\right]$$

$$= E\left[\left((z_m - z) + (z - z_j)\right)\left((z_m - z) + (z - z_j)\right)^T\right]$$

$$= E\left[\left(\varepsilon^T - H_j(\theta_j - \theta)\right)\left(\varepsilon^T - H_j(\theta_j - \theta)\right)^T\right]$$

(Equations 5.8 & 5.11)

$$= H_j E\left[(\theta_j - \theta)(\theta_j - \theta)^T\right] H_j^T - H_j E\left[(\theta_j - \theta)\varepsilon\right]$$

$$- E\left[\left((\theta_j - \theta)\varepsilon\right)^T\right] H_j^T + E\left[\varepsilon^T \varepsilon\right]$$

$$= H_j V_j H_j^T - H_j D_j - D_j^T H_j^T + V_\varepsilon \; . \qquad \text{(Equations 5.9 \& 5.13)}$$

Equation 5.19. The correlation matrix D_j may be updated by

$$D_{j+1} = E\left[\theta_{j+1}\varepsilon\right]$$

$$= E\left[\theta_j \varepsilon + T(z_m - z_j)\varepsilon\right] \qquad \text{(Equation 5.14)}$$

$$= D_j + T\, E\left[(z_m - z)\varepsilon + (z - z_j)\varepsilon\right]$$

$$= D_j + T\, E\left[\varepsilon^T \varepsilon - H_j(\theta_j - \theta)\varepsilon\right] \qquad \text{(Equations 5.8 \& 5.11)}$$

$$= D_j - T\left(H_j D_j - V_\varepsilon\right) \qquad \text{(Equations 5.9 \& 5.13)}$$

$$= D_j - \left(V_j H_j^T - D_j\right) V_{zj}^{-1}\left(H_j D_j - V_\varepsilon\right)$$

Equation 5.22. The expression for the next parameter estimate is derived from minimising the cost function given in equation 5.21 with respect to θ. Using equations 5.8 and 5.11

$$\begin{aligned} \varepsilon^{T} &= z_m - z \\ &= (z_m - z_j) - (z - z_j) \\ &= (z_m - z_j) - H_j(\theta - \theta_j) \end{aligned}$$

and so

$$J(\theta) = (\theta - \theta_j)^T \left[H_j^T W_\varepsilon H_j + W_\theta\right](\theta - \theta_j) - (\theta - \theta_j)^T H_j^T W_\varepsilon (z_m - z_j)$$

$$- (z_m - z_j)^T W_\varepsilon H_j(\theta - \theta_j) + (z_m - z_j)^T W_\varepsilon (z_m - z_j)$$

Hence the least squares estimate is (equation 5.22)

$$\theta = \theta_j + \left[H_j^T W_\varepsilon H_j + W_\theta\right]^{-1} H_j^T W_\varepsilon (z_m - z_j)$$

Equations 5.23 and 5.24. By comparing equations 5.18 and 5.22 the two estimates of the parameters are equal if

$$\left[H_j^T W_\varepsilon H_j + W_\theta\right]^{-1} H_j^T W_\varepsilon = \left(V_j H_j^T - D_j\right) V_{zj}^{-1}$$

Since W_ε and V_{zj} are both square matrices and have the same dimension (equation 5.23) let

$$W_\varepsilon = V_{zj}^{-1}$$

Then the solution of the above equation for W_θ is obtained by rearranging

the above equation. A pseudo inverse is required to obtain the expressions for W_θ, the form of which will depend on the number of measurements and parameters. Thus

$$\left[H_j^T V_{zj}^{-1} H_j + W_\theta \right]^{-1} H_j^T = \left(V_j H_j^T - D_j \right) \qquad \text{(Equation 5.23)}$$

$$H_j^T = \left[H_j^T V_{zj}^{-1} H_j + W_\theta \right] \left(V_j H_j^T - D_j \right) \qquad \text{(Rearranging)}$$

$$W_\theta \left(V_j H_j^T - D_j \right) = H_j^T - H_j^T V_{zj}^{-1} H_j \left(V_j H_j^T - D_j \right)$$

$$= - H_j^T V_{zj}^{-1} \left(H_j D_j - V_\varepsilon \right)^T \qquad \text{(Equation 5.17)}$$

which is equation 5.24.